ANL/ES-CEN-1015
and
FE-1780-4

ANL/ES-CEN-1015
and
FE-1780-4

A DEVELOPMENT PROGRAM ON PRESSURIZED FLUIDIZED-BED COMBUSTION

Quarterly Report
January—March 1976

by

G. J. Vogel, I. Johnson, P. Cunningham,
B. Hubble, S. Lee, J. Lenc, J. Montagna,
S. Siegel, R. Snyder, S. Saxena, G. Smith,
W. Swift, G. Teats, I. Wilson, and A. A. Jonke

ARGONNE NATIONAL LABORATORY, ARGONNE, ILLINOIS
Operated for the U. S. ENERGY RESEARCH
AND DEVELOPMENT ADMINISTRATION
under Contract W-31-109-Eng-38

DISCLAIMER

Printed in the United States of America
Available from
National Technical Information Service
U. S. Department of Commerce
5285 Port Royal Road
Springfield, Virginia 22161
Price: Printed Copy $5.50; Microfiche $2.25

ANL/ES-CEN-1015
and
FE-1780-4
Coal Conversion and Utilization—
Direct Combustion of Coal
(UC-90e)

ARGONNE NATIONAL LABORATORY
9700 South Cass Avenue
Argonne, Illinois 60439

A DEVELOPMENT PROGRAM ON PRESSURIZED FLUIDIZED-BED COMBUSTION

Quarterly Report
January—March 1976

by

G. J. Vogel, I. Johnson, P. Cunningham,
B. Hubble, S. Lee, J. Lenc, J. Montagna,
S. Siegel, R. Snyder, S. Saxena,* G. Smith,
W. Swift, G. Teats, I. Wilson, and A. A. Jonke

Chemical Engineering Division

Prepared for the
U. S. Energy Research and Development Administration
under Contract No. 14-32-0001-1780

and the

U. S. Environmental Protection Agency
under Agreement IAG-D5-E681

*University of Illinois - Chicago Circle

BIBLIOGRAPHIC DATA SHEET	1. Report No. ANL/ES-CEN-1015	2.	3. Recipient's Accession No. FE-1780-4
4. Title and Subtitle: A Development Program on Pressurized Fluidized-Bed Combustion			5. Report Date: April 1976 6.
7. Author(s): G. J. Vogel *et al.*			8. Performing Organization Rept. No. ANL/ES-CEN-1015
9. Performing Organization Name and Address: Argonne National Laboratory, 9700 South Cass Avenue, Argonne, Illinois 60439			10. Project/Task/Work Unit No. 11. Contract/Grant No. 14-32-0001-1780 (ERDA) IAG-D5-E681 (EPA)
12. Sponsoring Organization Name and Address: U.S. Energy Research and Development Administration and the Environmental Protection Agency			13. Type of Report & Period Covered QUARTERLY January 1-March 31, 1976 14.

15. Supplementary Notes

16. Abstracts A development program on pressurized fluidized-bed combustion is being carried out in a bench-scale pilot plant capable of operating at 10-atm pressure. The concept involves burning fuels such as coal in a fluidized bed of particulate lime additive that reacts with the sulfur compounds formed during combustion to reduce air pollution. Nitrogen oxide emissions are also reduced at the combustion temperatures used, which are lower than those used in a conventional coal combustor. The $CaSO_4$ produced in the combustor is regenerated to CaO that is recycled to the combustor for removal of sulfur compounds.

This report presents information on: bench-scale regeneration experiments, TGA experiments on sulfation and regeneration rates of synthetic SO_2-sorbents containing metal oxides, bench-scale combustion, regeneration by the $CaSO_4$-CaS reaction, coal combustion reactions, status of equipment fabrication and methematical modeling of the gas-solid combustion reaction.

17. Key Words and Document Analysis. 17a. Descriptors

Air Pollution
Fluidized-Bed Processing
Sulfur Oxides
Dolomite
Fossil Fuel
Combustion
Coal
Calcium Sulfates
Additives
Sulfur
Calcium Oxides
Calcium Carbonate
Flue Gas
Roasting
Calcium Sulfide
Sorbents
Ashes
X-ray Diffraction
Desulfurization
Particle Shape
Particle Size
Flue Dust
Fly Ash
Particle Size Distribution
Fragmentation
Agglomeration

17b. Identifiers/Open-Ended Terms

Air Pollution
Stationary Sources
Fluidized-Bed Combustion
Supported Additives
Additive Regeneration

17c. COSATI Field/Group

18. Availability Statement	19. Security Class (This Report) UNCLASSIFIED	21. No. of Pages
	20. Security Class (This Page) UNCLASSIFIED	22. Price

TABLE OF CONTENTS

TABLE OF CONTENTS (Contd.)

LIST OF FIGURES

LIST OF FIGURES (Contd.)

LIST OF TABLES

LIST OF TABLES (Contd.)

A DEVELOPMENT PROGRAM ON PRESSURIZED FLUIDIZED BED COMBUSTION

Quarterly Report
January—March 1976

by

G. J. Vogel, I. Johnson, P. Cunningham, B. Hubble, S. Lee, J. Lenc, J. Montagna, S. Siegel, R. Snyder, S. Saxena, G. Smith, W. Swift, G. Teats, I. Wilson, and A. A. Jonke

ABSTRACT

A development program on pressurized fluidized-bed combustion is being carried out in a bench-scale pilot plant capable of operating at 10-atm pressure. The concept involves burning fuels such as coal in a fluidized bed of particulate lime additive that reacts with the sulfur compounds formed during combustion to reduce air pollution. Nitrogen oxide emissions are also reduced at the combustion temperatures used, which are lower than those used in a conventional coal combustor. The $CaSO_4$ produced in the combustor is regenerated to CaO that is recycled to the combustor for removal of sulfur compounds.

This report presents information on: bench-scale regeneration experiments, TGA experiments on sulfation and regeneration rates of synthetic SO_2-sorbents containing metal oxides, bench-scale combustion experiments, regeneration by the $CaSO_4$-CaS reactions, coal combustion reactions, status of equipment fabrication, and mathematical modeling of the gas-solid combustion reactions.

SUMMARY

In fluidized-bed combustion, coal is combusted in a fluidized bed of calcium-containing solids (limestone, dolomite, or synthetic stones) which react with the sulfur compound released in coal combustion, forming calcium sulfate. In another step, the calcium sulfate may be regenerated for reuse in the combustor.

Current objectives of the ANL fluidized-bed combustion-regeneration program are (1) to select and optimize a regeneration process, (2) to test the behavior of different limestones, dolomites, and synthetic additives during combustion and regeneration, and (3) to assess the behavior of biologically toxic trace elements and corrosive elements.

One-Step Regeneration of Additive, Bench-Scale Studies

A process for the one-step reductive regeneration of additive in a fluidized bed is being investigated in which the required heat and

reductants are provided by partial combustion of coal in the bed. In current studies, sulfated dolomite and limestone have been regenerated, fusion temperatures of mixtures of ash and partially sulfated additive have been determined, and the distributions of sulfur in sample particles have been examined with the electron microprobe instrument.

Regeneration of Sulfated Greer Limestone. Experiments have been initiated in which sulfated Greer limestone from Pope, Evans and Robbins is regenerated. The first bench-scale experiment was performed at 1040°C with a solids feed rate of 4.9 kg/hr. A SO_2 concentration of 2.2% in the wet effluent gas was obtained from which a sulfur regeneration of 68% was calculated. These results are comparable with those obtained in a similar experiment with sulfated Tymochtee dolomite. In another experiment at 1100°C with a solids feed rate of 5.4 kg/hr, a SO_2 concentration of 2.8% in the wet effluent gas and a sulfur regeneration of 75% were obtained. The COS and CS_2 concentrations were 0.02% and ∿0.01%, respectively, for both experiments.

At a higher additive feed rate (8.6 kg/hr), the average SO_2 concentration in the wet effluent gas was 3.6%, which was higher than any obtained in previous regeneration experiments which used coal to supply heat. Solids throughput rate will be increased in future experiments to investigate the feasibility of obtaining high SO_2 concentrations in the effluent gas stream.

In these coal-combustion regeneration experiments, the extent of regeneration was also calculated from chemical analyses of regenerated dolomite and limestone samples. The values obtained were 19 to 25% higher than those calculated from SO_2 and H_2S concentrations in the effluent gas. The extent of elemental sulfur formation is being evaluated as a possible explanation for these differences.

The Effect of the Relative Sizes of the Oxidizing and Reducing Zones During Regeneration. Two experiments have been performed at relatively high reducing gas concentrations (∿4% in the effluent gas, which is approximately twice as high as in other regeneration experiments with coal) to test the effect of the relative lengths of the oxidizing and reducing zones on the steady state concentrations of CaS in the regenerated product. Increasing the length of the oxidizing zone relative to the length of the reducing zone resulted in a drastically reduced CaS concentration in the regenerated product and an increase in the extent of regeneration.

Fusion of Sulfated Additive and Coal Ash. Ash fusion temperatures of Arkwright coal ash were measured (ASTM-D-1857-74). It was found that the initial deformation temperature of this ash under reducing conditions was ∿1100°C. Since some regeneration experiments are being performed at or near this temperature, it was decided to use coal (Triangle coal) with a higher ash fusion temperature.

Mixtures of ash and sulfated Tymochtee dolomite (10.2 wt % S) and mixtures of ash and sulfated Greer limestone were prepared. The plots of

fusion temperature versus ash content indicated the possibility that a eutectic forms in mixtures of 60 to 70% ash content. X-ray diffraction analysis of fused samples of Tymochtee dolomite and ∿50% ash revealed that spinel type compounds had formed. Fused samples of Greer limestone and ∿70% ash contained calcium-aluminum silicate compounds.

Sulfated Greer limestone from Pope, Evans and Robbins (Test 620) was analyzed, and its composition was compared with that of unsulfated Greer limestone. Based on composition changes of silicon, ∿10% ash content was estimated for the sulfated stone.

Effect of Regeneration Temperature on Sulfation and Regeneration of Tymochtee Dolomite. In the FAC-series of regeneration experiments with sulfated Tymochtee dolomite, it was found that as the regeneration temperature was increased from 1010°C to 1095°C, the extent of CaO regeneration increased from 20% to 90% and the SO_2 concentration in the wet effluent gas increased from 0.7% to 5.4%.

To evaluate the effect of regeneration temperature on the quality of regenerated dolomite as an SO_2 acceptor, the pore size distributions for several regenerated samples were obtained. It was found that the dolomite that had been regenerated at the higher temperature (1095°C as compared with 1040°C) contained a greater amount of larger pores (>0.4 μm). These larger pores have been shown by others to be beneficial to sulfation. However, when the reactivity of these samples as SO_2 acceptors was evaluated in TGA experiments, the sample regenerated at the lower temperature (1040°C) was found to be more reactive.

Although higher regeneration rates are obtained at higher regeneration temperatures, the effect of regeneration temperature on the reactivity of the additive in subsequent cycles also has to be considered.

Electron Microprobe Analysis of Sulfated and Regenerated Tymochtee Dolomite. Electron microprobe analyses were made of sulfated and regenerated Tymochtee dolomite particles. Radial concentration profiles for calcium and sulfur are given. Generally, the regenerated particles examined showed no sulfur concentration irregularities that might lead to poor utilization in subsequent sulfation cycles.

Correlation of Reaction Kinetic Data Associated with the Bench-Scale Regeneration of Sulfated Dolomite. Data from the FAC-series regeneration experiments with sulfated dolomite has been correlated. This analysis considers the quantitative contribution of the gaseous composition, not at the concentrations within the reactor zone, but at the concentrations before introduction into the fluidized-bed reactor. The interdependence of the feed gas concentrations, Y_{CH_4} and Y_{O_2}, and the fluidized-bed height, h, for the FAC experiments has been obtained as:

$$R_{av} = k\, Y_{CH_4}\, Y_{O_2}^{0.68}\, h^{-1.33}$$

where R_{av} is similar to extent of solid regeneration and k is a constant.

Development of Synthetic SO_2-Sorbents

Synthetic SO_2-sorbents prepared by the impregnation of alumina pellets with CaO are being investigated for possible use to capture SO_2 during the fluidized-bed combustion of coal. Sorbents containing 2-21% CaO have been tested for their reactivity with SO_2. It was observed that except for one composition, as the CaO content of the sorbent increased, the rate of reaction decreased; the rate of reaction of the 20.9% CaO in α-Al_2O_3 sorbent increased anomalously.

Other metal oxides, Li_2O, Na_2O, K_2O, SrO, and BaO, have been impregnated into alumina and tested as SO_2 sorbents. Lithium sulfate was found to be unstable at sulfation conditions (900°C). Sodium oxide and potassium oxide sorbents have a higher rate of reactivity with SO_2 than does CaO sorbent; however, their sulfates would have appreciable volatility at regeneration conditions (1100°C). Strontium oxide and barium oxide sorbents have essentially the same reactivity as calcium oxide sorbents.

Porosity measurements have been made on granular supports that had been heat treated at 1100, 1200, and 1500°C. The higher heat-treatment temperatures produced supports containing larger pores. The supports that contained larger pores produced sorbents having a higher reactivity with SO_2 and a greater calcium utilization.

Some Dow chemical sorbents were reacted with a synthetic combustion gas. They performed poorly due to the formation of stable calcium-aluminum silicates.

Bench-Scale, Pressurized Fluid-Bed Combustion Experiments

In the utilization of regeneration technology, it is important that additive can be recycled a sufficient number of times without losing its reactivity for either sulfation or regeneration and without decrepitating severely. An experimental effort is being made at ANL, therefore, to evaluate the effects of cyclic operation on the resistance to decrepitation and the reactivity of Tymochtee dolomite in ten combustion/regeneration cycles. Reported here are the results of (1) an initial experiment and (2) the first in a series of cycling experiments.

Experiment RC-1A was performed at the initial step in the evaluation of the effects of additive recycling on additive reactivity and decrepitation. A limited quantity of Tymochtee dolomite ($\sim$120 lb) which had been sulfated, regenerated under various operating conditions, and then thoroughly mixed was used as the additive in the experiment. Arkwright coal was combusted at a bed temperature of 840°C, 810 kPa pressure, and $\sim$17% excess combustion air. The Ca/S mole ratio, which was used on the unreacted calcium in the regenerated dolomite (additive contained $\sim$4.3% sulfur), was 1.6 for the experiment.

Based on the flue-gas analysis for SO_2 (250 ppm), sulfur retention (based on sulfur in coal and ignoring the sulfur in the original additive) was determined to be ∿90%. This agrees well with correlations of previous combustion experiments, indicating that the additive retained its reactivity for sulfur removal into the second combustion cycle.

A calcium material balance at steady-state conditions revealed that ∿32% of the additive fed to the combustor was entrained in the off-gas and recovered in the primary and secondary cyclone ash materials. Although the evidence is inconclusive at this point, it seems apparent from the screen analyses of the dolomite feed and overflow and the primary and secondary cyclone materials that the high additive entrainment was not the result of additive decrepitation in the combustor. More rigorous determinations of additive decrepitation are planned during the full 10-cycle combustion/regeneration series of experiments.

To compensate for anticipated losses of additive in ten cycles of combustion and regeneration, a large amount of Tymochtee dolomite is currently being sulfated as part of the first combustion phase of the cyclic experiments. At the end of 1 1/2 cycles, the material from experiment RC-1A will be blended in for the remaining cyclic experiments.

The first combustion cycle experiment, REC-1, in the cyclic series of experiments is nearly completed; over 1000 lb of the dolomite has been sulfated. In the two extended runs in the first cycle, the level of SO_2 in the flue gas was ∿300 ppm, which corresponds to a sulfur retention of 86% and an SO_2 emission of 0.58 lb/10^6 Btu. Chemical and physical analyses of sulfated dolomite and fly-ash samples are being performed to determine the extent of decrepitation during the first combustion cycle.

Regeneration Chemistry

Additional information is given on the chemistry of regeneration reactions. Results are reported for experiments on gas phase reduction of $CaSO_4$ at several hydrogen reducing gas concentrations and at temperatures of 950, 900, 850, and 800°C. The results indicated that CaO is formed at 950°C at all reducing gas concentrations; at 900, 850, and 800°C, CaO is formed only at low reducing gas concentrations. This is interpreted to suggest that in the reducing step of the two-step regeneration method, the $CaSO_4$-CaS reaction is a competing reaction with the reduction reaction under most experimental conditions.

Preliminary experiments were made to test the implication of this interpretation on the carbonation reaction in the two-step regeneration scheme and are discussed.

Coal Combustion Reactions

The Determination of Inorganic Constituents in the Effluent Gas from Coal Combustion

Some chemical elements carried by combustion gas are known to cause

severe metal corrosion. The purpose of this study is to determine quantitatively which elements are present in the hot combustion gas of coal, in either volatile or particulate form, and to differentiate between volatile and particulate species. Identification of the compound form and amount of particulate species, as well as determination of the amount and form of condensable species, are of interest.

The laboratory-scale batch-unit fixed-bed combustor designed for this study is being constructed in the central shop of ANL. The ceramically bonded fused-alumina filter to be used in the combustor for the removal of particulates from the hot combustion gases of coal has been received. The Tocco induction heating unit, which will be used with the combustor, has been installed, tested, and found to be in good working condition. The coupling between the induction heating unit and combustor has been adjusted by using as a stand-in a 3-ft length of stainless steel pipe of the same size as the combustor.

Systematic Study of the Volatility of Trace Elements in Coal

Knowledge of the vaporization characteristics of trace elements in coal and the rate of their volatilization is important for combined-cycle turbine operation. The objective of this study is to obtain data on the volatility of these elements under practical coal combustion and gasification conditions. Those elemental analyses not completed in time for the preceding report are presented. The results indicate that most of the chlorine in coal evolves at temperatures below 640°C and that the metallic elements are generally retained in the ash up to 990°C under oxidizing conditions.

This study has been extended to a high heat-treatment temperature range. In the Series-2 experiments, coal ash was heat-treated in a platinum combustion boat to temperatures between 850 and 1250°C for 20 hr in either air or an oxygen-enriched air flow of 0.6 scfh. Some elemental analyses for this series of experiments are reported. The metallic elements Fe, Al, Na, K, Zn, Mn, and Ni are found to remain in the ash up to 1250°C under the oxidizing environment. The retention of these elements in the ash is not affected by the oxygen concentration in the flowing gas.

Fabrication of New Equipment

To improve experimental capabilities relating to the pressurized combustion of coal in a fluidized bed of SO_2-retaining additive and subsequent regeneration of the sulfated additive, several new pieces of equipment are to be fabricated. Major equipment items include a new regenerator, a new combustor, and a cyclic system for continuous recycling of additive between the combustor and the regenerator.

The scheduled completion date for fabrication of a new regenerator of improved design is June 15, 1976. Design of a new, pressurized, fluidized-bed combustor is being reviewed, prior to fabrication, for conformance to the ASME Boiler and Pressure Vessel Code.

Various pieces of equipment are being either fabricated or purchased that will permit continuous cycling (instead of manual transfer) of sulfated additive from the combustor to the regenerator and of regenerated additive from the regenerator back to the combustor. In current investigations related to the effect of additive recycling on such variables as decrepitation, reactivity for SO_2 retention, and buildup of coal ash in the additive, manual transfer of the additive is required. The status of the various components required for the cyclic system is presented.

Mathematical Modeling. Noncatalytic Gas-Solid Reaction with Changing Particle Size: Unsteady State Heat Transfer

A mathematical expression for the unsteady state heat balance is derived for a nonisothermal, noncatalytic, first order gas-solid reaction. The formulation is based on a shrinking core model and takes into account the changing size of the spherical particle during reaction. Thus, the model has two moving boundaries, *viz.*, the reaction front and the external particle diameter which grows or shrinks due to reaction. This complicates the numerical solution considerably.

Limestone and Dolomite for the Fluidized-Bed Combustion of Coal: Procurement and Disposal

A report on the potential demand, supply, cost, and disposal aspects associated with the use of limestone or dolomite as sulfur-accepting additives in the fluidized-bed combustion coal was prepared by B. S. Friedman, a consultant to Argonne National Laboratory. It is appended to this report.

INTRODUCTION

In this program, funded by the Energy Research and Development Administration and the Environmental Protection Agency, fluidized-bed combustion is being studied as a method of removing from the gas phase nearly all atmospheric pollutants (sulfur and nitrogen compounds) generated during the combustion of fossil fuels. The concept involves burning of fuels such as coal in a fluidized bed of particulate lime solids that react with the sulfur compound formed during coal combustion. In another step, the sulfated lime may be regenerated for reuse in the combustor.

This quarterly report presents information on: bench-scale regeneration experiments, TGA experiments on sulfation and regeneration of synthetic additives containing metal oxides, bench-scale combustion experiments, regeneration by the $CaSO_4$-CaS reaction, coal combustion reactions, status of equipment fabrication, and mathematical modeling of the gas-solid combustion reactions.

ONE-STEP REGENERATION OF ADDITIVE, BENCH-SCALE STUDIES

A process is being investigated for the one-step reductive regeneration of additive in a fluidized bed in which the required heat and reductants are provided by partial combustion of coal in the regeneration reactor. One reaction by which regeneration of CaO occurs is given below:

$$CaSO_4 + CO \xrightarrow{1100°C} CaO + SO_2 + CO_2 \qquad (1)$$

Other reductants such as H_2 and CH_4 can play the same role as CO.

Equipment

The bench-scale experimental system used for previous regeneration experiments has been previously described.[1] Recently, the experimental regeneration system was separated from the combustion system and the regenerator was rebuilt and modified. Figure 1 is a schematic diagram of the new regeneration system. As previously reported, the inside diameter of the reactor vessel has been enlarged from 7.62 cm (3.0 in.) to 10.8 cm (4.25 in.), and the inside metal overflow pipe (formerly used to control the fluidized-bed height) has been replaced with an overflow pipe that is external to the fluidized bed. The coal and the sulfated additive are fed separately for independent control to a common pneumatic transport line which enters the bottom of the reactor. Other modifications to the experimental system have been previously described.[2]

Solids transport air constitutes ~40% of the total fluidizing gas in the reactor. The remaining fluidizing gas is a mixture of pure N_2 and O_2.

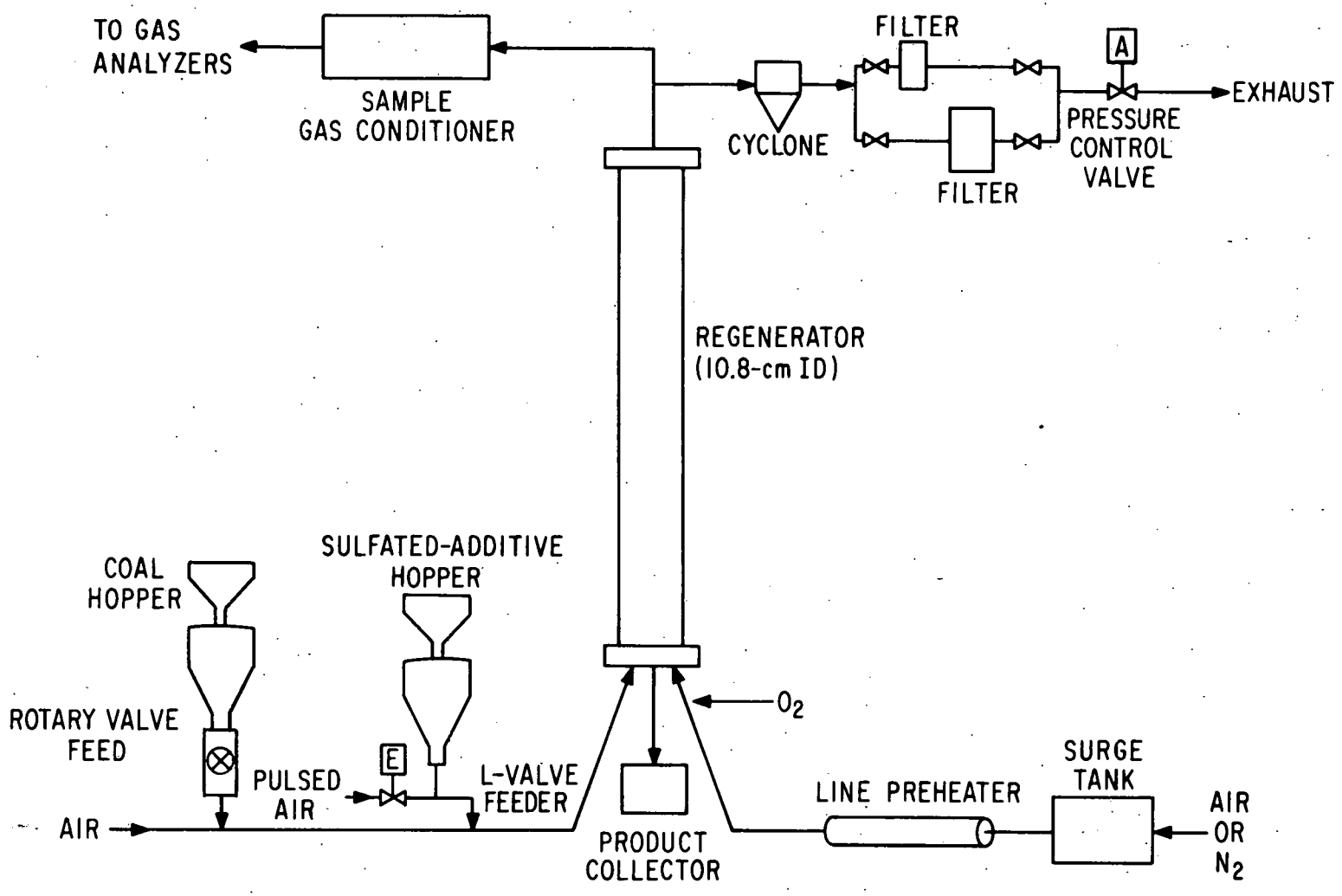

Fig. 1. Schematic Diagram of New Regeneration System

The gases are added separately to permit better temperature control in the fluidized bed (if there should be a mild temperature excursion, combustion can be stopped without defluidizing the bed by shutting off the oxygen). Also, an oxygen concentration in the entering gas higher than that in air can be used, allowing more coal to be combusted without significantly changing the fluidization gas velocity. Larger amounts of heat are required to compensate for (1) the heat losses in the comparatively small experimental system and (2) the heat load imposed by feeding cold sulfated additive to the system.

Regeneration of Sulfated Greer Limestone

Sulfated Greer limestone from Pope, Evans and Robbins (Test 620) has been regenerated, with the reducing gas and required heat generated by combustion in the regenerator of Arkwright or Triangle coal.

In experiments LCS-1, Greer limestone was regenerated at the same experimental conditions as were used in CS-5, in which Tymochtee dolomite was regenerated.[3] The results for these experiments are given in Table 1. A SO_2 concentration of 2.2% in the wet effluent gas and a sulfur regeneration of 68% were obtained for LCS-1. These results are similar to the regeneration results obtained for sulfated Tymochtee dolomite (CS-5). The extent of regeneration was slightly better for sulfated limestone than for sulfated dolomite, as estimated by flue-gas analysis for SO_2 and H_2S. However, the extent of regeneration based on chemical analysis of the regenerated products from these experiments were almost identical. The steady-state concentrations of COS and CS_2 in the flue gas, obtained by mass spectrometric analysis, were 0.02% and $\leq$0.01%, respectively, in LCS-1.

Experiment LCS-2 with Greer limestone was performed at a higher bed temperature of 1100°C. The experimental conditions are shown in Fig. 2 and the results are given in Table 1. The feed rate in this experiment was 5.4 kg/hr, in comparison to 4.9 kg/hr in LCS-1. The SO_2 concentration in the wet flue gas was 2.8% in LCS-2, and the sulfur regeneration based on flue gas analysis was 75%. In comparison with LCS-1 (performed at 1040°C), the extent of regeneration and the SO_2 content of the effluent gas were improved by increasing the temperature in LCS-2. The concentrations of COS and CS_2 in the flue gas for LCS-2 were 0.02% and 0.01%, respectively.

An additional experiment was performed with sulfated Greer limestone. Instead of partially combusting Arkwright coal as in previous experiments, Triangle coal (a bituminous coal with a higher ash fusion temperature than Arkwright coal) was used. This regeneration experiment (LCS-3) was performed with a higher additive feed rate (8.6 kg/hr) than in earlier experiments at a bed temperature of 1060°C, a fluidizing-gas velocity of 1.0 m/sec, and a reducing gas concentration of 1.6% in the effluent gas. The operating temperature and the concentrations of components in the effluent gas are given in Fig. 3; the experimental results are given in Table 1. From the average SO_2 concnetration of 3.6% in the wet

Table 1. Experimental Conditions and Results for Regeneration Experiments with Combustion of Arkwright and Triangle Coal in a Fluidized Bed.

Nominal Particle Residence Time: 15-30 min
Nominal Fluidized-Bed Height: 46 cm
Reactor ID: 10.8 cm
Coal: Arkwright Coal (2.82 wt % S). Ash fusion temp. under red. conditions, 1105°C.
Triangle Coal (0.98 wt % S). Ash fusion temp. under red. conditions, 1390°C (initial deformation)
Additive: (a) Sulfated Tymochtee dolomite (11.1 wt % S) -14 +50 mesh (CS-5)
(b) Sulfated Greer limestone (9.48 wt % S) -10 +50 mesh (LCS-1, -2, -3).

Exp. No.	Pressure (kPa)	Bed Temperature (°C)	Feed O_2 Conc. (%)	Fluidizing Gas Velocity (m/sec)	Feed Rate (kg/hr)	Reducing Gas Concentration in Effluent (%)	Measured SO_2/H_2S in Wet Effluent Gas (%)/(ppm)	Sulfur Regeneration (%)[a]/(%)[b]
CS-5[c]	184	1040	22.5	0.93	5.0	~2	2.4/435	64/89
LCS-1	184	1040	18.9	0.91	4.9	1.3	2.2/96	68/88
LCS-2	153	1100	18.6	1.1	5.4	1.3	2.8/235	75/94
LCS-3[d]	153	1060	23.6	1.0	8.6	1.6	3.6/76	63/84

[a]Based on flue gas analysis.

[b]Based on chemical analysis of dolomite and limestone samples.

[c]Results previously reported in Ref. 3.

[d]Triangle coal was used; in other experiments, Arkwright coal was used.

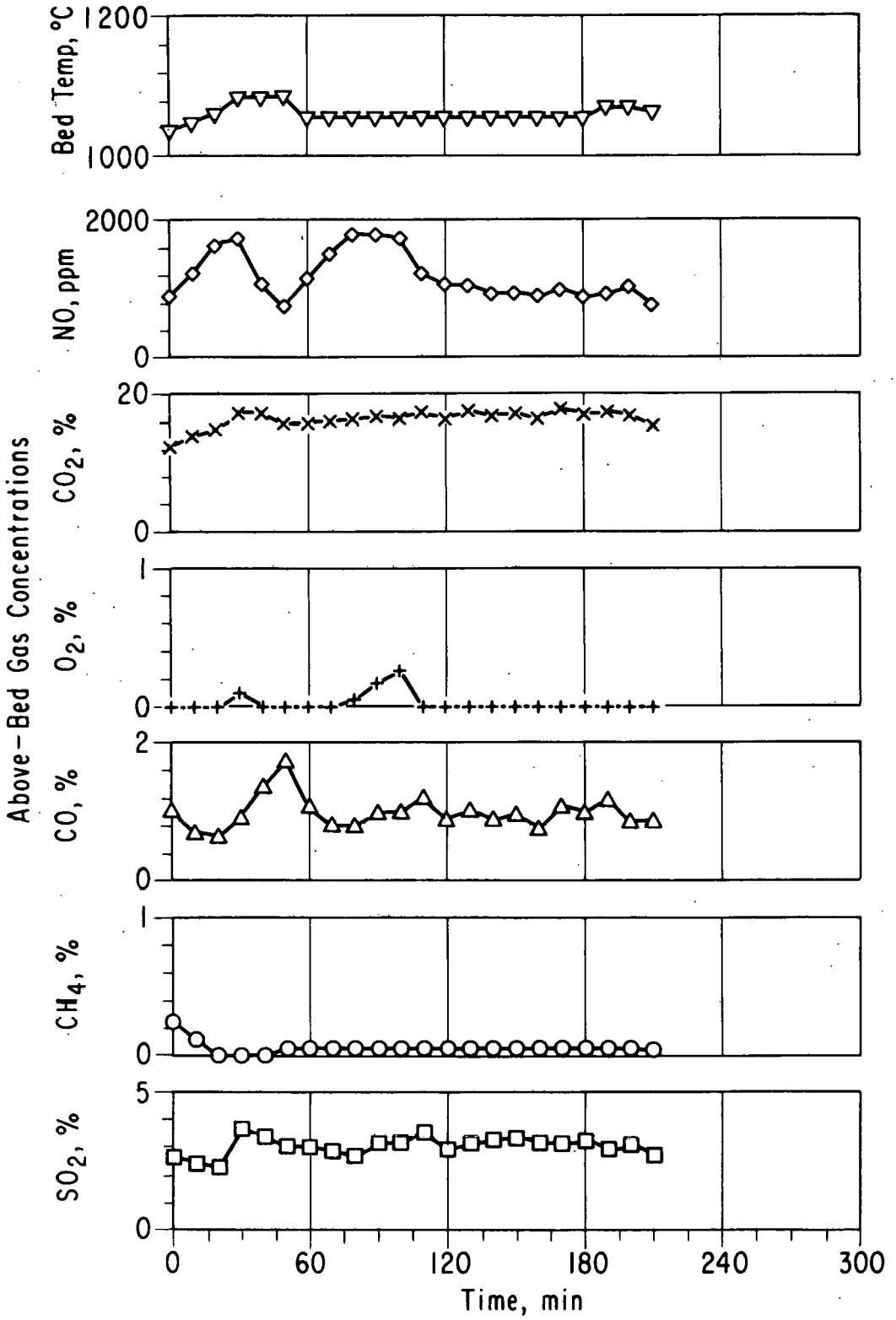

Fig. 2. Bed Temperature and Gas Concentrations in Off-Gas, Experiment LCS-2.

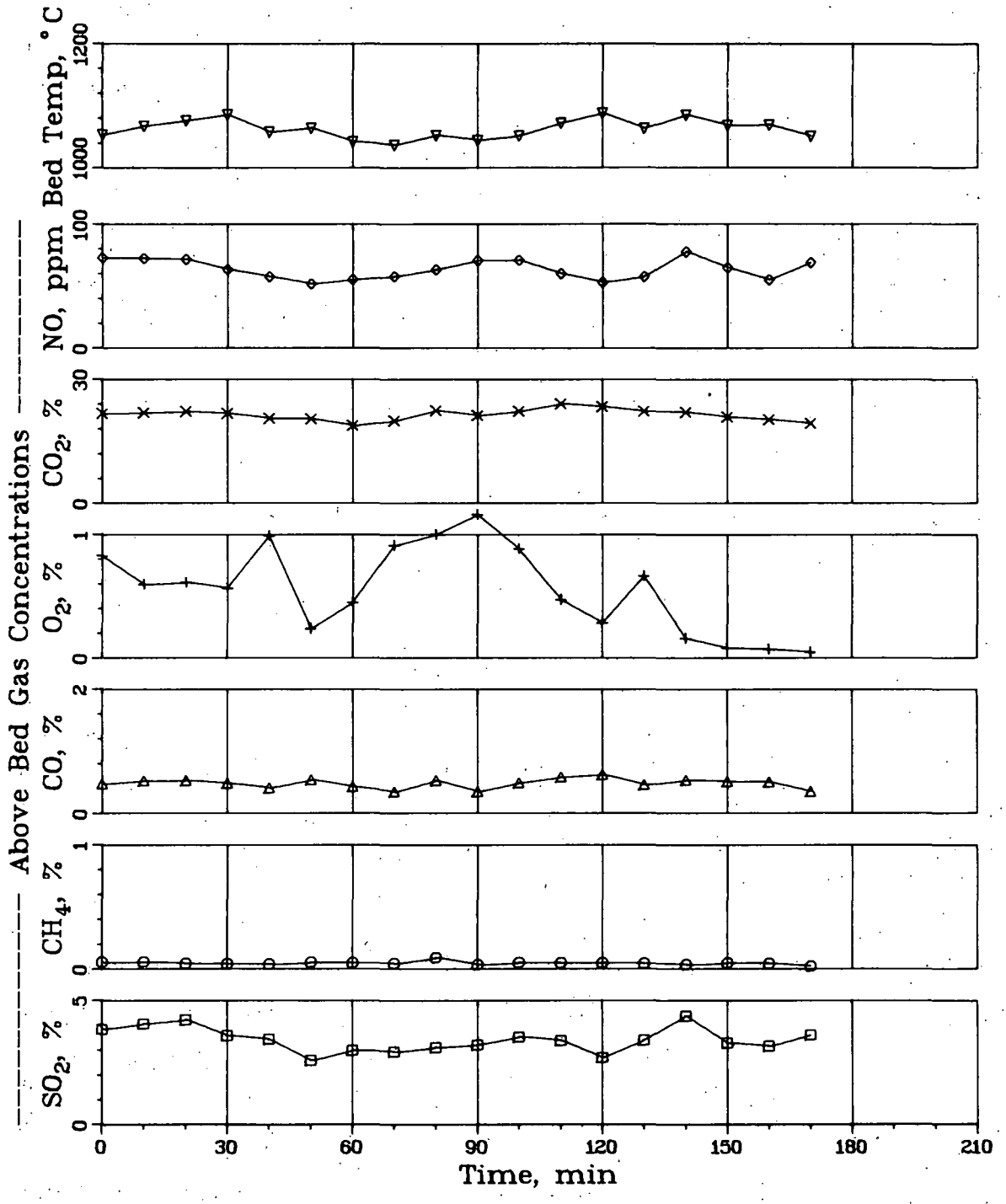

Fig. 3. Bed Temperature and Gas Concentrations in Off-Gas, Experiment LCS-3.

effluent gas, a sulfur (or CaO) regeneration of 63% was calculated. A larger sulfated additive feed rate (*i.e.*, reduced solids residence time) in this experiment increased the SO_2 concentration in the effluent gas without greatly decreasing the extent of regeneration. Because the reaction rates are relatively high, sulfated additive feed rates will be increased in future experiments to investigate the feasibility of obtaining high SO_2 concentrations in the effluent gas streams.

From the chemical analyses of the regenerated samples, the extents of regeneration can be calculated. These results, given in Table 1, are 19 to 25% higher than those calculated from the SO_2 concentrations in the effluent gas. The consistent discrepancy suggests the possibility that sulfur is being released in forms other than SO_2, H_2S, CS_2, and COS (concentrations of these compounds have all been measured in some of these experiments). The extent of elemental sulfur formation is being investigated as a possible explanation of these differences.

Effect of Relative Lengths of Oxidizing and Reducing Zones during Regeneration of Greer Limestone

When fuel (coal) is combusted under reducing conditions in the fluidized bed, both an oxidizing zone and a reducing zone are present. An oxidizing zone is established at the bottom of the fluidized bed (mainly below the coal injection point) where combustion air enters; a reducing zone is established in the upper, fuel-rich portion of the fluidized bed. Calcium sulfide is formed in the reducing zone by the following typical reaction:

$$CaSO_4 + 4CO \rightarrow CaS + 4CO_2$$

and its formation is favored by higher reducing gas concentrations. The presence of large amounts of CaS is detrimental to the regeneration of $CaSO_4$ to CaO since CaO does not form directly from CaS under the conditions used. However, since the additive is continually circulated in the bed, the CaS can be re-oxidized in the oxidizing zone of the bed by the reaction:

$$CaS + 2O_2 \rightarrow CaSO_4$$

An effective oxidizing zone is very important for preventing the buildup of CaS.

To test the effect of the relative lengths of the oxidizing and reducing zones on the steady-state level of CaS in the bed, two experiments have been performed with a reducing gas concentration of ∿4% in the effluent gas (approximately twice as high a concentration as in other regeneration experiments with coal). The results for these two experiments in which sulfated Greer limestone was fed to the regenerator are given in Table 2.

In the first experiment, LCS-4D, regeneration (conversion of $CaSO_4$ to CaO) was very poor, 41%, and sulfide ($S^=$) concentration was high, 4.9%.

Table 2. Experimental Conditions and Results for Regeneration Experiments Designed to Test the Effectiveness of the Two-Zone Reactor in Minimizing CaS Buildup.

Nominal Particle Residence Time: 15-30 min
Nominal Fluidized-Bed Height: 46 cm
Reactor ID: 10.8 cm
Temperature, °C : 1060
Pressure, kPa : 153
Coal: Triangle Coal (0.98 wt % S). Ash fusion temp. under red. conditions: 1390°C (initial deformation)
Additive: Sulfated Greer limestone (9.48 wt % S) -10 +30 mesh

Exp. No.	Fluidizing Gas Velocity (m/sec)	Feed Rate (kg/hr)	Reducing Gas Concentration in Effluent (%)	Total Sulfur/Sulfide in Regenerated Additive (%)/(%)	Measured SO_2/H_2S in Wet Effluent Gas (%)/(ppm)	Sulfur Regeneration (%)[a]/(%)[b]
LCS-4D	0.97	5.3	3.8	7.5/4.9	0.55/625	10/41
LCS-7	0.95	5.9	4.1	2.3/1.1	1.5/1900	56/71

[a]Based on flue gas analysis.

[b]Based on chemical analysis of limestone samples before and after regeneration.

The intermittent flue gas analysis for this experiment is given in Fig. 4. The ratio of the nominal heights of the reducing zone and the oxidizing zone was 5, and the total fluidized-bed height was 46 cm (illustrated in Fig. 5).

In experiment LCS-7, the coal injection line was ∿13 cm longer than that formerly used, decreasing the ratio of the heights of the reducing and oxidizing zones from 5 in LCS-4D to ∿1.3 in LCS-7 and subsequent experiments.

Since ∿40% of the total fluidizing gas is used to inject the coal and additive into the fluidized bed, a fluidizing-gas velocity discontinuity existed between the portion of the fluidized bed below and above the injection line. To compensate for this discontinuity, a 20-cm-long ceramic insert with an ID of 8.9 cm (3.5 in.) was installed above the gas distributor, as illustrated in Fig. 5.

The experimental conditions and the results for LCS-7 are given in Table 2. The intermittent flue gas analyses are given in Fig. 6. Solids regeneration was 71%, and the regenerated additive contained 1.1% sulfide. By increasing the length of the oxidizing zone relative to the size of the reducing zone, the buildup of CaS was reduced and greater regeneration was obtained.

Fusion of Sulfated Additive and Coal Ash

In current bench-scale regeneration efforts, CaO is regenerated from sulfated additive by reductive decomposition. Coal is combusted in the regenerator to generate the necessary heat and reducing gases. To investigate the possibility that constituents of sulfated additives combine with coal ash during regeneration and form mixtures that have lower melting points of either the additive or the ash, preliminary tests have been performed. The composition of additive agglomerated in regeneration experiments was reported earlier.[3] Fusion temperatures of coal ash and mixtures were measured by Commercial Testing & Engineering Co. by the standard method (ASTM D-1857-74) used for measuring ash fusion temperatures.

Arkwright coal No. 2, a bituminous coal, was ashed and its ash fusion temperature under oxidizing and reducing conditions was determined. The results for reducing conditions are given in Table 3 along with those for Sewickley and Triangle coal ashes. Since the fusion temperature under reducing conditions of Arkwright coal (which has been used in bench-scale regeneration experiments) is very close to the regeneration temperatures used, it has been decided to use Triangle coal in subsequent experiments.

The fusion temperatures (ASTM D-1857-74) were determined for Arkwright coal ash, sulfated Tymochtee dolomite (10.2 wt % S), and mixtures of these containing 10-90% ash. The initial deformation temperatures and the fluid temperatures of the mixtures under reducing conditions are given in Fig. 7 as a function of ash content. As the ash content increased, the fusion temperature generally decreased. However, near 70% ash content,

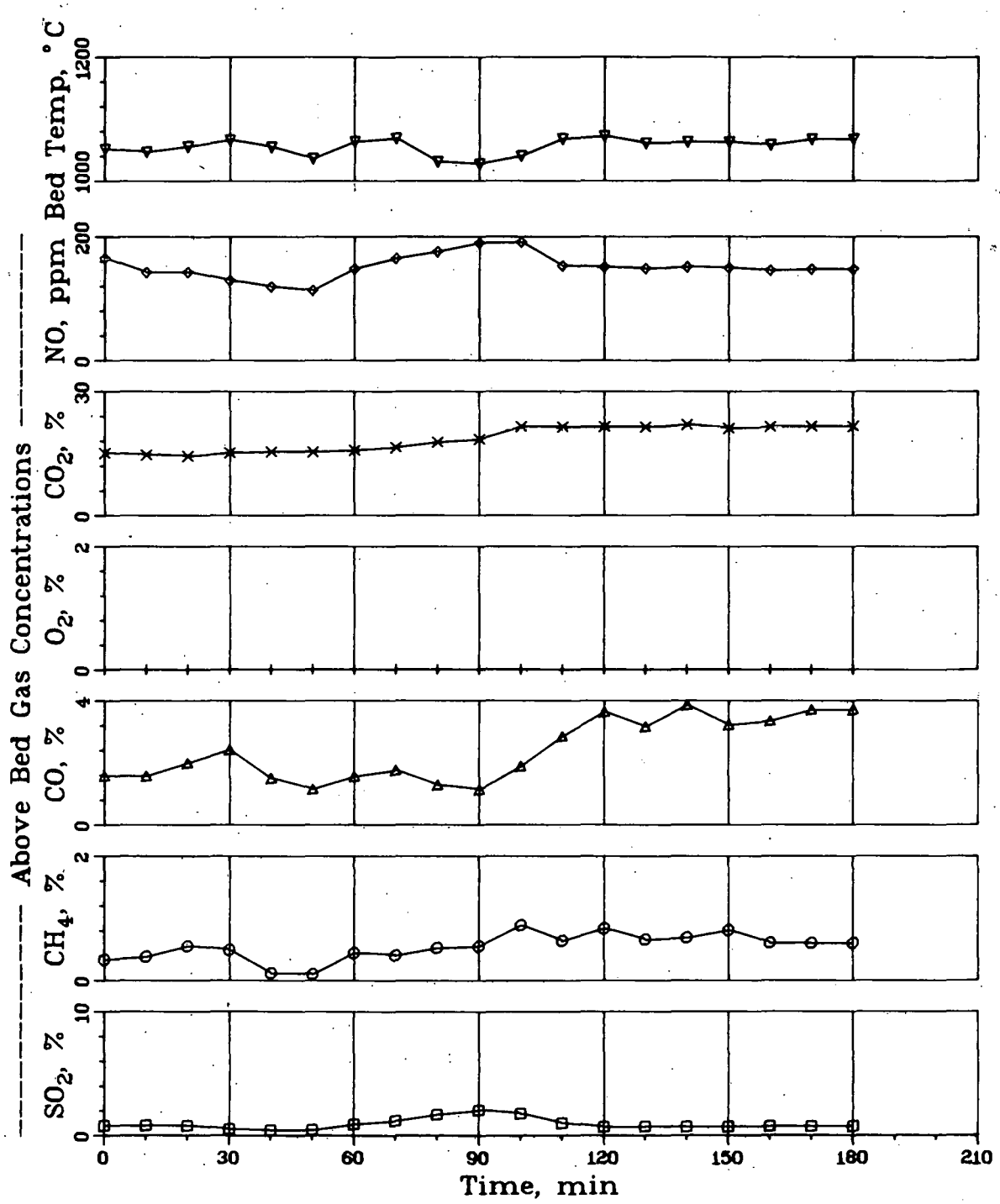

Fig. 4. Bed Temperature and Gas Concentrations in Off-Gas, Experiment LCS-4D.

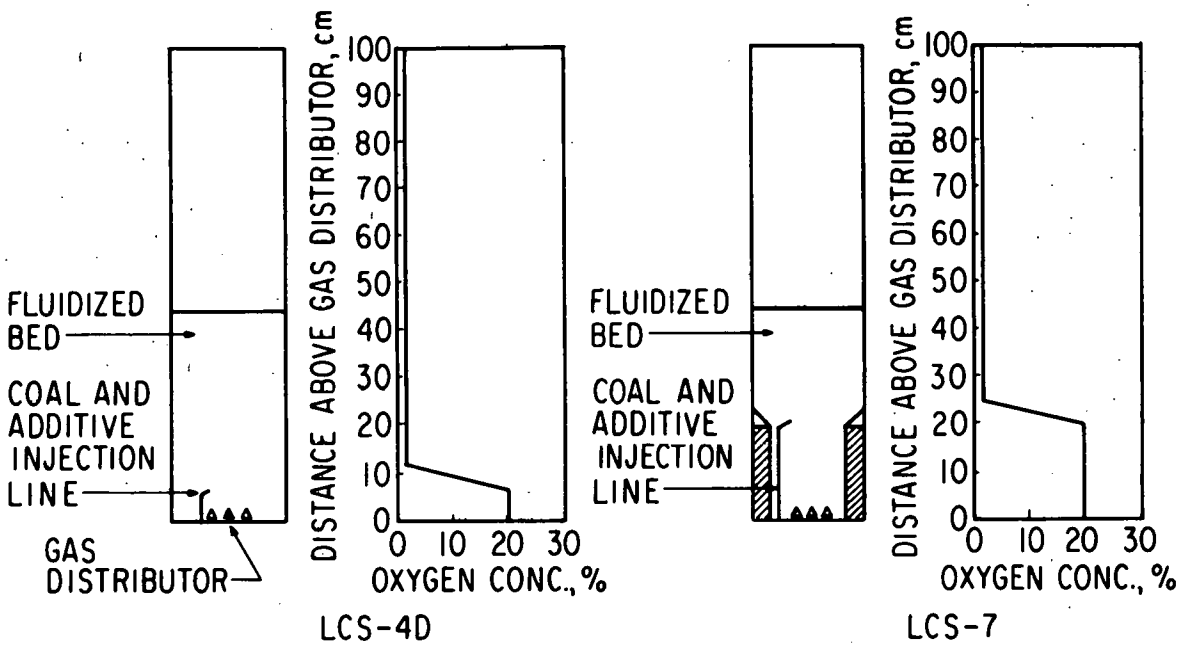

Fig. 5. Geometry of Oxidizing and Reducing Zones in Relation to Position of Coal Injection Line.

Table 3. Fusion Temperatures, Under Reducing Conditions, of Ash from Arkwright Coal No. 2, Sewickley Coal, and Triangle Coal.

	Arkwright (°C)	Sewickley (°C)	Triangle (°C)
Initial Deformation	1104	1100	1383
Softening (H = W)	1177	1188	1444
Softening (H = 1/2 W)	1193	1215	1485
Fluid	1232	1288	1510

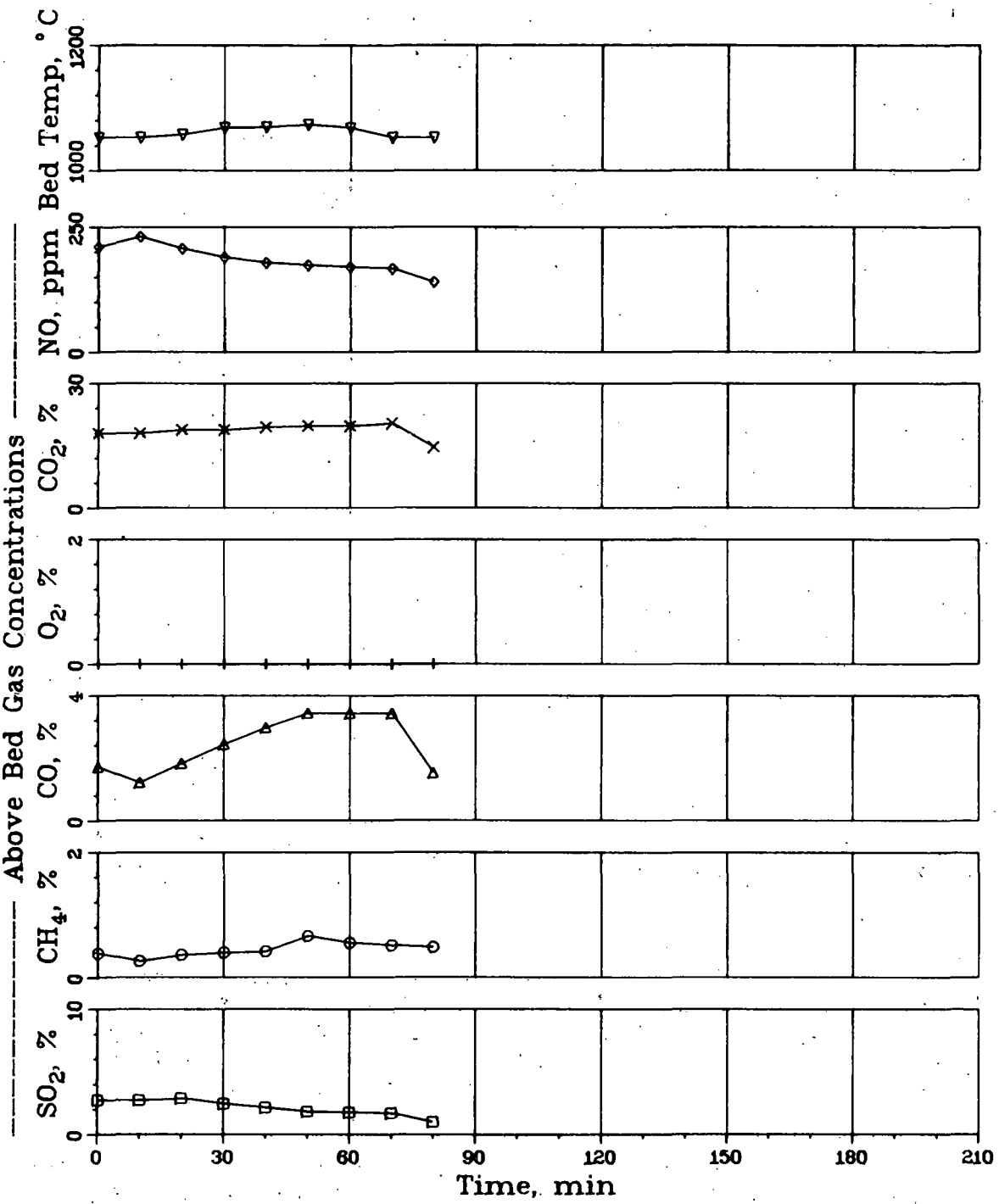

Fig. 6. Bed Temperature and Gas Concentrations in Off-Gas, Experiment LCS-7

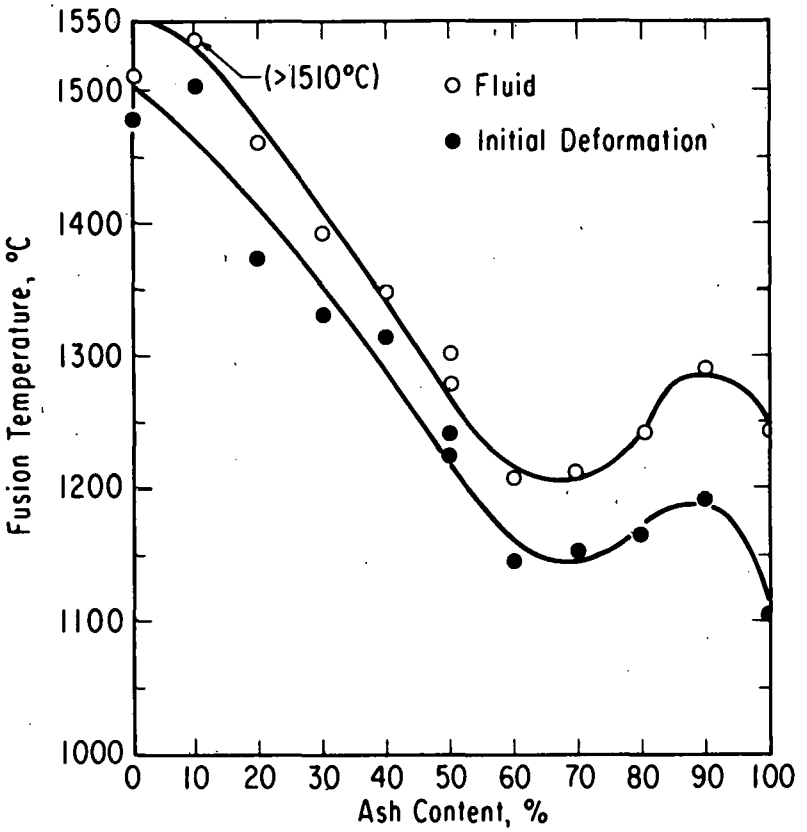

Fig. 7. Fusion Temperature in a Reducing Atmosphere of Mixtures of Arkwright Coal Ash and Sulfated Tymochtee Dolomite.

the fusion temperature seems to be at a minimum. This suggests the possibility that near the 70% ash content a eutectic formed from constitutents of the ash and the sulfated dolomite.

Mixtures were also made of Arkwright coal ash and sulfated Greer limestone furnished by Pope, Evans and Robbins (Test PER 620), and their fusion temperatures were determined. The initial deformation temperatures and the fluid temperatures of the mixtures under reducing conditions are given in Fig. 8 as a function of ash content. Again, the possibility that a eutectic forms near the 70% ash content is suggested by the results.

Fused samples of mixtures of ∿50% ash and sulfated Tymochtee dolomite were analyzed by X-ray diffraction, and spinel type compounds were found to have formed. Fused samples of ∿70% coal ash and sulfated Greer limestone were found to contain calcium-aluminum-silicate compounds. These ash-additive fusion tests were preliminary experiments. To understand

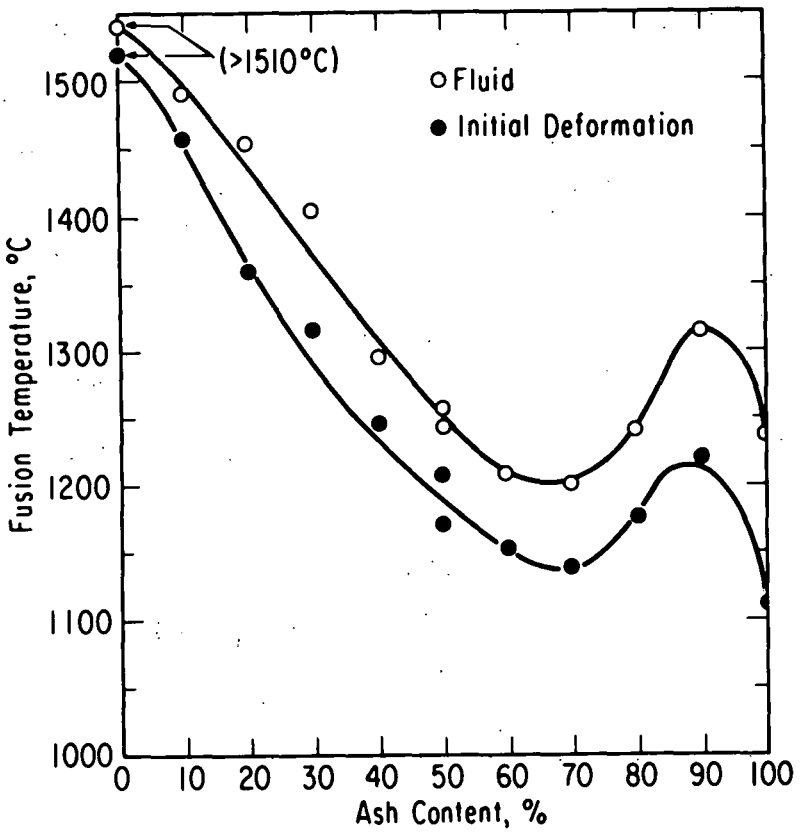

Fig. 8. Fusion Temperatures in a Reducing Atmosphere of Mixtures of Arkwright Coal Ash and Sulfated Greer Limestone (from Test PER 620).

the agglomeration mechanism of additive and coal ash during regeneration, additional fusion temperature data is being obtained with a differential thermal analyzer.

Partial agglomeration of sulfated additive (specifically, sulfated Greer limestone from Pope, Evans and Robbins) has been found to occur, even during mild temperature upsets near 1100°C. Observations of agglomerated interior surfaces with an optical microscope revealed ash cenospheres, which appeared as tiny glass-like beads. These beads are formed as tiny bubbles as gases evolve from the ash. X-ray diffraction analysis showed them to be amorphous.

The agglomerating tendency of molten ash (the Godel phenomenon) is utilized as a means of removing the ash from a fluidized bed of bituminous coke in Ignifluid gasification boilers,[4] which are operated at high fluidizing-gas velocities (10-15 m/sec) and at temperatures of 1200-1400°C.

A suggested mechanism for one type of agglomeration (in the presence of coal ash) is as follows: At temperatures where these spheres and/or the ash are molten, the spheres could serve as coalescing agents between adjacent additive particles in the regenerator. Although is has been reported that molten ash has a high surface tension,[5] its interfacial tension with sulfated additive at high temperature might be low enough so that it could wet the additive, causing the additive particles to become sticky and to agglomerate. This could occur at temperatures above the ash fusion point and below the fusion point of the additive. Other types of agglomeration (initiated by the fusion of the sulfated additive or the formation of eutectics) are also possible.

In recent experiments, agglomeration of additive and coal ash has occurred, even during mild temperature fluctuations which were due to upsets in the regenerating environment at ∿1100°C. Molten ash is believed to be responsible for the initiation of some agglomeration at these temperatures, and analyses of sulfated additive have been performed in an attempt to study this postulated mechanism.

The ash content of one of the sulfated additives regenerated was calculated. From a chemical analysis of once-sulfated Greer limestone (-8 mesh) provided by Pope, Evans and Robbins (Test 620), its composition was calculated and compared (Table 4) with the composition of unreacted Greer limestone.[6]

Table 4. Composition of Greer Limestone and Sewickley Coal Ash (used by Pope, Evans and Robbins).

	Unsulfated Limestone (wt %)	Sulfated Limestone (wt %)	Coal Ash (wt %)
CaO	44.80	36.3	5.0
$CaSO_4$	--	30.4	--
MgO	1.90	1.94	1.0
Fe_2O_3	0.80	2.53	20.3
SiO_2	10.50	16.63	49.8
Al_2O_3	3.60	5.75	19.5
S	0.17	7.16[a]	--
Others	0.71	--	4.4
CO_2 Loss	37.52	3.54	--
Total	100	104	100

[a] Also included in $CaSO_4$ value.

The concentrations of SiO_2, Al_2O_3, and Fe_2O_3 increased markedly during sulfation. These compounds are the major constituents of the ash of Sewickley coal (Table 4) used in Test 620. The fusion temperature of the ash from this coal under reducing conditions is ∿1100°C (initial deformation).

To estimate the amount of ash in the sulfated limestone, calcium was used as an element basis (ash contains only small amounts of calcium). Increases in silicon, iron, and aluminum were calculated from the analysis and are given in Table 5, together with the corresponding calculated ash contents of the sulfated limestone. Since SiO_2 is the most abundant ash constituent, constituting 50% of the ash, its chemical analysis is expected to give the most reliable result. The ash content of the sulfated limestone based on the silicon analyses was 10%, which is in good agreement with the remaining calculated ash contents. This buildup of ash constituents in addition to their high concentrations in the unsulfated limestone may have been responsibile for agglomerates forming during relatively mild temperature upsets (some below 1100°C).

The effect of the presence of these ash constituents on the fusion temperature of the limestone is being investigated with a differential thermal analyzer and by X-ray diffraction analysis.

Effect of Regeneration Temperature on Sulfation and Regeneration of Tymochtee Dolomite

The results of five FAC-series experiments reported earlier[1] are plotted in Fig. 9 as a function of regeneration temperature, the main variable in these experiments. (In the 1095°C experiment, a solids residence time of ∿18 min instead of ∿30 min was used.) As expected, higher temperatures were found to enhance the extent of regeneration of

Table 5. Ash Buildup in Sulfated Greer Limestone.
Mass basis: 100 g unsulfated limestone

	Unsulfated Limestone (mol)	Sulfated Limestone (mol)	Increase (mol)	Equivalent Ash Content (%)
Ca	0.8	0.800	0	0[a]
Fe	0.010	0.029	0.019	8.1
Si	0.175	0.254	0.079	10.4
Al	0.071	0.103	0.032	9.1

[a] It was assumed that the ash contributed no calcium (this ash contains only 3.6 wt % calcium).

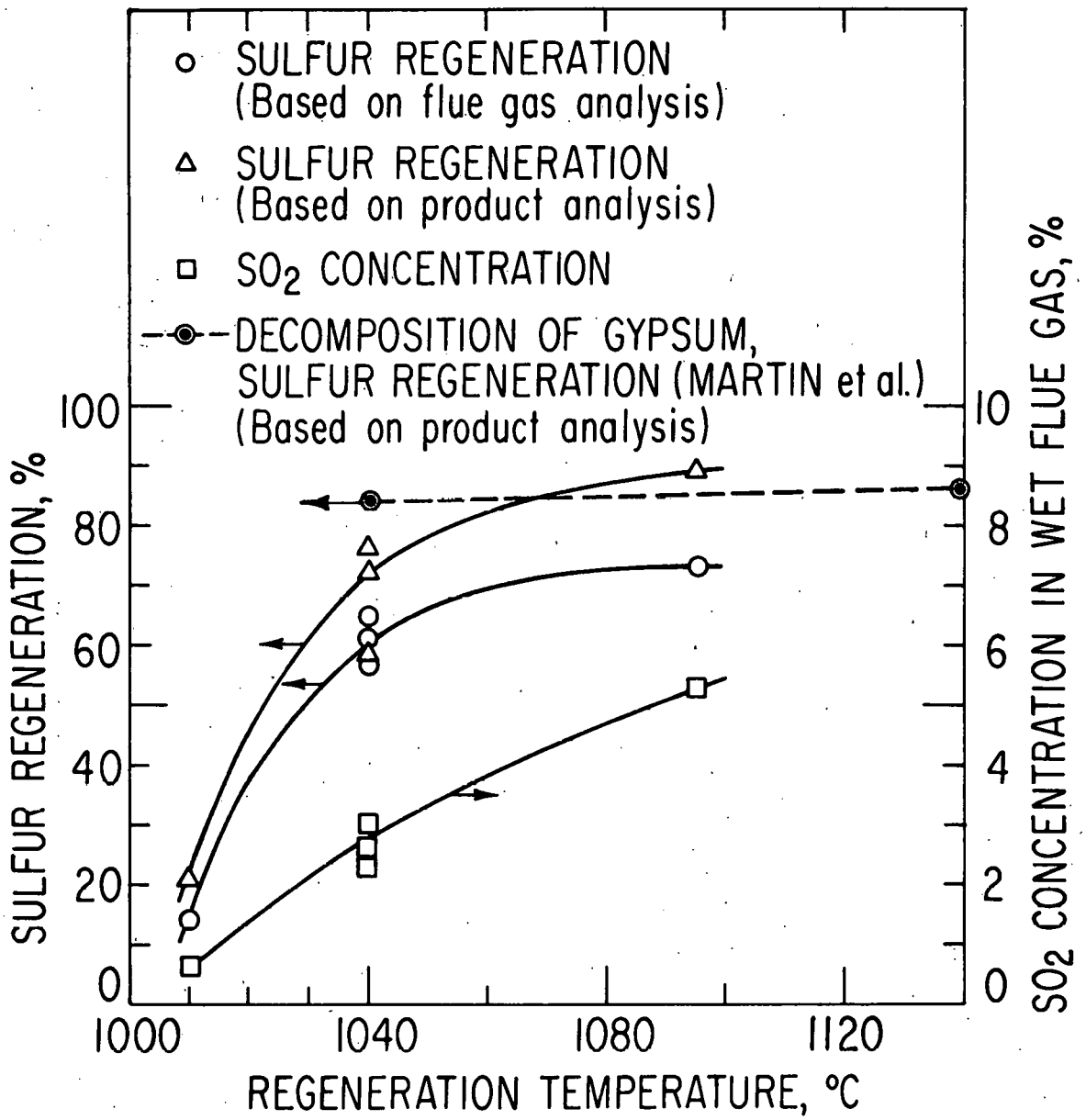

Fig. 9. Effect of Temperature on Sulfur Regeneration for Sulfated Tymochtee Dolomite.

CaO and/or sulfur from sulfated dolomite. As the temperature increased from 1010°C to 1095°C and the solids residence time remained constant or decreased, sulfur regeneration (based on analysis of the regenerated product) increased from 21% to 89%.

In these five experiments, the SO_2 concentration in the wet flue gas increased from 0.7% to 5.4% with increasing bed temperature (similarly increasing from 0.8% to 7.3% in the dry flue gas with increasing bed temperature).

The temperature dependence of the regeneration of sulfated Tymochtee dolomite in these experiments with a solids residence time of ∿30 min can be compared in Fig. 9 with similar results obtained by Martin *et al.*[7] for the decomposition of gypsum in a 10-in.-dia fluidized bed with a solids residence time of ∿90 min. In the latter investigation, carbon was used as the reductant and the extent of regeneration was based on chemical analysis of the gypsum before and after decomposition.

To evaluate the effect of regeneration temperature on the quality of the regenerated dolomite as a SO_2-acceptor, porosity measurements of several samples (-25 +35 mesh particles) have been made (Fig. 10). Porosity was measured as the extent of penetration of mercury as a function of pressure. The cumulative pore volume (Hg penetration) per given mass is plotted as a function of pore diameter. The pore distribution of fully calcined virgin dolomite was used for comparison because dolomite is fully calcined during regeneration.

Curve A represents the pore structure of fully calcined virgin dolomite. [This sample was calcined by placing dolomite in a preheated furnace (900°C) for 2 hr with a 20% CO_2 and 80% air environment.] The cumulative pore volume for pores $\geq$0.4 μm was found to be 0.1 cm^3/0.5g. Since pores smaller than ∿0.4 μm are relatively small and easy to plug, they contribute little to the extent of sulfation. This was reported by Hartman.[8]

Curve B represents the pore structure of dolomite which was sulfated (10.2 wt % S) during coal combustion experiments at 900°C. The cumulative pore volume for pores $\geq$0.4 μm was found to be 0.045 cm^3/0.5g. This was the feed dolomite for the FAC-regeneration experiments. In contrast to the curve A pore volume distribution, the pores of the sulfated material are very much plugged by sulfation. Most sulfation takes place in the larger pores ($\geq$0.4 μm).[8] These larger pores shrink during sulfation of CaO by the changes in occupied molecular volume.

Curves C and D illustrate the pore structures of dolomite regenerated at 1040°C and 1095°C. At the higher regeneration temperature, a greater volume of the large pores (>0.4 μm) is formed. On the basis of this result, it was believed that the reactivity of the dolomite regenerated at the higher temperature would be greater.

Sulfation experiments were performed with a TGA at 900°C with these regenerated samples and with calcined virgin dolomite samples, and the

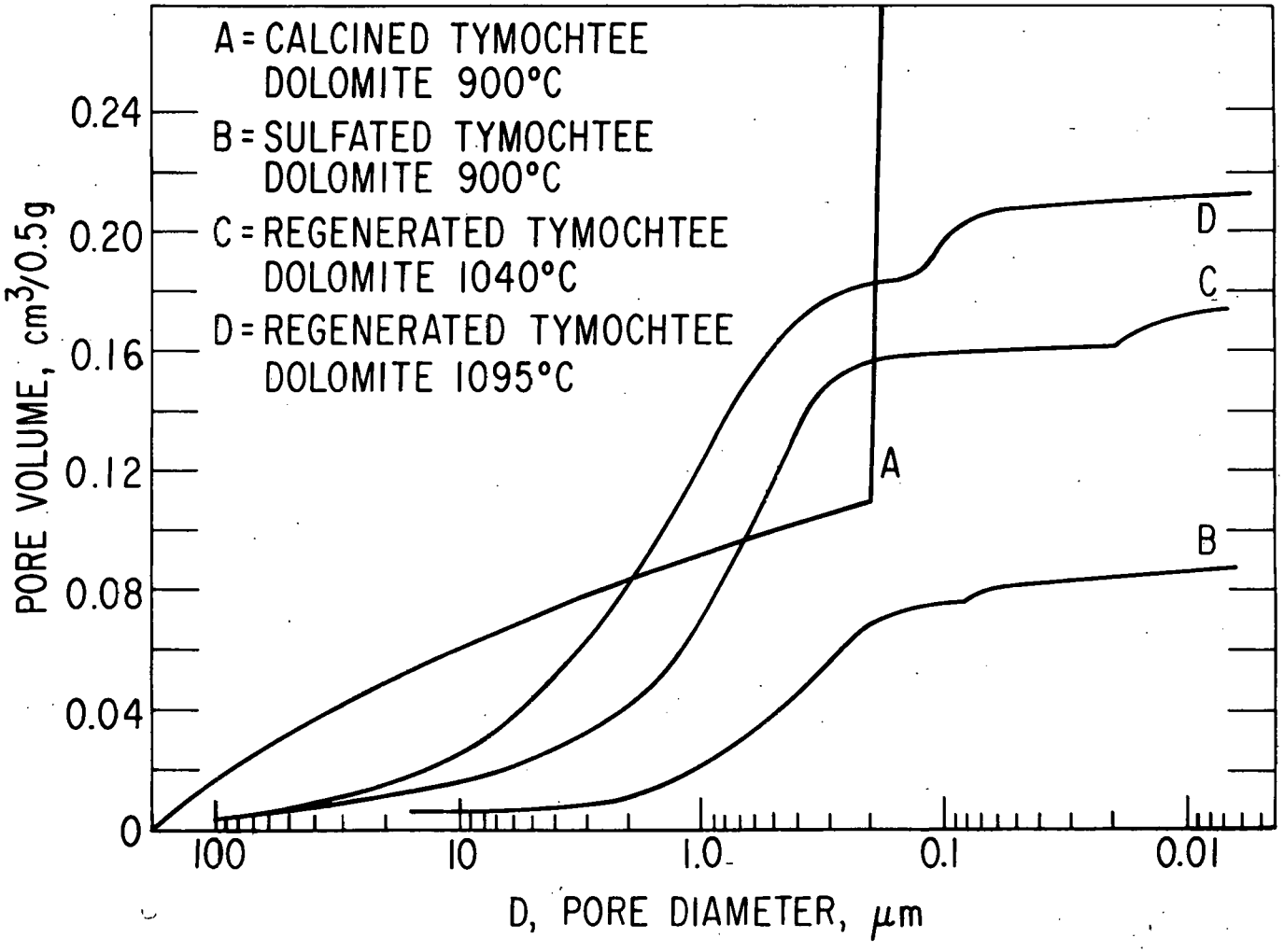

Fig. 10. Pore Distributions of Various Dolomite Samples.

results are given in Fig. 11. It was found that the higher regeneration temperature of 1095°C (instead of 1040°C) was not beneficial to the reactivity of the dolomite with SO_2. The 1095°C regenerated dolomite is less reactive than is the 1045°C regenerated dolomite and the precalcined dolomite, but is still fairly reactive. Its reactivity is about the same as the reactivity of (virgin) dolomite (calcined differentially) in other TGA sulfation experiments.

Although higher regeneration rates are obtained at higher regeneration temperatures, the effects of regeneration temperature on the reactivity of the additive in subsequent sulfation cycles must also be considered. A more extensive evaluation of the effect of cycling on sulfation reactivity of additive is planned.

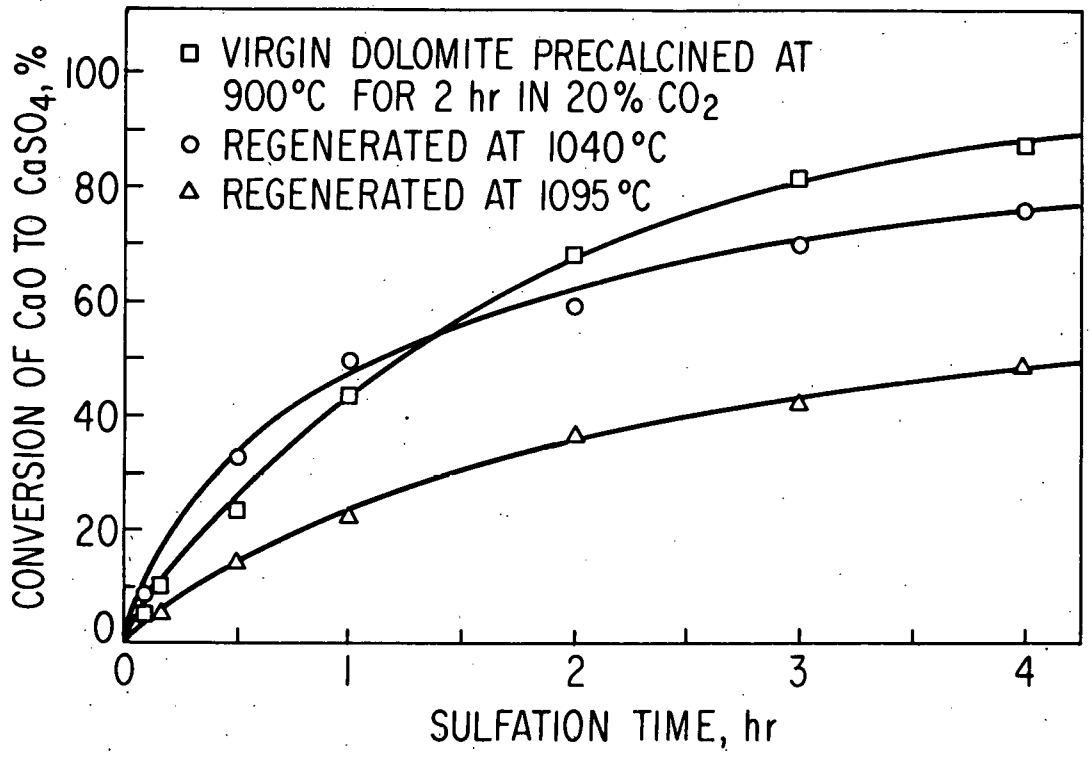

Fig. 11. Sulfation Reaction Data Obtained with a TGA at 900°C, 0.3% SO_2, and 5% O_2.

Electron Microprobe Analysis of Sulfated and Regenerated Particles

Regenerated Tymochtee dolomite particles from some of the FAC experiments, as well as nonregenerated sulfated Tymochtee dolomite particles, have been analyzed with an electron microprobe to determine the effect of regeneration on the sulfur concentration profiles. The FAC-regeneration experiments were performed by incomplete combustion of methane and were discussed in Ref. 3. The electron microprobe was used to analyze a number of particles in the sulfated Tymochtee dolomite feed and in each steady-state regeneration sample from FAC-1R2 and FAC-4. The radial distributions of calcium, magnesium, and sulfur in these particles were measured.

A random sample of particles from each sample was screened, and about twenty -20 +25 mesh (707-841 μm) particles were mounted in epoxy. The mounted samples were machined to remove the equivalent of one-half the diameter of a typical mounted particle (∿390 μm), and a thin gold layer (∿50 angstroms) was sputtered on the machined surface to enhance the conductivity of the mounts. About half the mounted particles were analyzed.

Standards were used to calibrate the probe to obtain a rough quantitative estimate of the local component concentrations. The materials used as calibration standards were apatite (38.9 wt % Ca), FeS_2 (53.4 wt % S), and MgO (60.3 wt % Mg).

Wet chemical analyses of aliquots of the samples analyzed with the electron microprobe indicated that the average sulfur and calcium contents of the sulfated Tymochtee dolomite were 10.2 wt % and 22.2 wt %, respectively. The component radial concentration distributions as obtained by the electron probe for calcium and sulfur for three typical sulfated particles are given in Fig. 12 (magnesium concentration profiles are not given because they are similar to those for calcium). Since these particles had not been in the continuously fed, fluidized-bed coal combustor for equal periods of time (solids are back-mixed), the extent of sulfation in these particles varied. The extent of sulfation was smallest for the particle at the top of Fig. 12 and the greatest for the bottom particle. As sulfation progressed, the edge of the sulfated shell moved towards the center of the particle. The local sulfur and calcium concentrations obtained by electron microprobe analysis were lower than the true local concentrations because the sample surfaces could not be machined as smoothly as were the calibration sample surfaces and the irregularities on the sample surfaces caused scattering of the characteristic X-rays emitted.

Chemical analyses indicated that regenerated particles from experiment FAC-1R2 (performed at 1040°C) contained 5.1 wt % S and 26.2 wt % Ca. The electron probe analyses of two sample particles from this experiment are given in Fig. 13. In the particle whose analysis is given at the top of Fig. 13, regeneration seems to be in the first stage, with the primary desulfurization reaction zone moving radially into the uniformly sulfated particle. Some residual sulfur (which is less available due to a limitation probably imposed by diffusion) is left behind the primary reaction zone. The bulk of the sulfur is removed in the first regeneration stage.

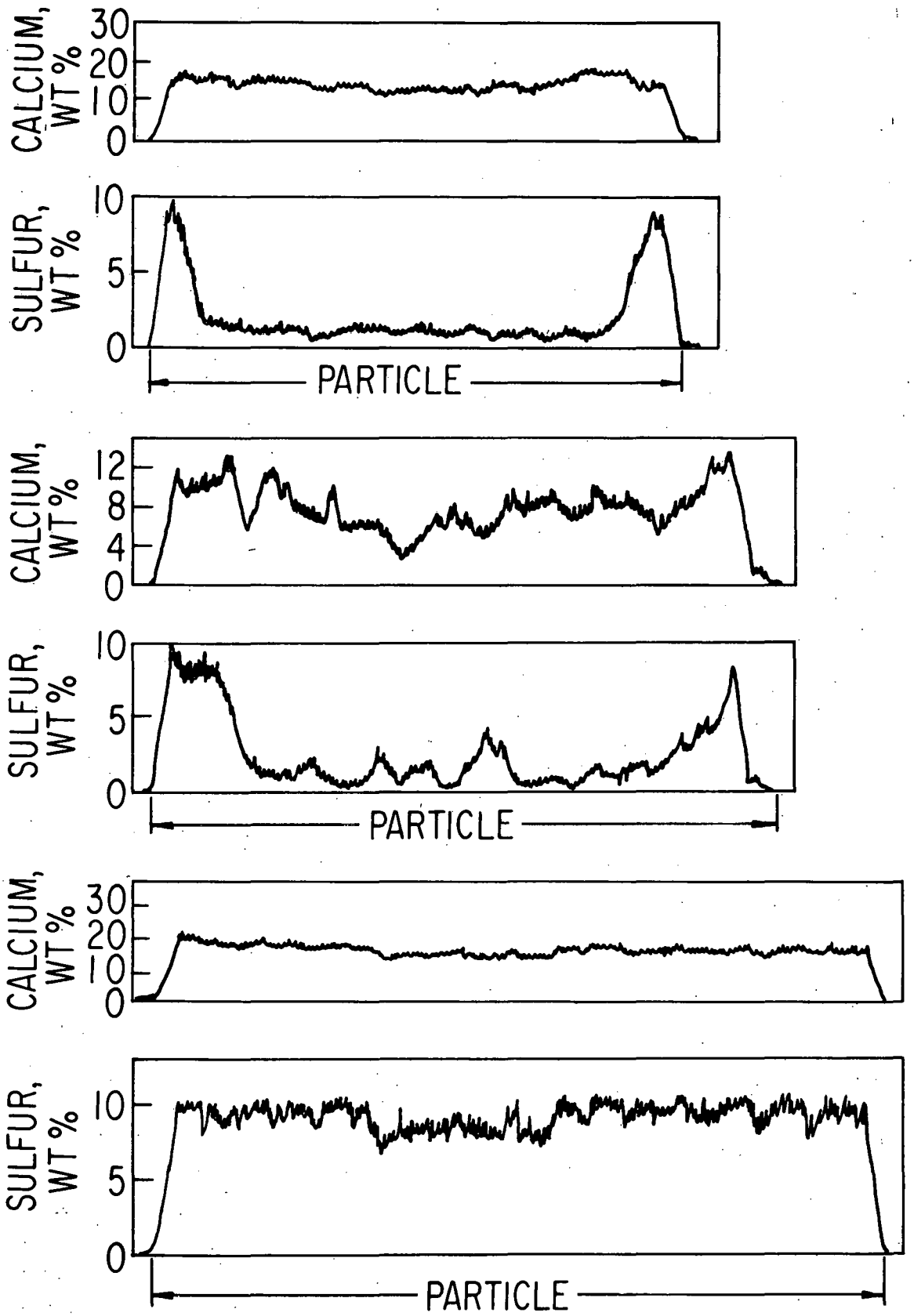

Fig. 12. Electron Microprobe Analysis of Three Sulfated Tymochtee Dolomite Particles.

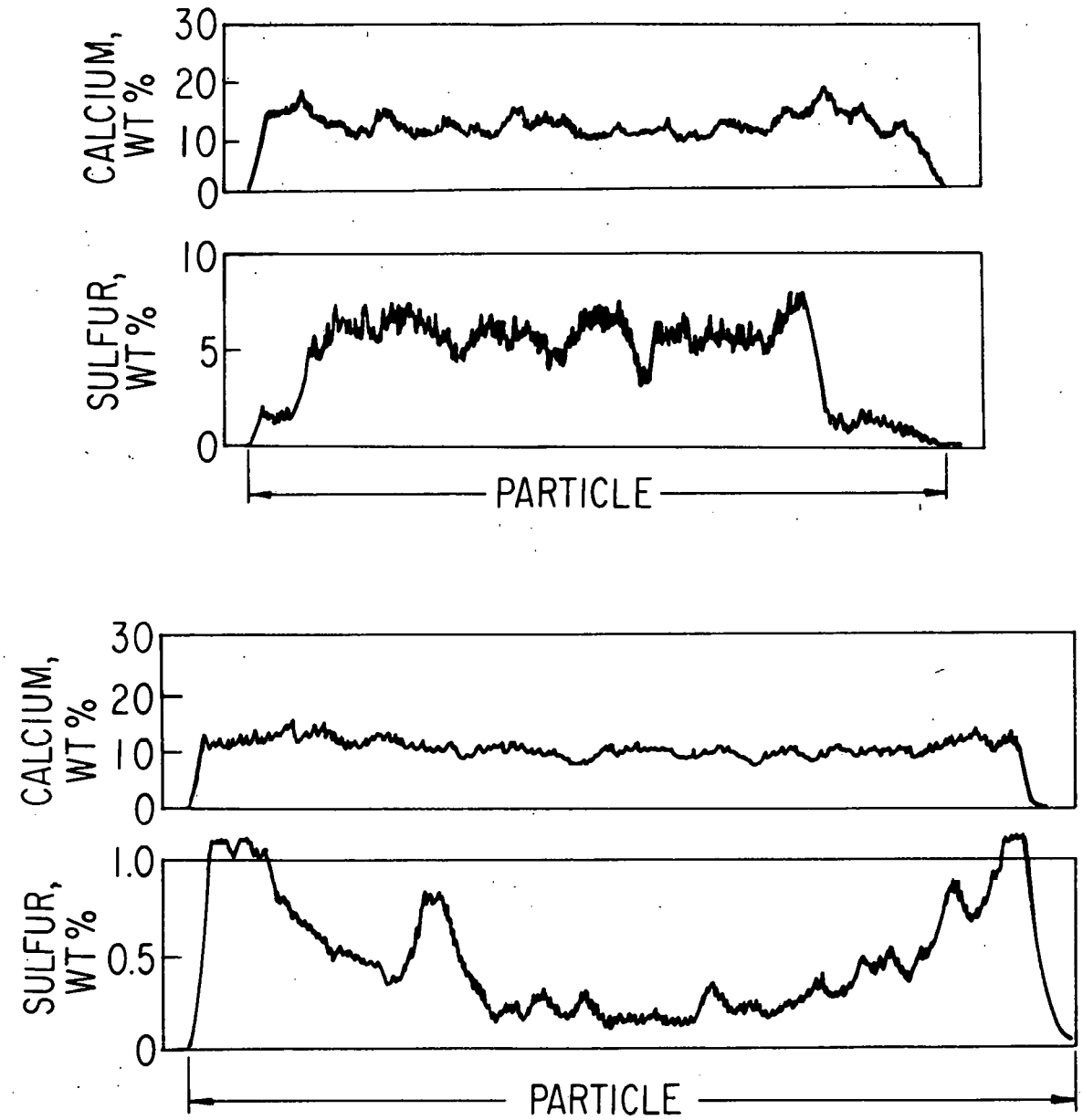

Fig. 13. Electron Microprobe Analysis for Two Regenerated Tymochtee Dolomite Particles from Experiment FAC-1R2.

Regeneration in the particle represented by the bottom electron probe analysis is in the second (slower) stage, and the residual concentration of sulfur in the entire particle is low. In an industrial process, the solids residence time would be low (high solids throughput), and probably only the first (rapid) stage of regeneration would occur. Hence, most but not all of the sulfur would be removed.

Regenerated particles from experiment FAC-4 (performed at 1095°C) also were analyzed with the electron microprobe. The calcium and sulfur concentrations for regenerated Tymochtee dolomite from this experiment were 30 wt % and 1.5 wt %, respectively. The electron probe analysis for calcium and sulfur in sample particles from this experiment is shown in Fig. 14.

The particle whose analysis is given at the top of Fig. 14 appears to be near the end of the first regeneration stage; the primary desulfurization reaction zone has almost reached the center of the particle. The other two particles are more nearly regenerated, and only the sulfur that is more slowly reacting (probably due to diffusion limitation) is left. Regeneration was more complete in particles from FAC-4 than in particles from FAC-1R2. Generally, the regenerated particles examined showed no sulfur concentration irregularities that might lead to poor utilization in subsequent sulfation cycles.

Correlation of Reaction Kinetic Data Associated with the Bench-Scale Regeneration of Sulfated Dolomite

Use of experimental data to establish a reaction kinetic model for the regeneration of sulfated dolomite can, at best, yield a first approximation. Difficulty exists because of the complex nature of the reducing environment within the fluidized bed in the course of the reaction. Several reducing constituents (methane, hydrogen, and carbon monoxide) are simultaneously involved in the reduction steps of this reaction, making a rigorous analysis of the reaction mechanics most difficult, particularly since the composition of the reducing environment at the zone of reaction is known only superficially.

To establish a quantitative assessment of some variables associated with the regeneration reactions, the involvement of these variables has been subjected to a screening analysis for the FAC-series regeneration experiments. This analysis, though empirical, considers the quantitative contribution of gaseous composition, not at the concentrations within the reaction zone, but at concentrations before introduction into the fluidized-bed reactor. The gas feed rates and compositions for the FAC-series are given in Table 6.

Reaction rates for the disappearance of sulfur dioxide from sulfated dolomite have been based on one pound of SO_2-free solid. Since the additive, fed at rates of 6 and 10 lb/hr, constitutes the only sulfur input in these studies, the corresponding feed rates of SO_2-free solids of 4.78 and 7.96 lb/hr have been utilized to establish the average rates of regeneration.

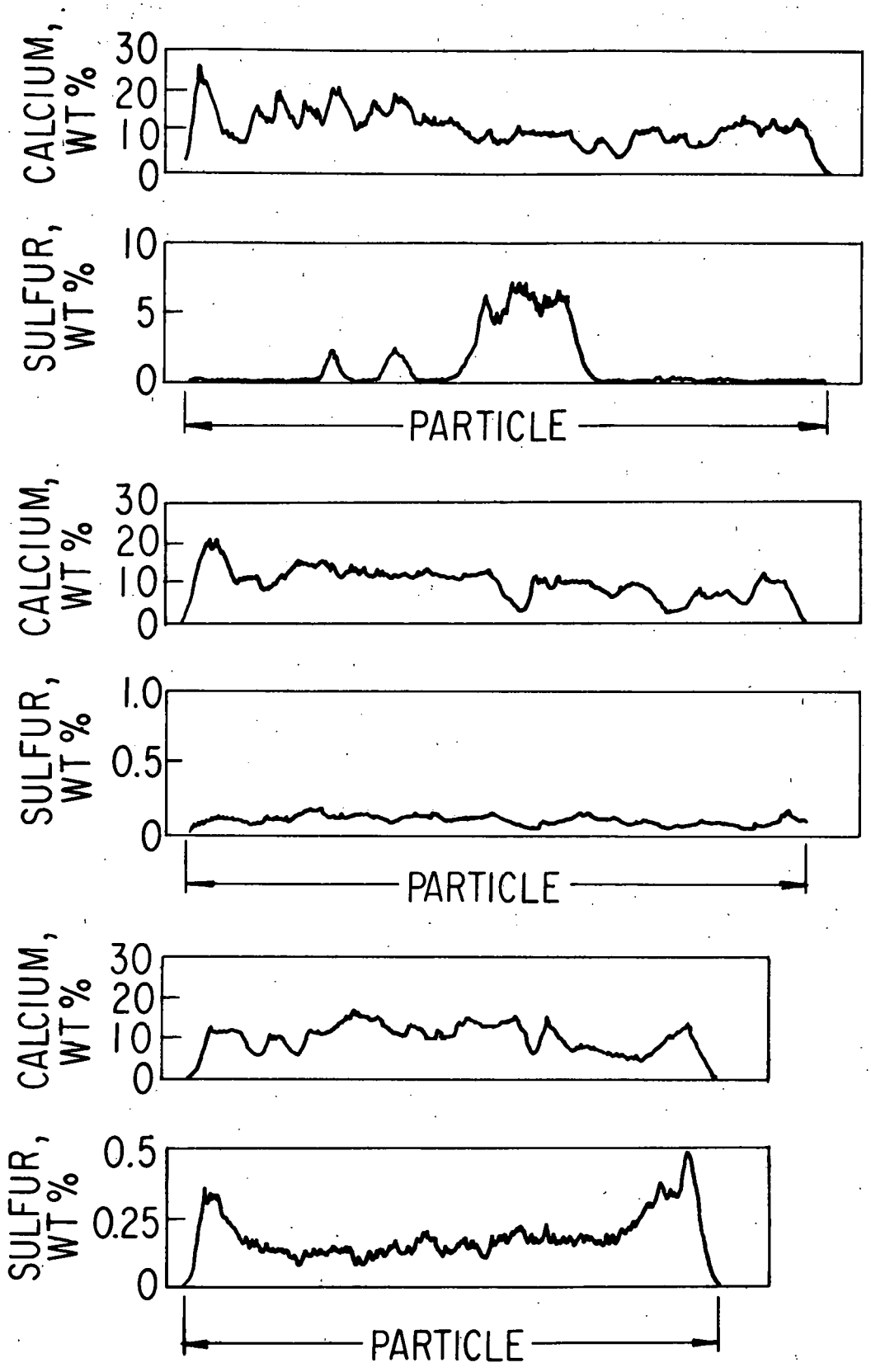

Fig. 14. Electron Microprobe Analysis of Three Regenerated Tymochtee Dolomite Particles from Experiment FAC-4.

Table 6. Experimental Gas Feed Rates and Compositions for the FAC-Series of Experiments

	Feed Rate[a] (ft^3/min)					Composition		
Exp.	Air	N_2	O_2	CH_4	Total	N_2	O_2	CH_4
FAC-1	--	1.39	0.84	0.45	2.68	0.518	0.314	0.168
FAC-1R1	0.08	1.6	0.778	0.417	2.875	0.578	0.277	0.145
FAC-1R2	0.08	1.71	0.778	0.441	3.019	0.587	0.267	0.146
FAC-3	0.08	1.26	1.02	0.756	3.116	0.424	0.333	0.243
FAC-4	0.08	1.18	1.04	0.551	2.851	0.436	0.370	0.194
FAC-5	0.08	1.3	1.08	0.756	3.206	0.425	0.339	0.236
FAC-7	0.09	1.414	1.01	0.52	3.304	0.490	0.338	0.172
FAC-8	0.08	1.66	0.66	0.36	2.76	0.624	0.245	0.131
FAC-9	0.08	1.71	0.755	0.386	2.931	0.605	0.263	0.132
FAC-9A	0.27	2.24	0.72	0.403	3.633	0.676	0.214	0.110

[a] At 21°C and 1-atm absolute pressure.

The SO_2 removal (as lb SO_2 generated/lb SO_2-free solid) from the sulfated dolomite during regeneration has been estimated from (1) the difference in sulfur content of the additive before and after regeneration, R_1, and (2) the SO_2 content of the effluent gas, R_2. Therefore, two rates for SO_2 removal have been obtained for each experiment. The average of these two regeneration rates, R_{av}, is used in this correlation. These three rates for the FAC-series of experiments are given in Table 7.

To correlate the effect of pertinent feed-gas concentration with the rate of regeneration, R_{av}, the average rate of SO_2 generation (R_{av}) at 1040°C was plotted against the concentrations of CH_4 (Y_{CH_4}) and O_2 (Y_{O_2}) on log-log coordinates (Fig. 15). The first plot, R_{av} versus Y_{CH_4}, the concentration of CH_4 in the feed, shows an approximately linear relationship with a slope of +1 for all experiments with a fluidized-bed height, h, of 1.5 ft. The results for FAC-5 and FAC-7 (performed with a fluidized-bed height of 2.5 ft) show the same linear relationship.

This result suggests that the ratio, R_{av}/Y_{CH_4}, can be used to establish the dependence of regeneration rate on Y_{O_2}, the feed-gas concentration of O_2. This is shown in the second plot of Fig. 15. An approximately linear relationship with a slope of +0.68 is obtained for experiments performed with a fluidizing-bed height of 1.5 ft.

Since the points representing experiments performed with a fluidized-bed height of 2.5 ft were not near the lines representing the results

Table 7. Comparison of Experimental SO_2 Regeneration Rates with Rates Calculated with Correlation Equation.

Exp.	Temp (°C)	Experimental Regeneration Rate[a] R_1	R_2	R_{av}	Calculated Regeneration Rate,[a] R_{cal}	Deviation (%)
FAC-1	1040	0.190	0.171	0.180	0.187	-4
FAC-1R1	1040	0.188	0.159	0.174	0.148	15
FAC-1R2	1040	0.147	0.148	0.148	0.145	2
FAC-3	1040	0.248	0.163	0.186	0.281	-51
FAC-4	1095	0.235	0.193	0.214	0.214	0
FAC-5	1040	--	0.143	--	0.140	1
FAC-7	1040	0.101	0.104	0.102	0.102	0
FAC-8	1010	0.138	0.038	0.088	0.089	-1
FAC-9	1040	0.203	0.081	0.142	0.130	8
FAC-9A	1040	--	0.100	--	0.094	6
					Average	9

[a] lb SO_2 removed per lb SO_2-free additive.

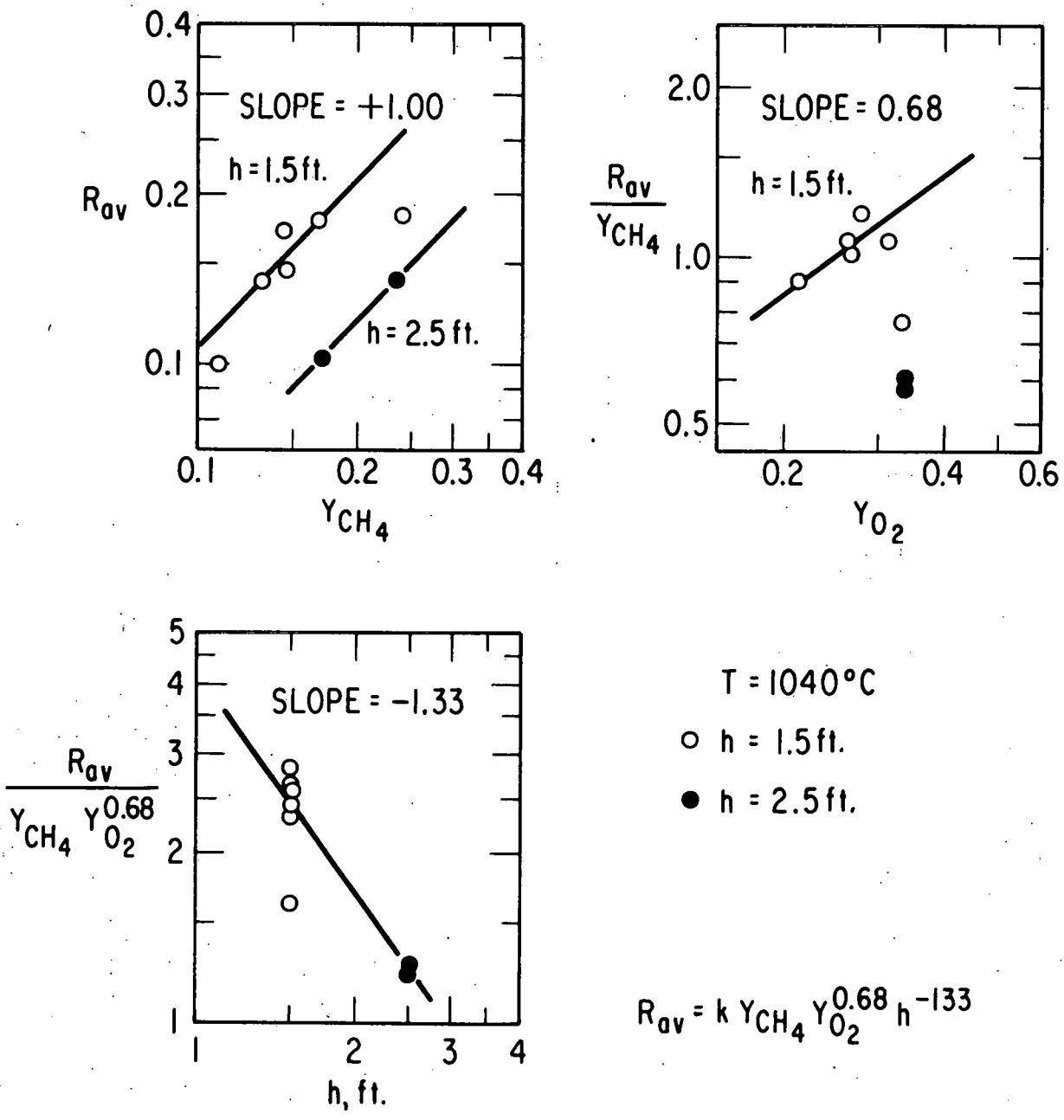

Fig. 15. Correlation of Experimental Data for the Regeneration of Sulfated Dolomite.

for a fluidized-bed height of 1.5 ft in the first two plots in Fig. 15, a dependence of SO_2 generation on fluidized-bed height was suggested. A plot of $R_{av}/Y_{CH_4}\ Y_{O_2}^{0.68}$ versus the fluidized-bed height, h, is also given in Fig. 15. An approximately linear relationship with a slope of -1.33 is obtained.

The interdependence of Y_{CH_4}, Y_{O_2}, h, and the average rate of regeneration of sulfated dolomite is given by:

$$R_{cal} = k\ Y_{CH_4}\ Y_{O_2}^{0.68}\ h^{-1.33} \qquad (2)$$

Values of k have been calculated for all experiments of the FAC-series, including an average value of k for the experiments at 1040°C. The values obtained were:

k	Temp, °C
3.04	1010
4.18	1040
3.71	1095

These three values have been fitted to a second order equation. The resulting non-Arrhenius type equation is

$$\ln k = -252 + \frac{121 \times 10^4}{T} - \frac{14.6 \times 10^8}{T^2} \qquad (3)$$

where T = regeneration temperature (°R).

Using Equations 2 and 3, R_{cal} values have been calculated (Table 7) at the experimental values of Y_{CH_4}, Y_{O_2}, and h.

Variables associated with regeneration have been correlated to establish some dependence of regeneration of sulfated dolomite on these external variables.

DEVELOPMENT OF SYNTHETIC SO_2-SORBENTS

A research program is under way to investigate the utility of synthetic additives for reducing the SO_2 content of the combustion gas in fluidized-bed combustors. Use of these synthetic SO_2-sorbents in place of limestone or dolomite is proposed.

Reactivity of CaO in α-Al_2O_3

Sulfation results are given below for a sorbent containing 20.9% CaO in α-Al_2O_3 (Girdler T-708, supplied by Chemetron Catalyst Division and used in all experiments reported previously). The Girdler T-708 designation is being used to distinguish it from other supports used in some of the experiments reported below.

In the preceding quarterly report, the reactivity of SO_2 and O_2 with synthetic sorbents containing 2-16.5% CaO was reported. In Fig. 16, the conversion of CaO to $CaSO_4$ as a function of time for the 20.9% CaO in α-Al_2O_3 sorbent is given and compared with the conversions for the above sorbents. All reactions were run at 900°C and 1 atm, using a 0.3% SO_2 - 5% O_2 in N_2 synthetic combustion gas.

An unexpectedly high sulfation rate was found for the 20.9% CaO in α-Al_2O_3 sorbent. The rate is equivalent to that of the 14.8% CaO in α-Al_2O_3 sorbent. Except for the 20.9% CaO sorbent, the sulfation rate decreases with increasing CaO concentration. The reason for this reversal in functional dependence is not known. If not all of the CaO had been tied up as aluminates, this might account for the increased rate. X-ray diffraction analysis of the 20.9% CaO in α-Al_2O_3 additive indicated that only $CaO \cdot Al_2O_3$ and $CaO \cdot 2Al_2O_3$ were present. However, up to about 5 percent CaO could have been present without being detected by the X-ray diffraction method of analysis.

Table 8 compares the sorbent weight gain for 20.9% CaO in α-Al_2O_3 due to the addition of SO_3 to that (previously reported) for the 2-16.5% CaO in α-Al_2O_3 sorbents. This particular sorbent, which had the largest SO_3 capture rate of the synthetic sorbents, captured approximately two-thirds as much SO_3 as did Tymochtee dolomite at any given residence time.

Figure 17 shows the weight gain data from Table 8 for 1, 3, and 6 hr. The sorbent weight gain as SO_2 is given as a function of the percent CaO in the support. This graph clearly shows the anomalous behavior of the supported additive containing 20.9% CaO.

Metal Oxides in α-Al_2O_3

Metal oxides other than CaO have been tested for their ability to react with SO_2 and O_2 and for the ability of the sulfated sorbent to be regenerated. Phillips[9,10] and Cusumano and Levy[11] have made thermodynamic calculations to determine the most promising compounds for reacting with SO_2 and for subsequent regeneration with a reducing gas. Phillips suggested that $LiAlO_2$ and Li_2TiO_3 are the most promising candidates. They were chosen from a list of 16 shown in Table 9 (Cusumano and Levy have suggested twelve candidate materials, all of which were suggested previously by Phillips).

Neither $LiAlO_2$ nor Li_2TiO_3 appear to be good choices in view of the instability of Li_2SO_4 at high temperatures. Li_2SO_4 has been reported by Stern and Weise[12] to decompose at a noticeable rate not far above its melting point (860°C). Ficalora *et al.*[13] report that Li_2SO_4 decomposed into gaseous Li, O_2, and SO_2 at temperatures about about 760°C. Nevertheless, 4.5 Li_2O in α-Al_2O_3 was prepared and tested. X-ray diffraction results indicated that $LiAl_5O_8$ was present in the sample. The sample was found to lose weight rather than gain weight under sulfation conditions. The weight loss was presumably due to decomposition of the Li_2SO_4 formed by the sulfation reaction. No further tests are planned with this material.

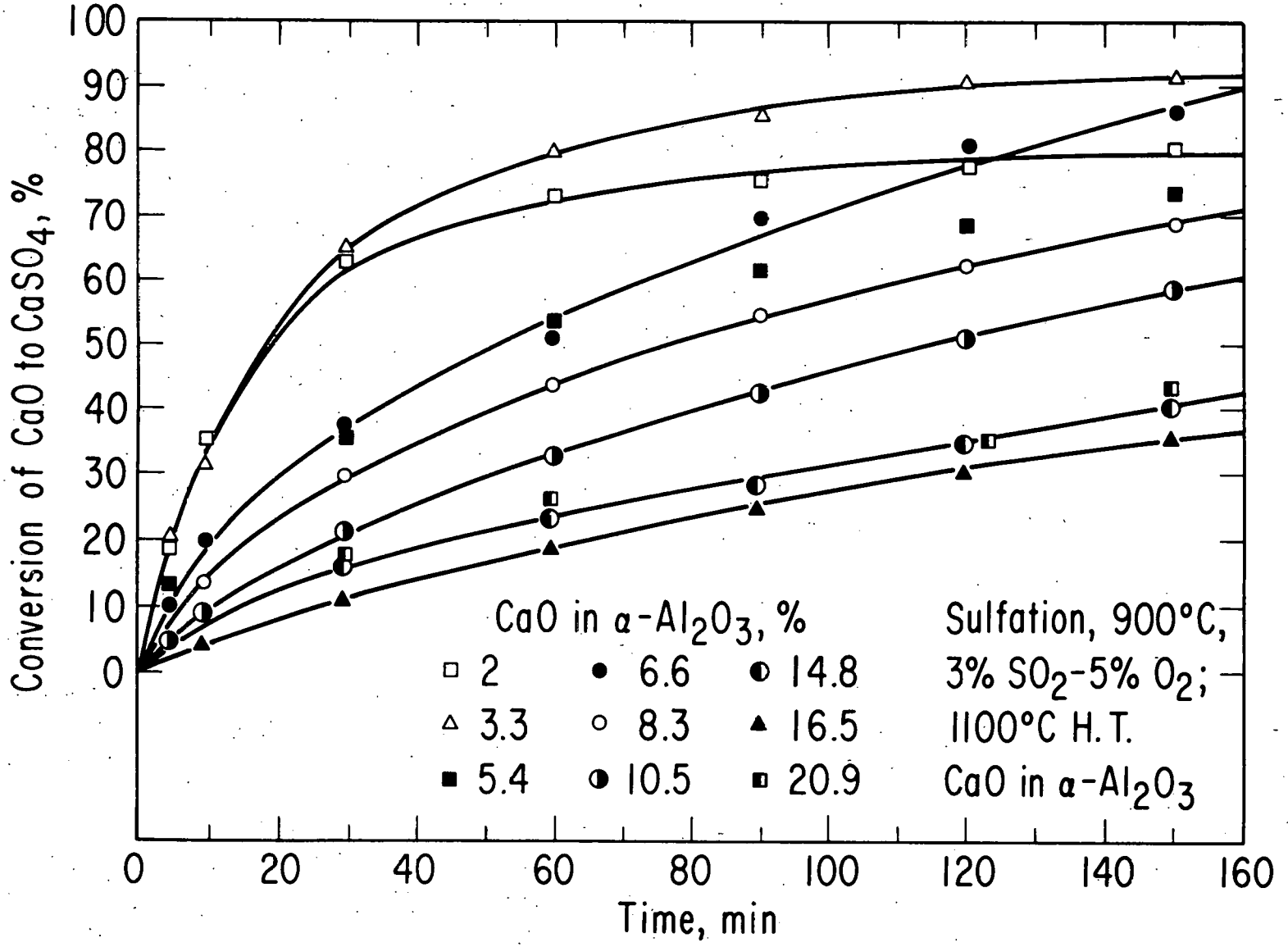

Fig. 16. Sulfation of Synthetic SO_2-Sorbents with Various CaO Loadings.

Table 8. Synthetic Sorbent Weight Gain during Sulfation for Various Calcium Oxide Concentrations.

Sulfation Conditions Feed Gas: 0.3% SO_2, 5% O_2
Temp: 900°C

	Weight gain, g/kg of additive (1100°C H.T.)									
Hours into Run	2% CaO	3.3% CaO	5.4% CaO	6.6% CaO	8.3% CaO	10.5% CaO	14.8% CaO	16.5% CaO	20.8% CaO	Dolomite
0.5	18.0	30.2	27.5	34.9	34.4	31.5	32.6	24.3	54.3	93.4
1	21.0	38.1	40.6	48.1	51.8	49.3	49.0	43.9	77.9	--
2	22.5	42.9	53.2	76.7	74.7	77.7	74.0	72.6	107.7	161.2
3	23.7	44.6	60.7	84.4	88.6	95.3	94.7	96.0	128.9	191.2
4	--	45.4	64.5	88.2	96.7	109.2	112.7	112.0	145.0	213.1
5	--	--	67.0	--	100.7	119.4	126.0	126.4	158.1	230.0
6	--	--	--	--	102.9	123.6	136.3	140	171.0	243.0
Max possible wt gain	28.6	47.1	77.1	94.3	119.0	150	211.4	235.8	298.4	546.0

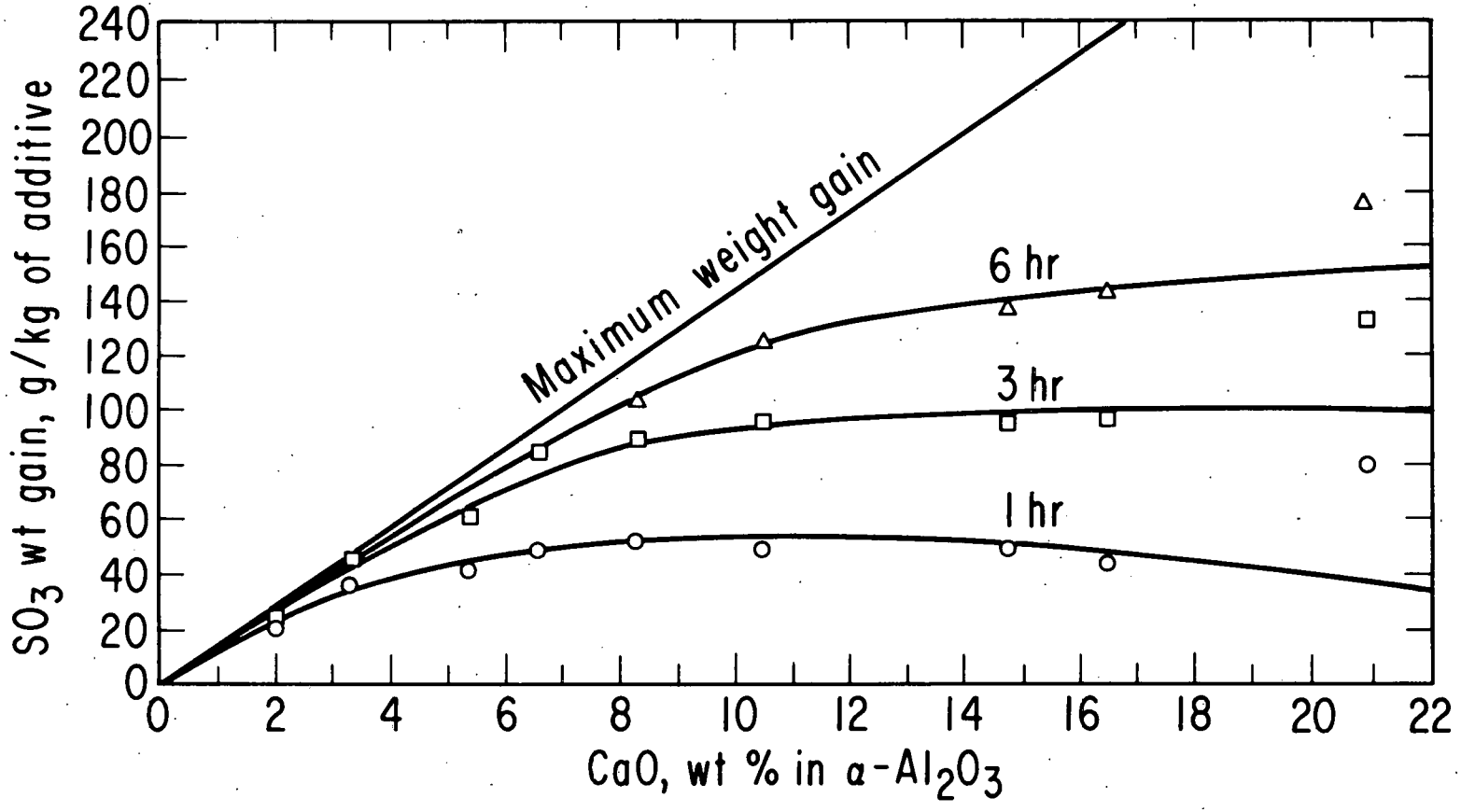

Fig. 17. Sorbent Weight Gain as a Function of Calcium Loading of Synthetic Sorbent (data for 20.9% CaO added to previously reported data).

Table 9. Most Promising SO_2-Sorbents Based on Thermodynamic Screening Results[a]

Sorbent	Temperature Range (°C)
Na_2O	1100-1200
CaO	750-1090
SrO	950-1200
BaO	1080-1200
$LiAlO_2$	750-1200
$LiFeO_2$	750-950
Li_2TiO_3	750-1200
$NaAlO_2$	750-820
$NaFeO_2$	750-1020
$CaAl_2O_4$	750-950
$Ca_2Fe_2O_5$	800-1150
$CaTiO_3$	830-1150
$SrAl_2O_4$	750-1000
$SrTiO_3$	750-920
$BaAl_2O_4$	750-1000
$BaTiO_3$	750-1000

[a] Selected from Reference 1.

The sorbents 7.9% Na_2O in α-Al_2O_3, 5% K_2O in α-Al_2O_3, 14.4% SrO in α-Al_2O_3, and 5.2% BaO in α-Al_2O_3 have been tested. Their rates of sulfation at 900°C using 0.3% SO_2 - 5% O_2 in N_2 are compared with the rates for 6.6% and 14.8% CaO in α-Al_2O_3 in Fig. 18. Potassium and sodium sorbents clearly have higher rates of sulfation than the CaO sorbents while the rates of sulfation of the BaO, SrO, and CaO sorbents are essentially the same. X-ray diffraction results indicated that the starting materials were β-$NaAlO_2$, $KAl_{11}O_{17}$, $BaAl_2O_4$, $CaAl_2O_4$, and $SrAl_2O_4$ in α-Al_2O_3. The products of sulfation were Na_2SO_4, K_2SO_4, $BaSO_4$, $SrSO_4$, and $CaSO_4$. After regeneration, the original aluminates given above were found. The regeneration rates using 3% H_2 at 1100°C are shown in Fig. 19, where they are compared with the regeneration rate of $CaSO_4$ in α-Al_2O_3 using 3% H_2 at 1100°C. The regeneration rates for all metal sulfates were extremely high compared with their sulfation rates. A maximum of 5 min was required for regeneration. The percent regeneration ranged from 85 to 94%. The reason for not attaining 100% regeneration has not yet been determined.

The regeneration results for K_2SO_4 are in disagreement with the thermodynamic calculations of Phillips.[9] In his report, potassium was rejected on the premise that potassium sulfate was theoretically stable under regeneration conditions. As can be seen in Fig. 19, experimentally the regeneration of K_2SO_4 was comparable to the regeneration rate of $CaSO_4$. However, the instability[13] of both Na_2SO_4 and K_2SO_4 at the regeneration temperature of 1100°C must also be considered. A part of the weight loss observed during regeneration may have been due to decomposition of the compounds.

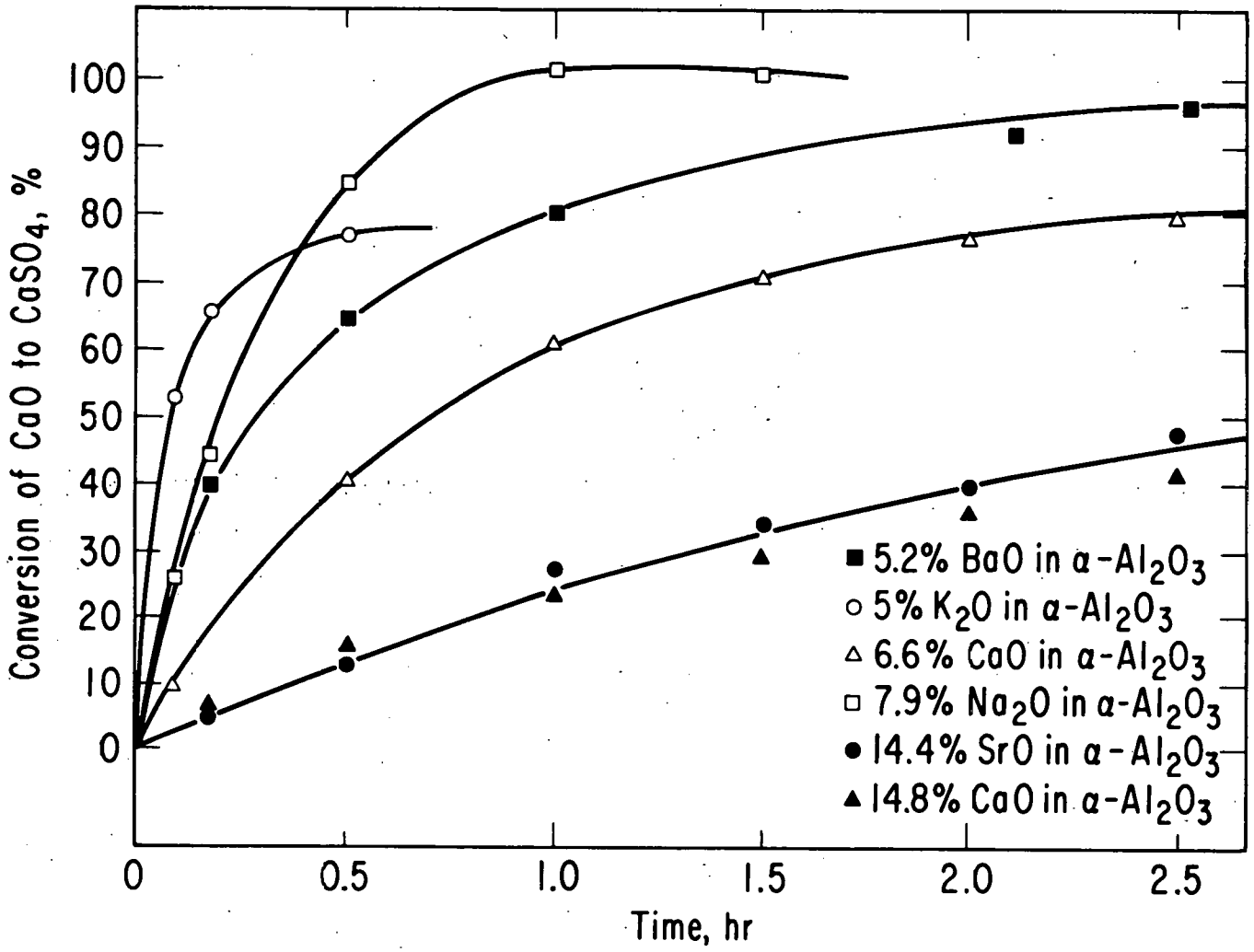

Fig. 18. Comparison of Sulfation Rates of Various Metal Oxides at 900°C.

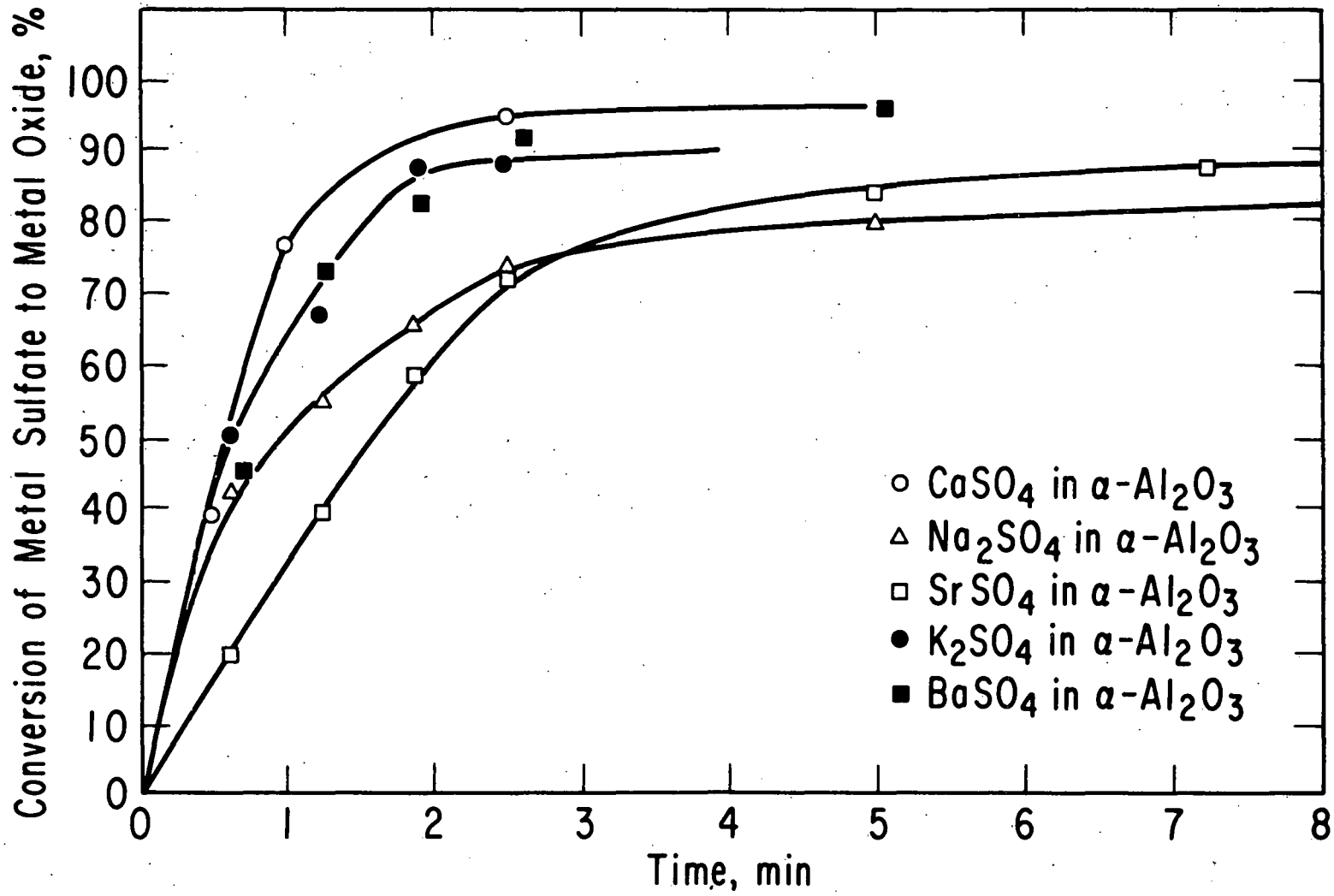

Fig. 19. Regeneration Rate of Various Metal Sulfates in α-Al_2O_3 at 1100°C using 3% H_2.

Since CaO, BaO, and SrO sorbents containing comparable amounts of metal oxides have the same sulfation rate and since calcium is most likely to be the least expensive material, calcium is probably the most desirable. Potassium and sodium sorbents have a higher sulfation rate than CaO; however, due to their sulfate instabilities, they do not seem promising.

Support Development

An investigation has been initiated of methods of producing supports with the required properties (surface area, porosity, and strength). Porosity measurements have been performed on a number of granular supports to determine what effect pore size distribution has on the synthetic sorbent reactivity during sulfation. All synthetic supports tested to date were prepared from granular (-14 +30 mesh) boehmite (γ-AlOOH) obtained from Alcoa (Aluminum Co. of America). Samples were heat treated (H.T.) at 1100°C, 1200°C, and 1500°C for 8 hr. (The rate of heating the sample to the heat treatment temperature has no effect on the sample's pore size distribution.) The pore size distributions (cumulative pore volume versus pore diameter) of the 1100°C, 1200°C, and 1500°C H.T. supports are given in Fig. 20. The pore size distribution for as-received boehmite is also shown. As can be seen in Fig. 20, the higher the heat treatment temperature, the larger the pore diameters. Also, it should be noted that 76% of the pore volume of the 1500°C H.T. support is due to pores having a diameter larger than 0.3 μm and that this material contains essentially no pores smaller than 0.13 μm.

Synthetic sorbents containing 11.1 and 11.4% CaO were prepared from the 1500°C H.T. support; a sorbent containing 12.5% CaO was prepared using the 1200°C H.T. support; and a sorbent containing 8.8% CaO was prepared using the 1100°C H.T. support. These sorbents were sulfated on the TGA to determine their reactivity with 0.3% SO_2 - 5% O_2 in N_2 at 900°C. In Fig. 21, the rates of reaction (or conversion) of calcium oxide with SO_2 to form calcium sulfate are shown for the 8.8%, 11.1%, 11.4%, and 12.5% CaO in α-Al_2O_3 sorbents. Also, the sulfation rate for 10.5% CaO in α-Al_2O_3 (T-708) sorbent is shown. The sorbent prepared from the 1500°C H.T. support has the highest rate of conversion of the CaO to $CaSO_4$, and its reactivity is even higher than that for the 10.5% CaO in α-Al_2O_3 (T-708). There is a direct correlation between pore size distribution in supports and the sorbent reactivity with SO_2 made from these supports; the larger the pore diameter, the greater the reactivity. Synthetic sorbents prepared from supports containing a large percentage of pores smaller than 0.1-0.2 μm have a low sulfation rate.

The quantity of SO_2 captured for a given quantity of synthetic sorbent at various residence times is given in Table 10. The sorbents prepared from the 1500°C H.T. supports captured more SO_2 than did sorbents prepared from either the 1100°C or 1200°C H.T. supports. Also, this granular support performed better than did the 10.5% CaO in α-Al_2O_3 (T-708) sorbent.

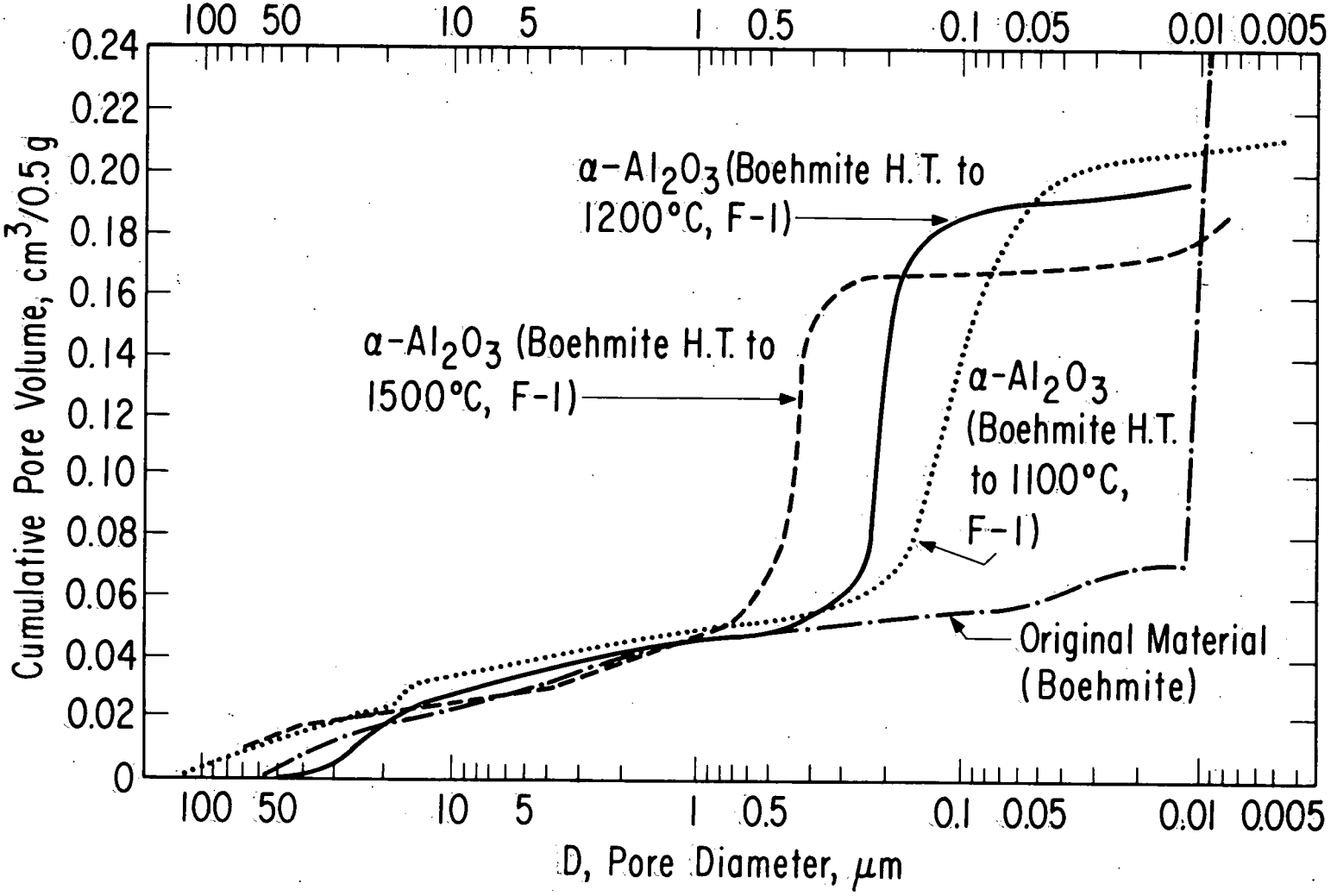

Fig. 20. Relationship of Cumulative Pore Volume to Pore Diameter.

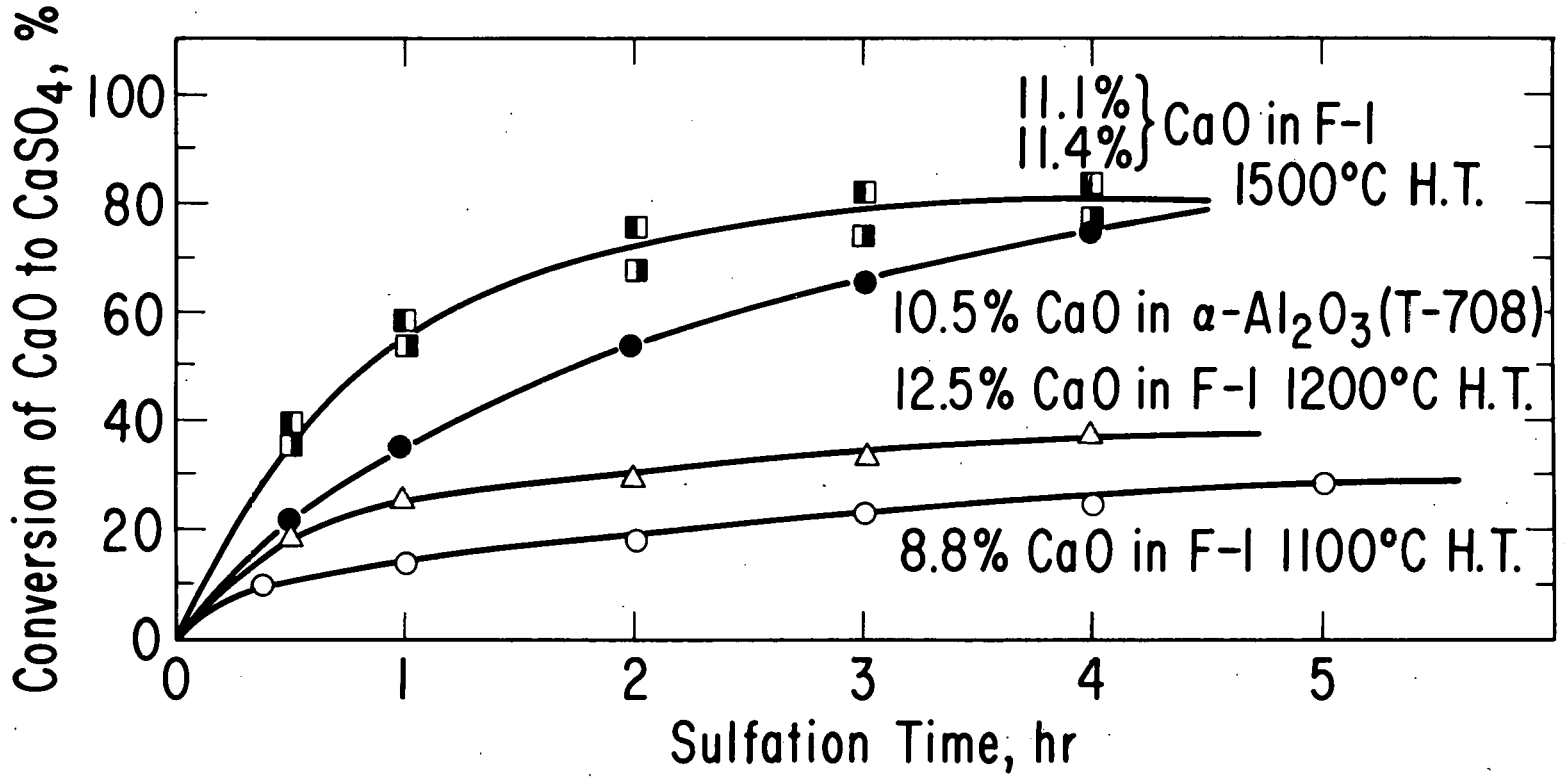

Fig. 21. Sulfation Rate of CaO in Granular Supports. Supports were heat-treated at different temperatures.

Table 10. Sulfation of Supported Sorbents

Residence Time (hr)	Wt Gain (g/kg of Additive)					
	8.8% CaO in F-1 Granular α-Al_2O_3 (1100°C H.T.)	12.5% CaO in F-1 Granular α-Al_2O_3 (1200°C H.T.)	11.1% CaO in F-1 Granular α-Al_2O_3 (1500°C H.T.)	11.4% CaO in F-1 Granular α-Al_2O_3 (1500°C H.T.)	1.05% CaO in T-708[a] -alumina	Tymochtee Dolomite
1/2	13	31	63	57	32	93
1	18	41	91	84	49	--
2	24	52	117	109	78	161
3	29	59	127	117	95	191
4	33	64	129	123	109	213
5	35	--	--	--	--	230

[a]T-708 is the support generally used in the supported additive experiments.

Dow Chemical Synthetic Sorbents

Several samples of CaO in granular α-Al_2O_3 obtained from the Dow Chemical Co. were tested on the TGA for their ability to react with SO_2 and O_2. After 4 hr of sulfation, synthetic sorbents containing 6.9% 10%, and 15.3% CaO in granular alumina had percent conversions of CaO to $CaSO_4$ of 14.8%, 13.3%, and 7.9%, respectively, which is much lower than the 80% conversion for the 11% CaO in F-1 1500°C H.T. sorbent. X-ray diffraction analyses showed that the Dow sorbents contained silica and that the calcium was in the form of stable calcium-aluminum silicates.

BENCH-SCALE, PRESSURIZED FLUID-BED COMBUSTION EXPERIMENTS

In the utilization of regeneration technology, it is important that additive can be recycled a sufficient number of times without losing its reactivity for either sulfation or regeneration and without decrepitating severely. If either assumption is not valid, the additive make-up rate will be sufficiently high (10-20%) that regeneration will not be justified. An experimental effort is being made at ANL, therefore, to evaluate the effects of cyclic operation on the resistance to decrepitation and the reactivity of Tymochtee dolomite in ten combustion/regeneration cycles. Reported here are (1) the results of an initial combustion experiment in which the Tymochtee dolomite used was material which had been previously sulfated in the 6-in.-dia combustor and regenerated in the 4.25-in.-dia regenerator, and (2) preliminary results of the first cycle in the planned ten-cycle combustion/regeneration experiments.

Equipment

The major items of the ANL bench-scale combustion equipment are coal and additive feeders, a preheater for the fluidizing gas, a 6-in.-dia combustor, cyclones and filters, and gas-sampling and analyzing equipment. The combustor is designed for operating at pressures up to 10 atm. The temperature of the combustor is regulated by electrical heaters and cooling coils. The gas analysis system provides on-line measurement of the flue gas constituents, SO_2, NO, NO_x, CO_2, O_2, CH_4, and total hydrocarbons, on a continuous basis. The system is thoroughly instrumented and equipped with an automatic data-logging system.

Sulfation of Regenerated Dolomite

Experiment RC-1A was performed as the initial experiment in a planned thorough evaluation of the effects of additive recycling on additive reactivity and decrepitation. The additive used in the experiments was Tymochtee dolomite ($\sim$50% $CaCO_3$, 39% $MgCO_3$ as received) which had first been sulfated in the bench-scale combustor during the PSI-series of experiments (combustion with Arkwright coal).[2] At that point, utilization of the additive had been $\sim$62% and the sorbent contained $\sim$10-11% sulfur by weight. The additive had then been regenerated in the ANL 4.5-in.-dia

regenerator during several regeneration experiments under various operating conditions and had then been thoroughly mixed. The additive recycled to the combustor for experiment RC-1A contained 4.3 wt % sulfur, which corresponded to an additive utilization of 18%.

The experiment was performed over a period of three days; 120 lb of regenerated additive was recycled. Operating conditions and flue-gas analysis results are given in Table 11 for the steady state conditions during the longest (~6 1/2-hr) and most stable operating period of the experiment. Bed temperature and flue-gas analysis data for that period of operation are plotted in Fig. 22.

Sulfur Retention. Based on the flue gas analysis for SO_2 (250 ppm) sulfur retention (based on sulfur in coal and not including the sulfur in the original additive) was determined to be ~90%. The SO_2 level agrees very well with the expected level of 240 ppm SO_2 in the flue gas calculated from correlations of previous combustion experiments.[14]

If the sulfur content of the partially regenerated additive feed is included, a total sulfur retention of 93% is indicated by the flue-gas analysis. Based on chemical analysis of steady-state overflow, primary cyclone, and secondary cyclone samples, a total sulfur retention of only 82% is indicated. The discrepancy between the two sulfur retention values (93 and 82%) is explainable by the total sulfur mass balance of only 89%. Since the sulfur mass balance (hence sulfur retention) is much more sensitive to slight errors in the solid sample mass flow rates and/or sulfur analyses than to errors in the gas flow rate or gas analysis, the gas analysis is considered the more reliable indication of sulfur retention. Thus, the results indicate that the additive fully retained

Table 11. Operating Conditions and Flue-Gas Analysis for Combustion Experiment RC-1A

Combustor:	ANL, 6-in.-dia	Excess Air:	17%
Bed Temp:	840°C	Coal:	Arkwright
Pressure:	810 kPa	Additive:	Regenerated Tymochtee dolomite

Feed Rate (kg/hr)				Flue-Gas Analysis					
Coal	Additive	Ca/S Ratio[a]	Gas Velocity (m/sec)	SO_2 (ppm)	NO (ppm)	NO_x (ppm)	CO (ppm)	CO_2 (%)	O_2 (%)
14.1	3.2	1.6	1.0	250	120	150	40	17	3.1

[a] Based on unreacted calcium (CaO) in regenerated dolomite and sulfur in coal.

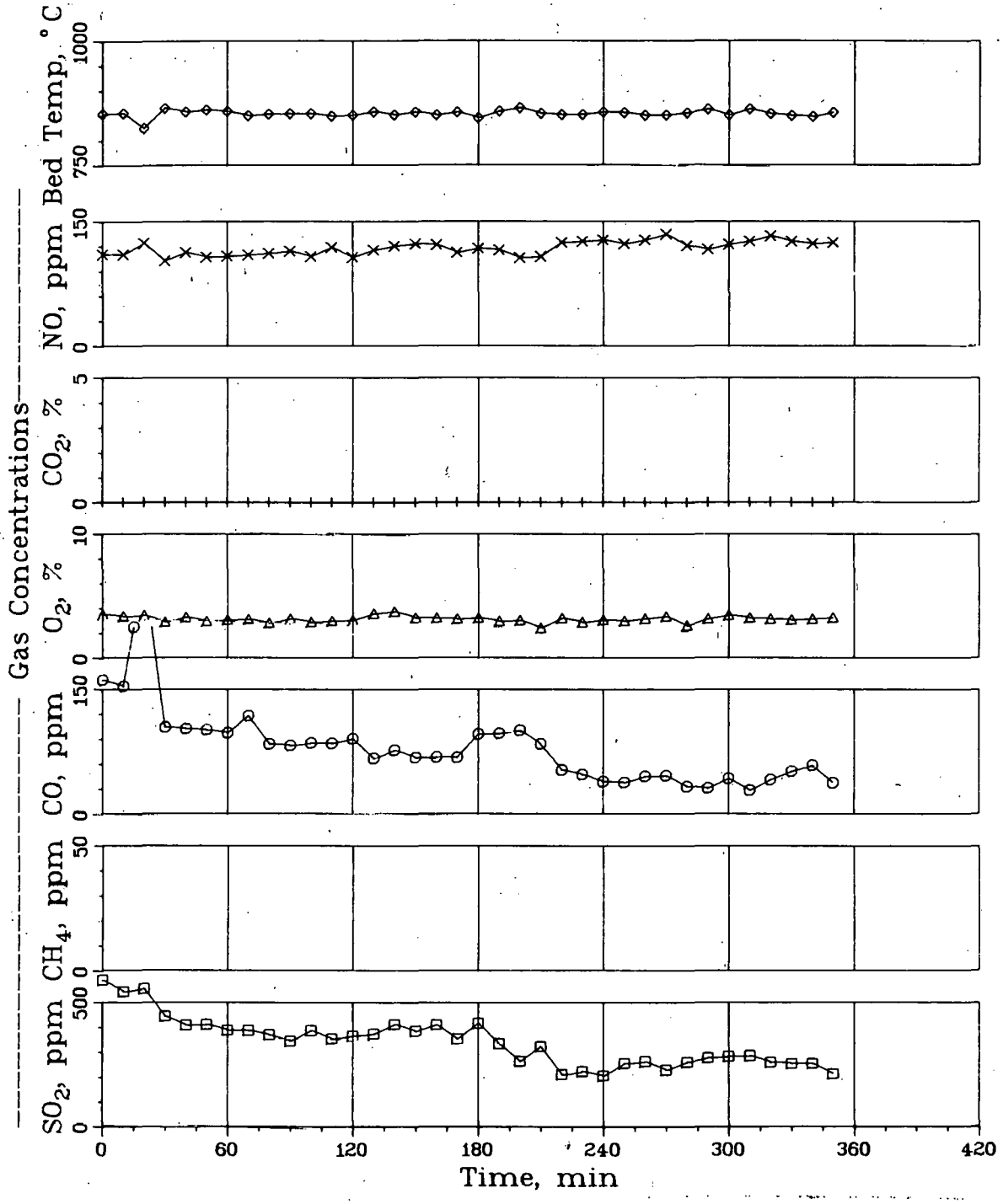

Fig. 22. Bed Temperature and Flue-Gas Composition, Experiment RC-1A.

is activity for sulfur removal into the second combustion cycle.

Additive Utilization. Calcium utilizations were calculated for steady-state overflow, primary cyclone, and secondary cyclone samples (Table 12). Utilizations based on the sulfur and calcium contents of the respective samples ranged from 56% in the overflow to 67% in the secondary cyclone. Also given in Table 12 are utilization values adjusted to reflect the 18% calcium utilization of the dolomite fed to the combustor. The adjusted utilizations ranged from 47% in the overflow to 60% in the secondary cyclone. These utilization values provide evidence of the higher activity of finer additive particles for SO_2 retention.

Based on the distribution of calcium in the samples of Table 12, a weighted average of 50% utilization was determined for the unreacted calcium in the feed. This utilization multiplied by the 1.6 Ca/S mole ratio suggests that 80% of the sulfur in the coal was retained by the additive. This value is very sensitive to small errors in the calcium and sulfur analyses of the various samples and to the calcium distribution in the product samples. The sulfur retention of 90% calculated on the basis of the SO_2 level in the flue gas is still considered the best value.

Additive Decrepitation. A calcium material balance for experiment RC-1A showed that of the additive fed to the combustor, ∿62% was removed in the product overflow, ∿30% was recovered in the primary cyclone, ∿2% was recovered in the secondary cyclone, and ∿6% was unaccounted for.

Screen analyses of samples of regenerated dolomite feed, overflow, primary cyclone, and secondary cyclone materials are presented in Table 13. Although conclusive evidence in the form of chemical determinations is

Table 12. Utilization of Calcium in Overflow, Primary Cyclone, and Secondary Cyclone Samples from Experiment RC-1A.

Sample	Calcium Utilization (mol S/mol Ca) x 100	
	Based on Sulfur and Calcium Content of Sample	As Adjusted for Feed with 18% Utilization
Overflow	56%	47%
Primary Cyclone	62%	54%
Secondary Cyclone	67%	60%
Weighted Average (based on product distribution of calcium)	∿59%	∿50%

Table 13. Screen Analysis Results for Combustion Experiment RC-1A

U.S. Sieve No.	Wt Fraction in Size Range: Regenerated Dolomite Feed	Steady State Overflow	U.S. Sieve No.	Wt Fraction in Size Range: Primary Cyclone	Secondary Cyclone
+14	0.00	0.00	+45	0.30	0.20
-14 +25	0.17	0.36	-45 +80	0.25	0.12
-25 +35	0.18	0.28	-80 +100	0.04	0.08
-35 +45	0.43	0.30	-100+170	0.10	0.10
-45 +80	0.22	0.05	-170+230	0.06	0.13
-80 +170	0.00	0.00	-230+325	0.08	0.14
-170	0.00	0.00	-325	0.16	0.24
Total	1.00	0.99	Total	0.99	1.01

lacking, it seems apparent from the screen analyses in Table 13 that the additive recovered in the primary and secondary cyclone ash products was elutriated in the off-gas without decrepitation of the additive in the fluidized bed. Comparison of the steady-state overflow with the regenerated dolomite feed shows an increasing loss by entrainment (in percent) with decreasing particle size. Examination of the primary cyclone screen analysis shows an unusually large amount of +80 mesh material, which is the size of the smallest particle in the regenerated dolomite feed. The limited evidence thus indicates very little decrepitation of the additive in the combustor. It also suggests that during the planned ten-cycle combustion/regeneration experiments, it may be necessary to recover the entrained additive from the cyclone ash material to reduce the amount of additive lost during each cycle. Also, during the ten-cycle series of experiments, more rigorous determinations of decrepitation during each cycle will be made.

Cyclic Combustion/Regeneration Experiments; Combustion Cycle One

As mentioned above, a series of combustion/regeneration experiments is planned to evaluate the effects of cyclic operattion on the resistance to decrepitation and the reactivity of Tymochtee dolomite over ten cycles. Since the quantity of additive in experiment RC-1A was insufficient to offset losses during ten combustion/regeneration cycles, a large amount of dolomite is being sulfated as part of the first combustion cycle. After this material undergoes 1 1/2 combustion/regeneration cycles, the material from experiment RC-1A will be blended in for the remaining experiments in the cyclic series. In anticipation of possibly large losses during ten complete cycles, ∿1000 lb of dolomite has been sulfated to date in the first combustion cycle (experiment REC-1). Nominal operating conditions for the first combustion cycle are a 900°C bed temperature, 810-kPa pressure, 1.5 Ca/S mol ratio, ∿17% excess combustion air, 0.91 m/s fluidizing gas velocity, and a 1.07 m bed height. Operating conditions and flue gas composition data for segments REC-1K and REC-1L of the first

combustion cycle experiment are presented in Table 14. Bed temperature and flue-gas data for both experiments are plotted in Fig. 23.

The sulfur dioxide level of ∿300 ppm (sulfur retention of 86%) was somewhat higher than that expected from correlations of previous combustion experiments.[14] The most probable causes of the slight increase in measured SO_2 level are a slightly larger additive particle size (-14 +30 mesh as compared with -14 +100 mesh) and modifications to the system to eliminate fluctuations in the bed level (replacement of a 1/4-in. overflow pipe with a purged 3/8-in. overflow pipe). The sulfur retention of 86% corresponds to an emission of 0.58 lb $SO_2/10^6$ Btu, as compared with the EPA emissions standard of 1.2 lb $SO_2/10^6$ Btu.

Chemical and screen analyses of sulfated product and fly ash samples are being done to evaluate the extent of decrepitation of additive during the first cycle. These results will be presented in a future report.

Table 14. Operating Conditions and Flue-Gas Compositions for Sulfation Experiments REC-1K and REC-1L in the First Combustion Cycle Experiment.

Combustor: ANL, 6-in.-dia — Temperature: 900°C
Coal: Arkwright, -14 mesh — Pressure: 810 kPa
Additive: Tymochtee dolomite, -14 +30 mesh — Excess Air: ∿17%

Operating Conditions	Experiment REC-1K	Experiment REC-1L
Coal feed rate, kg/hr	14.6	14.9
Additive feed rate, kg/hr	4.1	4.3
Ca/S mole ratio	1.6	1.6
Gas velocity, m/s	0.94	0.97
Bed height, m	1.1	1.1
Run duration, hr	11.2	10.3
Flue-Gas Analyses		
SO_2, ppm	290	300
NO, ppm	300	120
CH_4, ppm	32	25
CO, ppm	90	31
CO_2, %	16	17
O_2, %	3.4	3.4
Sulfur Retention	86%	86%

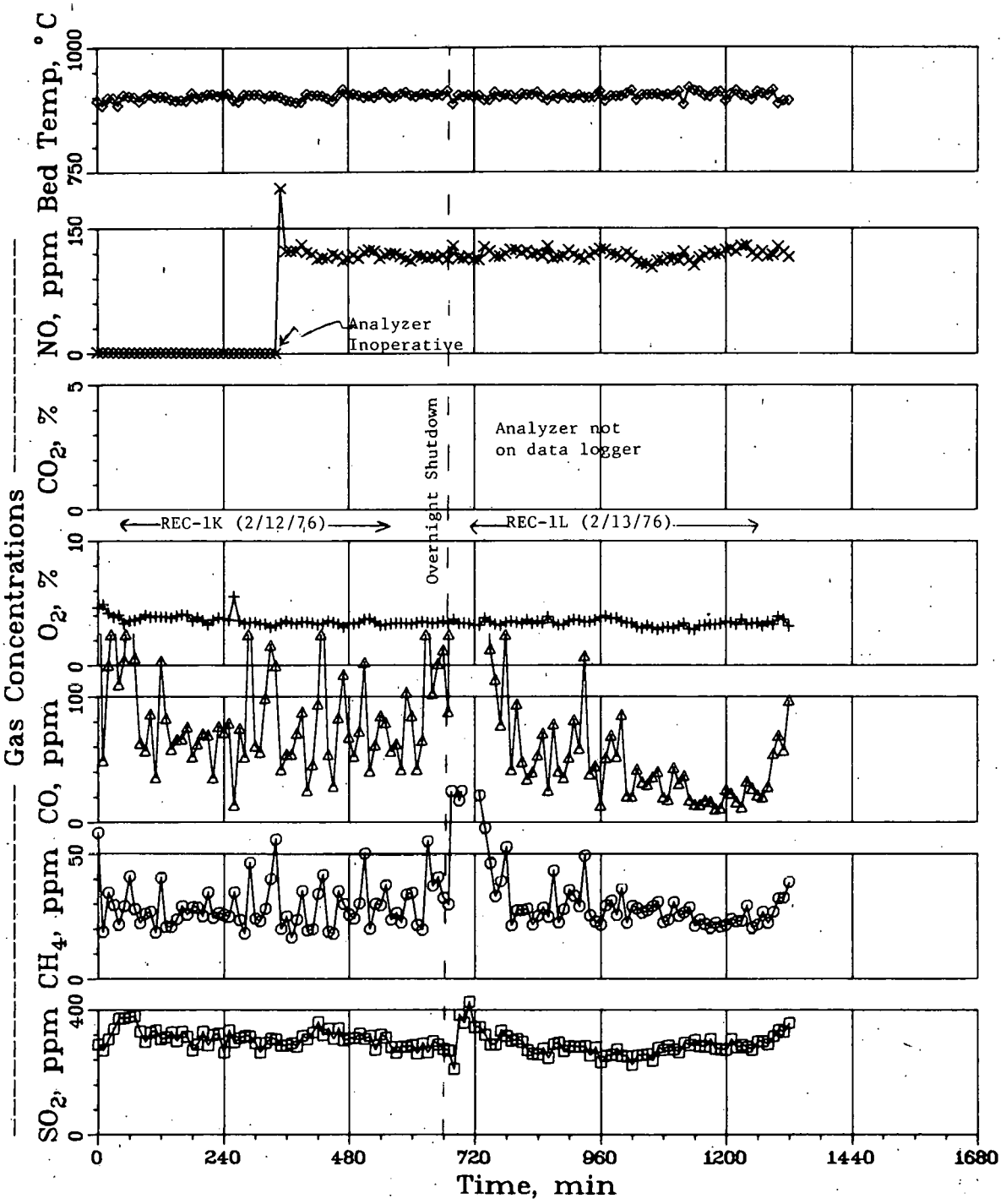

Fig. 23. Bed Temperature and Flue-Gas Composition, Experiments REC-k and -1L.

REGENERATION CHEMISTRY

Regeneration by the $CaSO_4$-CaS Reaction

Additional results are reported on the study of the solid-solid reaction

$$3[CaSO_4 + MgO] + [CaS + MgO] \rightarrow 4[CaO + MgO] + 4SO_2 \quad (1)$$

The earlier reported results[3] confirm that this reaction has potential as a regeneration scheme and illustrate that relatively high CaO yields are obtained by two different methods of carrying out the reaction: (a) a two-step process in which starting material for the reaction is prepared by partial reduction of the sulfated dolomite followed by the solid-solid reaction and (b) a single-step process in which the reductive and solid-solid reactions occur simultaneously. Additional results are presented on the single-step process. The earlier studies of this method[3] were performed at 950°C.

The experimental procedure followed in this series of experiments was similar to that used in the earlier studies. All experiments were performed using aliquots of a stock supply of sulfated 1337 dolomite, which was prepared in the same manner as in the earlier studies. An experiment consisted of placing an aliquot of the sulfated dolomite in the TGA (which was at the selected temperature) under a flow of the reducing gas and monitoring the weight change. Experiments were performed at several different reducing gas concentrations at the following temperatures: 950°C, 900°C, 850°C, and 800°C. The composition of the stones at the end of each experiment was determined by X-ray diffraction analyses of aliquots of 30 to 50 stones.

The results of these experiments are summarized in Table 15. The first column lists the experiment number; the second column, the reaction temperature; the third, the reducing gas concentration; the fourth, the reducing gas flow rate; the fifth, the reaction time; and the sixth, the chemical composition of the stones at the end of the experiments, as determined by X-ray diffraction analysis.

The results for CaO yields and reaction times at 950°C for low reducing gas concentrations are in general agreement with the earlier reported results.[3] These 950°C data indicate that the solid-solid and reduction reactions occur simultaneously at the higher as well as the lower reducing gas concentrations.

For the experiments carried out at temperatures lower than 950°C, the solid-solid reaction occurs at low reducing gas concentrations. For example, at 800°C and 0.1% H_2, the CaO concentration increased from 12% to 37%--a significant yield for the solid-solid reaction at a temperature 150 degrees lower than in the prior work.

Table 15. Simultaneous Reduction and Solid-solid Reaction Experiments

Expt. No. - Sample No.	Reaction Temperature (°C)	Reducing Gas Concentration (% H_2 in He)	Reducing Gas Flow Rate (cm^3/min)	Reaction Time (hr)	Stone Composition[a] - X-ray Diffraction
XVI[b]	750	0	0	0	12% CaO; 73% $CaSO_4$
XVII	950	6	200	0.7	25% CaO; 53% CaS
XVIII	950	3	300	0.9	34% CaO; 46% CaS
XIX	950	1	300	1.5	18% CaO; 54% CaS
XX	950	0.5	300	2.5	31% CaO; 42% CaS
XXI	950	0.1	300	4.7	49% CaO; 28% CaS
XXII	950	0.05	300	10.8	54% CaO; 26% CaS
XXIII	950	0.02	300	18.3	54% CaO; 19% CaS; 11% $CaSO_4$
XXIV	900	6	200	1.3	15% CaO; 60% CaS
XXV	900	3	300	2.4	15% CaO; 60% CaS
XXVI	900	1	300	6.0	20% CaO; 55% CaS
XXVII	900	0.4	300	7.6	23% CaO; 55% CaS
XXVIII	900	0.1	300	11.2	28% CaO; 46% CaS
XXIX	900	0.02	300	20.8	40% CaO; 25% CaS; 8% $CaSO_4$
XXX	850	6	200	2.5	8% CaO; 68% CaS
XXXI	850	4	300	2.9	11% CaO; 59% CaS
XXXII	850	2	300	5.6	10% CaO; 61% CaS
XXXIII	850	1	300	6.0	20% CaO; 54% CaS
XXXIV	850	0.3	300	7.6	27% CaO; 48% CaS
XXXV	800	6	200	7.2	8% CaO; 64% CaS
XXXVI	800	3	300	13.0	10% CaO; 63% CaS
XXXVII	800	1	300	15.5	6% CaO; 72% CaS
XXXVIII	800	0.1	300	15.7	37% CaO; 41% CaS

[a] Values given refer to percentages of maximum weight possible of calcium species if all the calcium present were that species.

[b] Starting material for remaining experiments described in this table.

Two-Step Regeneration Reaction Scheme

Reduction Step

The data given in Table 15 provide considerable information on the reduction of sulfated dolomite

$$[CaSO_4 + MgO] + 4H_2 \rightarrow [CaS + MgO] + 4\ H_2O \qquad (2)$$

The reduction reaction occurs at temperatures as low as 800°C. In general, its rate increases with temperature. It also can be concluded that the solid-solid reaction (Eq. 1) occurs as a competing reaction to reaction 2, which is the first step of the two-step regeneration scheme. This is certainly true at all temperatures studied, for the conditions defined as low hydrogen reducing gas concentration (<1%). In addition, it is true for the high-temperature-range data (950°C) for all concentrations of the reducing gas. The data obtained at higher reducing gas concentrations (>1%) in the 800°C to 900°C temperature range (Table 15) suggest that under these conditions, the solid-solid reaction does not occur to any great extent, if at all.

Carbonation Reaction Step

The above information on the reduction reaction possibly has implications on the chemistry associated with the carbonation reaction

$$[CaS + MgO] + H_2O + CO_2 \rightarrow [CaCO_3 + MgO] + H_2S \qquad (3)$$

which is the second reaction of the two-step regeneration scheme. The carbonation reaction does not proceed to completion, and this represents a major problem area for this regeneration scheme.

It can be speculated that the data given in Table 15 provides an explanation of why the carbonation reaction does not go to completion. If the solid-solid reaction is a competing reaction with the reduction reaction, it is possible that the CaO formed by this reaction, even if in small quantities, is the species that retards the carbonation reaction. For example, CaO existing as a thin film could act as a barrier to the diffusion of CO_2 and H_2O reactants in the carbonation reaction.

This suggests an experiment in which the reduction and carbonation reactions are performed simultaneously. This approach could result in the CaO being more finely dispersed in the stone so that CaO would not become a barrier--in other words, $CaCO_3$ might form before CaO has an opportunity to limit its formation.

To date, only two such experiments have been completed and analyzed, but the results (shown in Table 16) are encouraging. In these experiments, sulfated dolomite samples were placed in the TGA at temperatures, and the weight change process was monitored under the environment of 300 cm^3/min flow of the reaction gas mixture consisting of 3.6% H_2 and 40% CO_2 in helium.

Table 16. Simultaneous Reduction-Carbonation Reaction Experiments

Expt. No. - Sample No.[a]	Reaction Temperature (°C)	Reaction Gas Concentration	Reaction Time (hr)	Stone Composition[b] X-ray Diffraction Results
I	800	3.6% H_2; 40% CO_2	17	40% $CaCO_3$; 10% CaO; 34% CaS
II	750	3.6% H_2; 40% CO_2	42	46% $CaCO_3$; 22% $CaSO_4$; trace CaS

[a] Starting material for these experiments is sample XVI (Table 15).

[b] Values given refer to percentages of maximum weight possible of calcium species if all the calcium present were that species.

The composition of the stones at the end of the experiments was determined by X-ray diffraction analyses.

The results of these preliminary scoping experiments show that $CaCO_3$ yields were relatively high.

COAL COMBUSTION REACTIONS

The Determination of Inorganic Constituents in the Effluent Gas from Coal Combustion

Some chemical elements carried by combustion gas are known to cause severe metal corrosion. The objective of this study is to determine quantitatively which elements are present in the hot combustion gas of coal, either in volatile or particulate form, and to differentiate between volatile and particulate species. Identification of the compound form and amount of particulate species and determination of the amount and the form of condensable species are desirable.

The engineering drawings of the laboratory-scale batch-unit fixed bed combustor designed for this study have been approved, and fabrication of the combustor is under way in the central shop of ANL. The conceptual design of the combustor was presented in a previous report.[1] The combustor is being constructed under a fabrication specification and work plan that includes a manufacturing plan, a test plan, and a quality control plan.

The specially ordered "Kellundite" filter, a ceramically bonded fused-alumina product of Electro Refractories and Abrasives, a Division of Ferro Corporation, has been received. The filter is to be used in the combustor for the removal of particulates from the hot combustion gases of the coal.

Installation of the Tocco induction heating unit, which will be used with the combustor, has been completed. The unit has been tested and found to be in good working conditions. As a general procedure for operating an induction heating unit, the coupling between the unit and the workpiece (the combustor is this case) needs to be properly adjusted before the unit can be operated with the workpiece. The coupling adjustment of the unit has been made by using, as a stand-in for the combustor, a 3-ft length of stainless steel pipe of the same size as the combustor.

Systematic Study of the Volatility of Trace Elements in Coal

Knowledge of the vaporization characteristics of trace elements in coal and of the rate of their volatilization is important for combined-cycle turbine operation. The purpose of this study is to obtain data on the volatility of these elements under practical coal combustion conditions. This study is also intended to obtain data supporting "The Determination of Inorganic Constituents in the Effluent Gas from Coal Combustion" (above).

Some elemental analyses of high-temperature ashes (prepared in a muffle furnace from Illinois Herrin No. 6 Montgomery County coal; average temperature, 340°C; airflow, 9 liters/min; duration, 48 hr) were reported in a previous report.[3] The remainder of the elemental analyses (for lithium, sodium, magnesium, potassium, calcium, titanium, and chlorine) which were not available for the preceding report have now been obtained and are given in Table 17, together with the results previously reported. Unreasonably large increases in concentrations for aluminum, nickel, manganese, calcium, and magnesium are shown for samples obtained at 740°C and above, compared with the concentrations in the samples obtained below 740°C. As previously noted, the ash samples heated to 340, 542, and 640°C were analyzed in one group, while the remaining samples were analyzed in a second group at a later time.

For the purpose of checking on these doubtful values, the 340, 640, 940, and 990°C samples were reanalyzed, using the X-ray fluorescence method. Although reliable absolute elemental concentrations for these samples can not be obtained now, the X-ray fluorescence results show that, within the experimental error, the concentrations of aluminum and calcium for the 940 and 990°C samples are the same as those for the 340 and 640°C samples. The elements iron, potassium, and titanium were also analyzed by X-ray fluorescence and the concentrations remain reasonably constant for all four samples, as is also shown in Table 17. These X-ray fluorescence results appear to indicate that the observed increases in concentration for aluminum, nickel, manganese, calcium, and magnesium in the samples obtained at 740°C and above may not be real.

The only nonmetallic element analyzed in these ash samples is chlorine. Table 17 shows a significant decrease in chlorine concentration for samples heated above 640°C, indicating that most of the chlorine in coal evolves at temperatures below 640°C. In the X-ray fluorescence spectra, a small chlorine peak was also observed for each of the 640, 940, and

Table 17. Elemental Concentration[a] of High-Temperature Ash Corrected for Weight Losses at the Stated Temperatures. Ash prepared at 542 to 990°C by heating for 24 hours in air flow of 0.6 scfh.

		Heating Temperature (°C)						
		340	542	640	740	840	940	990
ppm	Be	6.5 ±0.6	6.3 ±0.6	6.2 ±0.6	6.2 ±0.6	6.8 ±0.7	7.2 ±0.7	6.3 ±0.6
	Pb	15±2	26±3	29±3	29±3	54±5	10±1	21±2
	V	210±50	200±50	230±60	150±40	130±30	150±40	130±30
	Cr	90±9	91±9	87±8	100±10	94±9	93±9	170±20
	Co	17.0 ±0.8	16.9 ±0.8	17.1 ±0.9	15.4 ±0.8	14.0 ±0.7	14.4 ±0.7	13.9 ±0.7
	Ni	52±5	52±5	53±5	62±6	60±6	66±7	100±10
	Cu	130±10	110±10	110±10	120±10	120±10	126±10	130±30
	Zn	540±30	510±30	520±30	460±20	480±20	560±30	560±30
	Mn	500±20	550±30	540±30	680±30	680±30	660±30	670±30
	Hg	0.01						
	Li	59±3	64±3	62±3	63±3	63±3	63±3	66±3
	Cl	90±10	91±10	22±10	17±10	17±10	13±10	21±10
%	Al	4.6 ±0.2	5.7 ±0.3	5.4 ±0.3	8.1 ±0.4	7.7 ±0.4	8.1 ±0.4	8.0 ±0.4
	Fe	10.5 ±0.5	10.7 ±0.6	11.1 ±0.6	11.2 ±0.6	11.3 ±0.6	11.5 ±0.6	11.5 ±0.6
	Na	0.74±0.04	0.75±0.04	0.87±0.04	0.79±0.04	0.80±0.04	0.81±0.04	0.76±0.04
	Mg	0.28±0.01	0.29±0.01	0.33±0.02	0.54±0.03	0.42±0.02	0.40±0.02	0.40±0.02
	K	1.08±0.05	1.26±0.06	1.21±0.06	1.24±0.06	1.25±0.06	1.29±0.06	1.28±0.06
	Ca	4.9 ±0.2	4.3 ±0.2	4.2 ±0.2	6.4 ±0.3	6.0 ±0.3	5.6 ±0.3	6.2 ±0.3
	Ti	0.6 ±0.1	0.6 ±0.1	0.5 ±0.1	0.4 ±0.1	0.4 ±0.1	0.4 ±0.1	0.5 ±0.1

[a] By atomic absorption. Each precision is based on an estimate of the precision of measurement obtainable with standard solution.

990°C samples. This indicates that trace amounts of chlorine still remained in the high-temperature ashes, as is also noted in Table 17. In contrast to nonmetallic chlorine, the metallic elements are generally retained in the ash up to 990°C. Under the oxidizing conditions present during heat treatment of these ash samples, no loss in sodium or potassium was observed.

This study has been continued to investigate the vaporization characteristics of these trace elements at a high temperature range. In the experiments of Series 2 (as compared with the Series-1 experiments presented above), 340°C ash was heat-treated in a platinum combustion coal (an Al_2O_3 boat was used in Series-1) to temperatures between 850 and 1250°C for 20 hr in either air or an oxygen-enriched air flow of 0.6 scfh.

The weight losses of the 340°C ash samples due to the heat treatments are given in Table 18. Tables 19 and 20 show some elemental analyses of ash residues for these Series-2 experiments.

The elemental concentrations reported in Tables 19 and 20 were calculated on the original 340°C ash basis, based on the percent weight losses given in Table 18.

Table 18. Effect of Temperature and Oxygen Concentration on Weight Loss of 340°C Ash.

Experimental Conditions: 0.6 scfh gas flow
20-hr heating time

Temperature (°C)	Oxygen Conc.[a] in Flowing Gas (vol %)	Wt of Sample (g)	Wt Loss as a Result of Heating (g)	Wt Loss (%)
850	21	1.1124	0.1022	9.19
950	21	1.1092	0.1141	10.29
1100	21	1.0987	0.1244	11.32
1150	21	1.1098	0.1279	11.52
1200	21	1.1054	0.1292	11.69
1250	21	1.1052	0.1304	11.80
1150	45	1.1015	0.1284	11.66
1150	68	1.1109	0.1305	11.75
1200	45	1.0949	0.1311	11.97
1200	68	1.0967	0.1335	12.17

[a]Balance was nitrogen.

Table 19. Elemental Concentrations in High-Temperature Ash Calculated on the Original 340°C-Ash Basis. Ashes prepared at 850 to 1250°C by heating for 20 hr in an air flow of 0.6 scfh.

	Element	Heating Temperature (°C) 340 AA	340 NAA[b]	850 AA	950 AA	1100 AA	1150 AA	1200 AA	1250 AA
%	Fe	11.9 ±0.6	11±2	11.8 ±0.6	11.4 ±0.6	11.4 ±0.6	11.2 ±0.6	10.9 ±0.5	11.8 ±0.6
	Al	9.5 ±0.5		9.7 ±0.5	9.6 ±0.5	10.0 ±0.5	9.8 ±0.5	8.6 ±0.4	9.9 ±0.5
	Na	1.00±0.05	0.8±0.2	1.14±0.06	1.04±0.05	1.15±0.06	0.97±0.05	0.94±0.05	1.13±0.06
	K	1.55±0.08	1.4±0.3	1.62±0.08	1.59±0.08	1.56±0.08	1.53±0.08	1.40±0.08	1.54±0.08
ppm	Zn	380±20		390±20	420±20	400±20	440±20	400±20	380±20
	Mn	360±20	380±80	340±20	300±20	300±20	320±20	320±20	320±20
	Ni	70±4		70±4	72±4	74±4	69±3	68±3	83±4

[a] AA - Atomic absorption; each precision is based on an estimate of the precision of measurement obtainable with standard solution.

[b] NAA - Neutron activation analysis; precision is estimated to be less than 20% at this stage.

Table 20. Elemental Concentrations[a] in High-Temperature Ash as a Function of Oxygen Concentration in Gas Flow. Ashes prepared by heating for 20 hr in a gas flow of 0.6 scfh.

	Element	Heating Temperature (°C)						
		340	1150			1200		
			Oxygen Concentration (vol %)[b]					
			21	45	68	21	45	68
%	Fe	11.9 ± 0.6	11.2 + 0.6	11.3 ± 0.6	11.3 ± 0.6	10.9 ± 0.5	11.2 ± 0.6	10.9 ± 0.5
%	Al	9.5 ± 0.5	9.8 ± 0.5	9.6 ± 0.5	9.5 ± 0.5	8.6 ± 0.4	8.5 ± 0.4	9.0 ± 0.4
%	Na	1.00± 0.05	0.97± 0.05	1.11± 0.06	1.08± 0.05	0.94± 0.05	1.14± 0.06	1.00± 0.05
%	K	1.55± 0.08	1.53± 0.08	1.52± 0.08	1.55±0.08	1.40± 0.07	1.44± 0.07	1.43± 0.07
ppm	Zn	380± 20	440± 20	440± 20	420± 20	400± 20	410± 20	400± 20
ppm	Mn	360± 20	320± 20	290± 15	310± 20	320± 20	290± 15	280± 15
ppm	Ni	70± 4	69± 3	78± 4	67± 3	68± 3	70± 4	--

[a] Calculated on the original 340°C ash basis; obtained by an atomic absorption method; each precision is based on an estimate of the precision of measurement obtainable with standard solution.

[b] Balance was nitrogen.

Since in Series-1 experiments significant analytical errors for several elements were observed in ash samples that had not been analyzed as one group, the ash samples for Series-2 experiments were specially analyzed as one group for each element during the same period of time. As a consequence, fairly consistent results were obtained, as indicated in Tables 19 and 20. Within the limits of experimental and analytical errors, Table 19 clearly shows that the elemental concentrations of the metallic elements iron, aluminum, sodium, potassium, zinc, manganese, and nickel remain constant up to 1250°C, indicating that these metallic elements generally remain in the ash up to 1250°C under the oxidizing environment. The retention of these elements in the ash was also independent of the oxygen concentration in the flowing gas, as shown in Table 20. Also included in Table 19 are the elemental concentrations in the 340°C ash, as determined by neutron activation analysis (NAA). Fairly good agreement of atomic absorption and NAA results is observed.

In Series-2 experiments, the ash residues obtained at both 850 and 950°C were light brown powder; however, those obtained at 1100°C and above were hard, glassy, black agglomerates, indicating fusion of the ash sample at the ashing temperature ranges.

The 340°C ash samples used in Series-1 and -2 experiments were prepared from the same batch of coal samples; however, for some elements, the elemental concentrations in the 340°C ash used in Series-1 experiments were surprisingly different from those in the 340°C ash used in Series-2 experiments. The elemental concentrations for both 340°C ashes have been recalculated on the original coal basis, and are given in Table 21. The observed difference in concentration can be explained on the basis of contamination of coal by the grinding equipment used for coal preparation. Series-1 340°C ash samples were prepared from coal powder that had been ground in a mill equipped with chilled-iron grinding plates; Series-2 340°C ash was obtained from coal that had been prepared using a ball mill with ceramic balls. The chemical composition of the chilled iron used in the grinding mill is not known; however, it is general practice to add certain types of alloys to chilled-iron castings to refine its grain structure, to improve the response to heat treatment, and to enhance the mechanical properties of the casting products. Based on this information, it seems reasonable to expect that the elemental concentrations of iron, zinc, and manganese would be higher for the coal prepared by the iron grinding mill and that the aluminum concentration would be higher for the coal prepared using ceramic balls in a ball mill, as is shown in Table 21.

Contamination of coal from a jaw crusher (made of manganese steel) has been reported by Schultz *et al.*[15] The coal, after crushing, showed a twofold increase in manganese concentration and significant increases in both chromium and copper elemental concentrations.

Table 21. Comparison of Elemental Concentrations[a] of 340°C Ash Prepared by Different Types of Grinding Methods.

	Element	Series-1[b] Chilled-Iron Grinding Mill	Series-2[c] Ball Mill with Ceramic Balls
%	Fe	2.5 ± 0.1	2.1 ± 0.1
	Al	1.10 ± 0.06	1.68 ± 0.08
	Na	0.18 ± 0.01	0.18 ± 0.01
	K	0.30 ± 0.02	0.27 + 0.01
ppm	Zn	121 ± 6	68 ± 3
	Mn	129 ± 6	64 ± 3
	Ni	12 ± 1	12 ± 1

[a] Calculated on the original coal basis.

[b] Results reported previously (ANL/ES-CEN-F083).

[c] Results obtained from Table 18 of this report.

FABRICATION OF NEW EQUIPMENT

To improve experimental capabilities related to the pressurized combustion of coal in a fluidized bed of SO_2-retaining additive and subsequent regeneration of the sulfated additive, several new pieces of equipment are to be fabricated. Major equipment items include a new regenerator, a new combustor, and a cyclic system for continuous recycling of additive between the combustor and the regenerator. The current status of fabrication of this new equipment is discussed below.

New Regenerator

The existing bench-scale regenerator, a 4.25-in.-dia reactor, is to be replaced with a new 6-in.-dia regenerator of improved design. A simplified schematic drawing of the new unit is shown in Fig. 24.

The new regenerator is being fabricated in two sections, a lower bed section and an upper freeboard section. Each section consists of an 18-in., Schedule S, carbon steel pipe (17.25-in. ID) lined with castable refractory and insulation to an inside diameter of 6 in. The refractory will be 3.125 in. thick and the insulation will be 2.5 in. thick. The inside diameter of the bed section can be reduced to 4 in. by increasing the refractory thickness to 4.125 in.

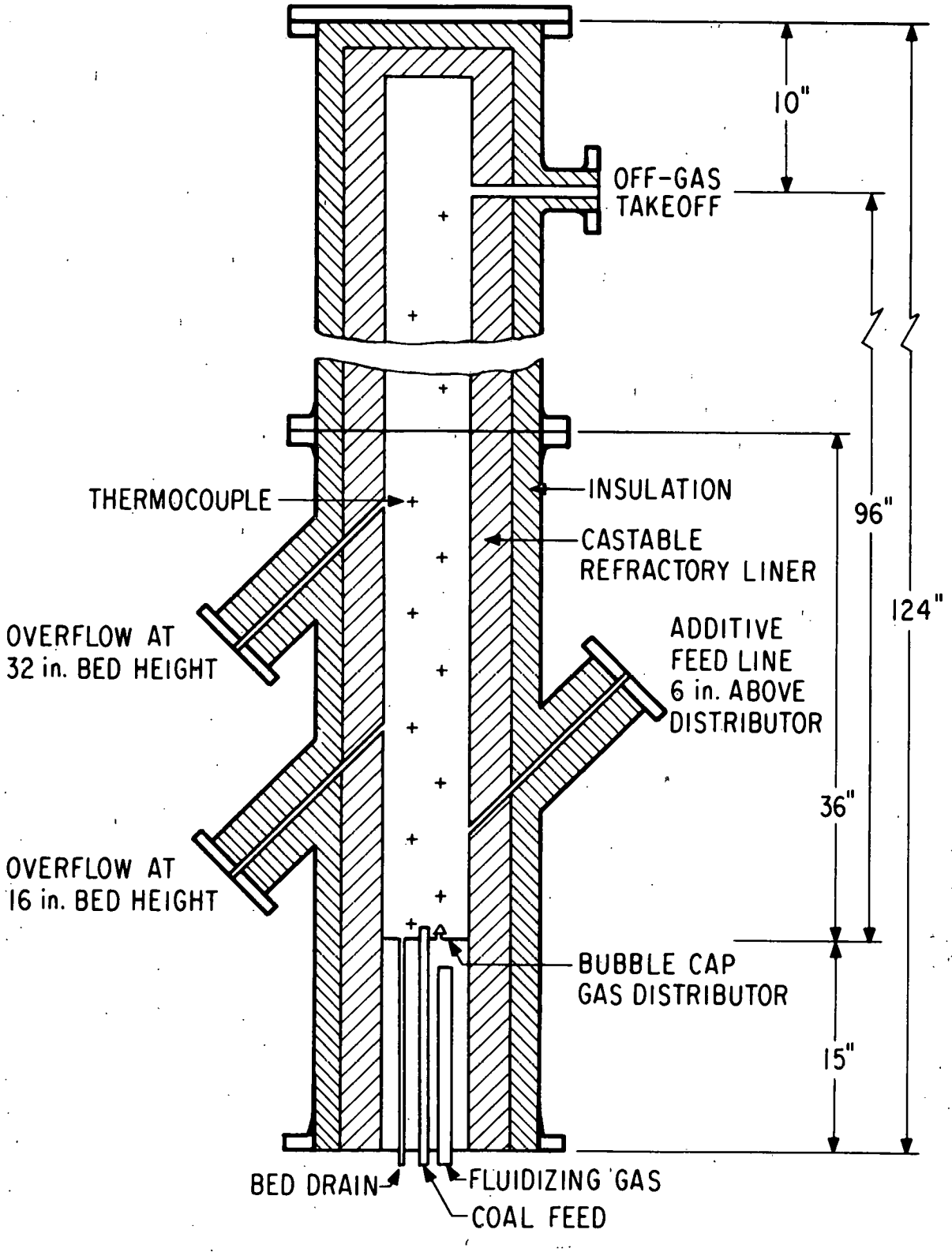

Fig. 24. Simplified Schematic Drawing of New 6-Inch-Diameter Regenerator.

In either bed section configuration, the unit will be capable of operating at pressures up to 10 atm absolute and at bed temperatures up to 1150°C (2100°F) with a relatively small heat loss of 1300 to 1500 Btu/(hr)(ft of bed). This heat loss is considerably less than the estimated heat loss of >4500 Btu/(hr)(ft of bed) for the existing regenerator. The lower heat loss for the new unit is expected to result in higher SO_2 concentrations in the off-gas.

In the new regenerator, the nominal bed height will be maintained at either 16 or 32 in. (a bed height to bed diameter ratio of 2.67 or 5.33 for the 6-in.-dia bed section configuration) by overflow of solids through side arms attached to the bed section. Sulfated additive from the combustor can be continuously fed to the regenerator through a third side arm that permits the additive to be introduced below the bed level 6 in. above the fluidizing-gas distributor plate.

A bubble-cap type gas distributor plate (only one bubble cap is shown in Fig. 24) is to be used that will be penetrated by a coal feed line and a bed drain line. The gas distributor plate is to be supported from the bottom flange and will be compression fitted between sections of castable refractory and insulation, using high-temperature gasketing material.

Side wall penetrations include several thermocouple wells for monitoring internal temperatures in and above the bed. The thermocouple wells will consist of metal-ceramic protection tubes to resist the effects of corrosive atmospheres and high bed temperatures.

The upper section of the new regenerator, which will have an inside diameter of 6 in., will provide sufficient freeboard space to minimize elutriation of bed material from the unit.

Fabrication of the new regenerator was started during the past quarter. The scheduled completion date for construction of the new unit is June 15, 1976.

New Combustor

The design of a new, pressurized, fluidized-bed combustor was described previously.[1] Construction drawings for the new unit were prepared and are currently being reviewed for design conformance to the ASME Boiler and Pressure Vessel Code, Section VIII, 1974. A formal design and preliminary safety review for the new combustor will be conducted prior to fabrication.

Cyclic System

Various pieces of equipment are being either fabricated or purchased that will permit continuous cycling (instead of manual transfer) of sulfated additive from the combustor to the regenerator and of regenerated additive from the regenerator back to the combustor. At present, manual

transfer of the additive between the two units is required in investigations related to the effect of additive recycling on such variables as decrepitation, reactivity for SO_2 retention, and buildup of coal ash in the additive.

The equipment to be fabricated or purchased includes solids product receivers, solids feeders with attached hoppers, system-pressure control valves, and inertial separators and filters for removing particulate solids from the off-gas. Fabrication of the inertial separators is complete; completion of the solids product receivers by April 1, 1976, is scheduled. The remaining equipment items are in various design stages prior to fabrication or procurement.

MATHEMATICAL MODELING. NONCATALYTIC GAS-SOLID REACTION WITH CHANGING PARTICLE SIZE: UNSTEADY STATE HEAT TRANSFER

Introduction

The knowledge of the interior (core) temperature of a solid reacting particle is important for catalytic as well as noncatalytic exothermic reactions inasmuch as this temperature may differ considerably from the surrounding temperature. In catalytic reactions, such temperature differences may lead to severe damage to catalyst reactivity. In noncatalytic reactions such as the combustion of coal to produce low-Btu gas, the composition of the product gas may differ considerably, depending on the temperature of the reaction front within the particle--for example, high temperatures may cause slagging of the solid reactant.

For many gas-solid reactions, it is reasonable to use the quasi-steady state approximation to provide a first approximate description of the reacting system. However, solution of the heat balance equation under quasi-steady state approximation can lead to errors in the estimates of (1) the reacting particle temperatures and (2) the instantaneous transition of the rate-controlling regime from kinetic to diffusion and vice versa. The particle temperature has a significant influence on the effective diffusivity and the reaction rate, since both of these are strongly dependent on temperature. For gas-solid reactions occurring in fluidized beds, the assumption that these are governed by the constant bed temperature is also not valid. Accurate data on internal particle temperature and change in particle size must be considered to obtain reasonable predictions either for design purposes or for comparison with the observed fluidized-bed operations.

Earlier Studies

For diffusion-controlled reactions, it has been shown[16] that a change in particle size as the reaction progresses has considerable influence on the conversion-time relationship. Generally, high temperatures are generated in the diffusion-controlled regime of the gas-solid reaction, and it is imperative that the changing size of the particle be included

in the analysis to obtain more realistic estimates of the internal particle temperatures. The effect of changing particle size on unsteady state heat transfer has not yet been analyzed in the literature. The inclusion of this phenomenon presents a unique problem of two moving boundaries--(1) the reaction front and (2) the external diameter of the particle (due to growth or shrinkage of the particle with reaction). The temperature rise during reaction, especially within a porous catalyst, has been investigated by many authors.[17-24] All workers have assumed that the particle size remains invariant throughout the reaction.

Prater[17] has derived the magnitude of the temperature difference between the unreacted core and the surface of the catalyst pellet at steady state. Assuming that a single reaction occurred having a known heat of reaction, he established the heat and mass transports following the Fourier and Fick's laws, respectively. He concluded that the maximum temperature difference occurred at the point where the concentration of the gaseous reactant dropped to zero. The maximum steady state temperature difference, termed the Prater temperature difference $(T_p)^*$ is given by:

$$T_p \equiv (T_c - T_s) = \frac{(-\Delta H_1) D_{eA} C_{AS}}{k_e} \qquad (1)$$

Bondi *et al.*[18] studied the unsteady state burning of coke in catalyst pellets in an effort to explain their rapid deactivation. The work involved approximately the spherical moving boundary problem with the corresponding semi-infinite slab problem and assumed that the mass transfer resistance of the gas film was negligible in comparison with the diffusional resistance of the ash layer. This assumption is not valid in the initial stages of the reaction, and hence erroneous conclusions could be drawn from their results. Wei[19] suggested that under transient conditions, the maximum temperature difference can greatly exceed the one obtained by Prater.[17] Wei has analyzed the temperature difference in terms of T_p and Lewis number, which is defined as the ratio of the catalyst thermal diffusivity to reactant diffusivity and is given by:

$$L = \frac{k_e}{\rho\ (S_1)\ C_p\ (S_1)\ D_{eA}} \qquad (2)$$

Under transient conditions, he concluded that the maximum temperature difference is given by:

$$(T_c - T_s) = T_p f(L,N) \qquad (3)$$

where f(L,N) is some function of Lewis number and the ratio of the catalyst pellet diameter to the hot spot diameter, and depends upon the geometry of the particles.

---

* Symbols are defined in the Notation subsection at the end of this report section.

Luss and Amundson[20] used the shrinking core model to determine the temperature rise in a spherical pellet for a diffusion-controlled gas-solid reaction. The effects of heat and mass transfer in the gas film, as well as inside the pellet, were investigated. For unsteady state conditions, the temperature rise was found to be much higher than that predicted for quasi-steady state conditions. They solved the system of heat and mass balance equations and derived an expression for the core temperature as a function of the decreasing core radius. The mass transfer process was assumed to be at quasi-steady-state, whereas the transient term was introduced in the heat balance equations. From the expression that they derived, the magnitude of the maximum temperature rise can be estimated. Among other variables, the temperature rise was found to be a strong function of the Sherwood number and Nusselt number. Both of these are strong functions of the particle size. Hence, the latter should not be ignored in the development of a reliable theory.

Beveridge and Goldie[21] discussed the general type of nonisothermal noncatalytic gas-solid reactions based on the shrinking-core model. They developed the heat and mass transfer equations for one reaction in a spherical pellet. Quasi-steady state was assumed for the mass transfer operation. The heat accumulation term was included in the heat balance equations. They claimed that the latter term avoids irrational solutions in the analysis of instability and makes it possible to identify instantaneous temperature and reaction rate transitions. They followed essentially the same method of solution as that used by Shen and Smith.[22] Thus, it was possible for them to determine the effect of adding a transient term to the steady state solution obtained by Shen and Smith.[22] They have primarily focused their attention on the effect of various parameters on the geometrical and thermal instability of a system. Wen and Yang[23] derived a more general case to demonstrate the differences between the quasi-steady state and unsteady state solutions of the heat balance equations by introducing radiation heat transfer and n-th order reaction. Their results are shown to correspond to the results of Beveridge and Goldie[21] in which radiation was ignored and the order of reaction was reduced to first order.

Knapp and Aris[24] have attempted to study the geometrical irregularities on the reaction front found by Cannon and Denbigh[25] in their studies of the oxidation of zinc sulfide particles. The latter study indicated that the formation of the oxide layer became very uneven and that a non-uniform surface developed at the interface. These irregularities were apparently due to locally enhanced reaction rates. Knapp and Aris[24] derived theoretical expressions for an unsteady state system to study these geometrical perturbations on the moving core surface and to determine if they disappear or develop into deeper perturbations as the reaction continues. They have simplified the resulting equations for a case of a dimple on a flat infinite plane, and the equations have been derived for its curvature on the center line. The shrinking-core model has been employed for the analysis, retaining the transient term in the heat balance equation. The physical interpretation of the equations and calculations suggests that in most cases the dimple is likely to flatten out, thus stablizing the geometrical perturbations. They concluded that the deep pits found were more likely to have been caused by local irregularities of porosity or a transition in rate-controlling regime.

In formulating a mathematical expression for the unsteady state heat transfer that addresses the problem of internal particle temperature, we shall introduce a parameter Z which characterizes the change in particle size as the reaction proceeds. The model governing such a system is developed below.

Model of the System

The analysis is based on a shrinking-core model for a spherical pellet, as shown in Fig. 25. The derivation essentially involves the same steps as are described in an earlier paper.[16] The following single reaction is considered in the present analysis.

$$aA(g) + S(s) \xrightarrow{k_1} eE(g) + jS_1(s) \tag{4}$$

The rate of reaction is assumed to be first order with respect to gaseous and solid reactants given by:

$$-r_A = k_1(T_c)\ C_{AC}C_{SO} \tag{5}$$

where the temperature dependence of the rate constant is assumed to be of the Arrhenius type. The reaction takes place at an interface situated at a distance r_c from the center. The solid reactant is assumed to lie within the interface ($0 < r < r_c$), and the solid product forms the surrounding shell ($r_c < r < R$). The particle is assumed to retain its spherical shape as it reacts. The overall size of the particle may change from its initial radius R_o as the reaction proceeds. The solid particle is immersed in a flowing gas mixture containing the gaseous reactant A whose concentration in the bulk phase is represented by C_{AO}. Our aim is to introduce the transient term in the energy balance equation and to examine its effects on both the conversion-time relationship and the interior particle temperature. Analysis of the system requires simultaneous solution of mass and heat balance equations in the particle. In the following analysis, we will employ the quasi-steady state approximation for the mass balance equation since such an assumption is justified by Bischoff.[26]

Based on a shrinking-core model for a nonisothermal system under the quasi-steady state assumption, a material balance for a gaseous reactant A leads to the following relation:

$$\frac{d}{d\xi}\ \xi^2\ \frac{d\omega_A}{d\xi} = 0 \tag{6}$$

The boundary conditions are:

$$\frac{d\omega_A}{d\xi} = N_{Sho}(1 - \omega_{AS})\ \text{at}\ \xi = \xi_s \tag{7}$$

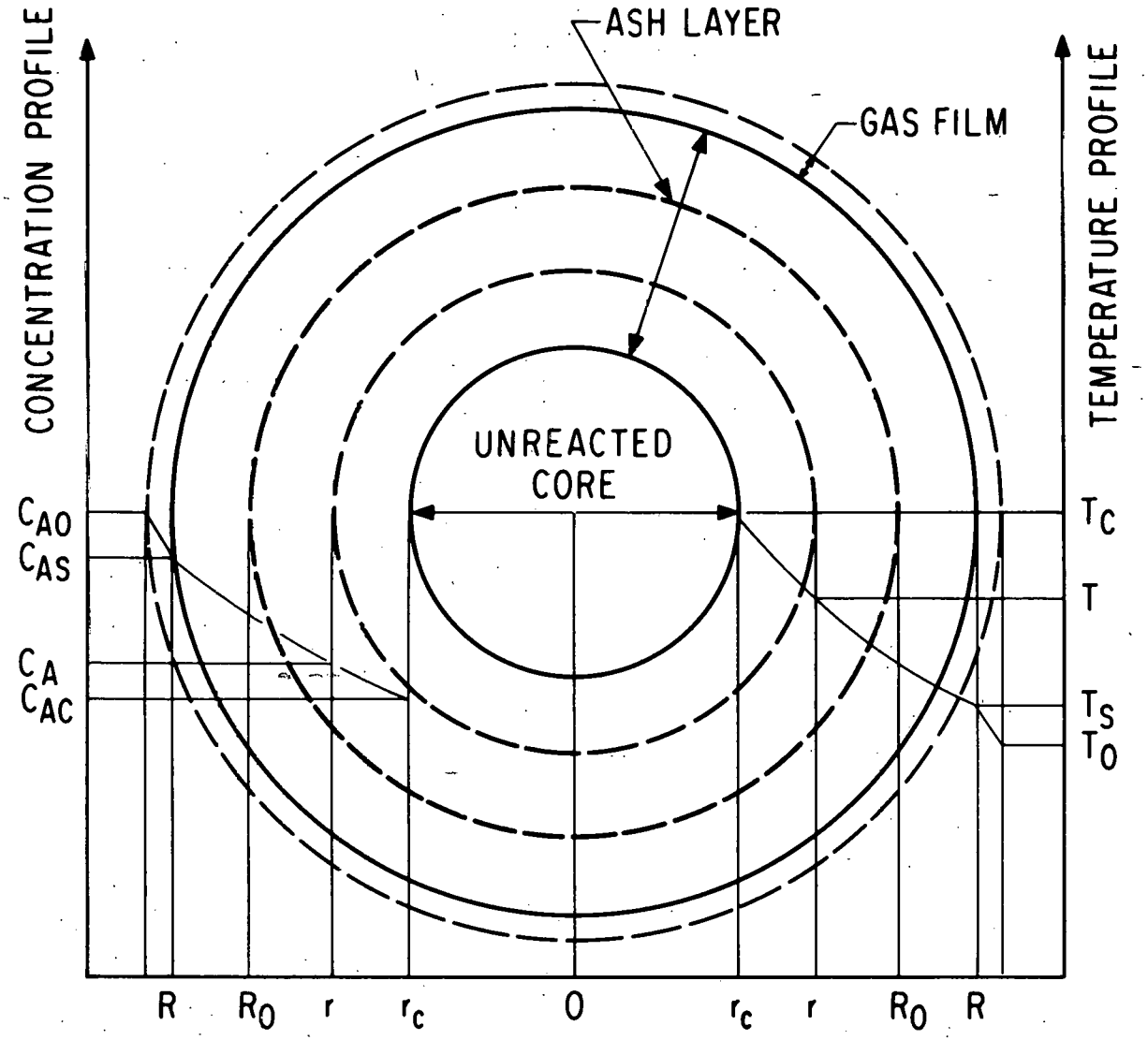

Fig. 25. Gas-Solid Reaction of a Growing Particle: The Concentration and Temperature Profiles.

and

$$\frac{d\omega_A}{d\xi} = \phi_1 \left(\frac{\omega_{AC}}{U_c}\right) \exp\left[\frac{E_1}{\bar{R}T_o}\left(1 - \frac{1}{U_c}\right)\right] \text{ at } \xi = \xi_c \tag{8}$$

Here

$$N_{Sho} = N_{Sh}(R_o/2R)(D_A/D_{eA}) \tag{9}$$

The solution of Eq. 6 in conjunction with the boundary conditions of Eq. 4 and 8 lead to the following relation for the concentration of A at the reaction surface:

$$\frac{1}{\omega_{AC}} = 1 + \frac{\phi_1 \xi_c^2 \exp\left[\frac{E_1}{\bar{R}T_o}\left(1 - \frac{1}{U_c}\right)\right]}{U_c N_{Sho} \xi_s^2} + \frac{\phi_1 \xi_c \left(1 - \frac{\xi_c}{\xi_s}\right)}{U_c} \exp\left[\frac{E_1}{\bar{R}T_o}\left(1 - \frac{1}{U_c}\right)\right] \tag{10}$$

The simplifying assumptions implicit in the above derivation are discussed in detail in reference 16.

Similarly, the heat balance equation with transient term included in the analysis is given by:

$$V\phi_1 \frac{\partial U}{\partial \theta} = \frac{\partial^2 U}{\partial \xi^2} + \frac{2}{\xi}\frac{\partial U}{\partial \xi} \tag{11}$$

with the following boundary conditions:

$$-\frac{\partial U}{\partial \xi} = N_{Nuo}(U_s - 1) + N_{NuR}\left(U_s^4 - 1\right) \text{ at } \xi = \xi_s \tag{12}$$

and

$$\frac{-\left(\frac{\partial U}{\partial \xi}\right)}{\beta_1 \phi_1 \left(\frac{E_1}{\bar{R}T_o}\right)} = \frac{\omega_{AC}}{U_c} \exp\left[\frac{E_1}{\bar{R}T_o}\left(1 - \frac{1}{U_c}\right)\right] - \frac{G\xi_c}{3}\frac{\partial U_c}{\partial \theta} \text{ at } \xi = \xi_c \tag{13}$$

The initial condition is given by:

$$U = U_c = 1 \text{ at } \theta = 0 \tag{14}$$

In the above, we have assumed that the core maintains a uniform temperature and that the walls of the reactor are maintained at the ambient temperature, T_o.

In the case of the quasi-steady state assumption, the above equations will not contain the accumulation term, and consequently $(\partial U/\partial\theta)$ and $(\partial U_c/\partial\theta)$ will both be zero. Thus, the equations will simplify to the following:

$$\frac{d^2U}{d\xi^2} + \frac{2}{\xi}\frac{dU}{d\xi} = 0 \tag{15}$$

with the boundary conditions given by

$$-\frac{dU}{d\xi} = N_{Nuo}(U_s - 1) + N_{NuR}(U_s^4 = 1) \text{ at } \xi = \xi_s \tag{16}$$

and

$$-\left(\frac{\bar{R}T_o}{E_1}\right)\frac{dU}{d\xi} = \phi_1\beta_1\left(\frac{\omega_{AC}}{U_c}\right)\exp\left[\frac{E_1}{\bar{R}T_o}\left(1 - \frac{1}{U_c}\right)\right] \text{at } \xi = \xi_c \tag{17}$$

The following abbreviations are used in the above equations:

$$N_{Nuo} = N_{Nu}(R_o/2R)(k/k_e) \tag{18}$$

$$N_{Nu} = h(2R)/k \tag{19}$$

$$N_{NuR} = \sigma R_o T_o^3/k \tag{20}$$

$$\beta_1 = C_{AO}D_{eA}(T_o)(-\Delta H_1)\bar{R}/k_e E_1 \tag{21}$$

$$V = C_{AO}D_{eA}(T_o)C_p(S_1)/aC_{SO}k_c \tag{22}$$

$$G = \rho(S)C_p(S)T_o/aC_{SO}(-\Delta H_1) \tag{23}$$

$$\phi_1 = aR_o k_1(T_o)C_{SO}/D_{e\Lambda}(T_o) \tag{24}$$

$$\tau = \rho(S)R_o/k_1(T_o)C_{AO}C_{SO}M(S) \tag{25}$$

and

$$\theta = t/\tau \tag{26}$$

Further, the following relations are also valid and apply to the system under analysis:

$$Z = jM(S_1)\rho(S)/M(S)\rho(S_1) \tag{27}$$

$$\xi_c^3 = Z + (1 - Z)\xi_c^3 \tag{28}$$

$$N_{Sho} = \frac{K_1'}{\xi_s} + \frac{K_2'(N_{Sc})^{1/3}(N_{Reo})^{1/2}}{\xi_s^{1/2}} \tag{29}$$

and

$$N_{Nuo} = \frac{K_1'}{\xi_s} + \frac{K_2'(N_{Pr})^{1/3}(N_{Reo})^{1/2}}{\xi_s^{1/2}} \tag{30}$$

The effect of the varying size of the particle is contained in Z.

Since N_{Sc}, N_{Reo}, and N_{Pr} refer to the properties at the constant ambient conditions and the initial size of the particle, Eq. 29 and 30 can be simplified further so that

$$N_{Sho} = \frac{K_1'}{\xi_s} + \frac{K_3}{\xi_s^{1/2}} \tag{31}$$

$$N_{Nuo} = \frac{K_1'}{\xi_s} + \frac{K_4}{\xi_s^{1/2}} \tag{32}$$

where

$$K_3 = K_2'(N_{Sc})^{1/3}(N_{Reo})^{1/2} \tag{33}$$

and

$$K_4 = K_2'(N_{Pr})^{1/3}(N_{Reo})^{1/2} \tag{34}$$

It can be seen from Eq. 31 and 32 that variations in K_3 and K_4 would result in the variation of N_{Sho} and N_{Nuo}. Thus, in our subsequent analysis, instead of varying N_{Sho} and N_{Nuo}, we will vary K_3 and K_4 to investigate the effect of mass and heat transfer coefficients, respectively.

Finally, we need an expression to relate conversion to time. Such an expression has already been derived[16] and has the following form:

$$-\frac{d\xi_c}{d\theta} = \frac{\omega_{AC}}{U_c} \exp\left[\frac{E_1}{\bar{R}T_o}\left(1 - \frac{1}{U_c}\right)\right] \tag{35}$$

with the boundary conditions given by

$$\xi_c = 1 \text{ at } \theta = 0 \tag{36}$$

The conversion of solid reactant X is related to the system parameter ξ_c and for a spherical pellet, it is given by:

$$X = 1 - \xi_c^3 \tag{37}$$

Equations 11, 12, 13, 14 in conjunction with Eq. 10, 35, and 36 are to be solved simultaneously to obtain conversion-time relationships.

Notation

a	Stoichiometric coefficient of gaseous component A
A	Gas reactant
C_A	Concentration of A at the radial distance r, mol/ft^3
C_{AO}	Concentration of A in bulk phase, mol/ft^3
C_{AC}	Concentration of A at the core of the particle, mol/ft^3
C_{AS}	Concentration of A at the surface of the particle, mol/ft^3
C_{SO}	Initial concentration of the solid reactant, mol/ft^3
C_p	Specific heat of the bulk gas at constant pressure, Btu/(lb)(°R)
$C_p(S)$	Specific heat of solid reactant S, Btu/(lb)(°R)
$C_p(S_1)$	Specific heat of solid product, S_1, Btu/(lb)(°R)
D_A	Molecular diffusivity of component A in the bulk gas phase, ft^2/hr
D_{eA}	Effective diffusivity of the component A in the ash layer, ft^2/hr
e	Stoichiometric coefficient for the gaseous component E
E	Product gas
E_1	Activation energy, Btu/mol
g	Signifies the gaseous state
G	Dimensionless quantity defined by Eq. 23
h	Convective heat transfer coefficient, Btu/(hr)(ft^2)(°R)
ΔH_1	Heat of reaction per mole of reactant Btu/mol
j	Stoichiometric coefficient of the solid component S_1
k	Thermal conductivity of the bulk gas, Btu/(hr)(ft)(°R)
k_1	Reaction rate constant, ft^4/(mol)(hr)
k_e	Effective thermal conductivity of the ash layer, Btu/(hr)(ft)(°R)
k_{ma}	Mass transfer coefficient for component A across the gas film, ft/hr
K_1	A numerical constant which occurs in the correlation of Sherwood and Nusselt numbers
K_1'	$K_1/2$, dimensionless
K_2	A numerical constant which occurs in the correlation of Sherwood and Nusselt numbers
K_2'	$K_2/2$, dimensionless
K_3	Defined by Eq. 33
K_4	Defined by Eq. 34
L	Lewis numbers, $K_e/\rho(S_1)C_p(S_1)D_{eA}$
M(S)	Molecular weight of solid S
$M(S_1)$	Molecular weight of solid S_1
N	Hot spot diameter, ft
N_{Nu}	Nusselt number, 2Rh/k, dimensionless
N_{Nuo}	Defined by Eq. 18, dimensionless
N_{NuR}	Defined by Eq. 20, dimensionless
N_{Pr}	Prandtl number $C_p\mu/k$, dimensionless

N_{Re}	Reynolds number $2ur\rho/\mu$
N_{Reo}	$N_{Re}(R_o/R)$, dimensionless
N_{Sc}	Schmidt number, $\mu/\rho D_A$
N_{Sh}	Sherwood number, $2Rk_{mA}/D_A$, dimensionless
N_{Sho}	Defined by Eq. 9, dimensionless
r	Radial distance from the center of the spherical particle, ft
r_A	Rate of reaction of A, mol/(hr)(ft^2)
r_c	Radius of the unreacted core, ft
R	Particle radius, ft
R_o	Initial particle radius, ft
$\bar{R}$	Gas constant, Btu/(mol)(°R)
s	Signifies solid state
S	Solid reactant
S_1	Solid product
t	Time, hr
T	Temperature, °R
T_o	Ambient temperature, °R
T_s	Temperature of the bulk gas, °R
T_c	Temperature of the unreacted core, °R
T_p	Prater temperature difference (T_c-T_s), °R
T_S	Temperature of the outer surface of the particle, °R
u	Flow velocity of bulk gas, ft/hr
U	Reduced temperature T/T_o, dimensionless
U_c	Reduced core temperature T_c/T_o, dimensionless
U_s	Reduced particle surface temperature T_S/T_o, dimensionless
V	Defined by Eq. 22, dimensionless
X_A	Mole fraction of component A, dimensionless
X_{AO}	Value of X_A in the bulk gas, dimensionless
X_{AC}	Value of X_A at the unreacted core surface, dimensionless
X_{AS}	Value of X_A at the center surface of the particle, dimensionless
X	Conversion of solid reactant S defined by Eq. 37, dimensionless
Z	A parameter to characterize growth or shrinkage of the particle, defined by Eq. 27, dimensionless

Greek Letters

β_1	Defined by Eq. 21, dimensionless
θ	Reduced time defined by Eq. 26, dimensionless
μ	Viscosity of bulk gas, lb/(ft)(hr)
ξ	Reduced distance r/R_o, dimensionless
ξ_c	Reduced core radius of the particle r_c/R_o, dimensionless
ξ_s	Reduced size of the particle R/R_o, dimensionless
ρ	Density of the bulk gas, lb/ft^3
$\rho(S)$	Density of the solid S, lb/ft^3
$\rho(S_1)$	Density of the solid, S_1, lb/ft^3
τ	Characteristic time defined by Eq. 25, hr
ϕ_1	A parameter to characterize the ratio of intraparticle diffusion resistance to the reaction resistance, defined by Eq. 24, dimensionless
ω_A	Reduced value of X_A, X_A/X_{AC}, dimensionless
ω_{AC}	Reduced value of X_{AC}, X_{AC}/X_{AO}, dimensionless
ω_{AS}	Reduced value of X_{AS}, X_{AS}/X_{AO}, dimensionless
σ	Radiative heat transfer coefficient, Btu/(hr)(ft^2)(°R^4)

REFERENCES

1. G. J. Vogel *et al.*, "A Development Program on Pressurized Fluidized-Bed Combustion," Annual Report, July 1974 to June 1975, ANL/ES-CEN-1011.

2. G. J. Vogel *et al.*, "A Development Program on Pressurized, Fluidized-Bed Combustion," Quarterly Report, July 1 - September 30, 1975, ANL/ES-CEN-1013.

3. G. J. Vogel *et al.*, "A Development Program on Pressurized, Fluidized-Bed Combustion," Quarterly Report, October 1 - December 31, 1975, ANL/ES-CEN-1014.

4. J. Yerushalmi *et al.*, "Agglomeration of Ash in Fluidized Beds Gasifying Coal: The Godel Phenomenon," Science 187, 646 (1975).

5. P. Nicholls and W. T. Reid, Trans. Am. Soc. Mech. Eng. 62, 141 (1940).

6 S. Ehrlich and W. A. McCurdy, "Developing a Fluidized-Bed Boiler," 9th Intersociety Energy Conversion Engineering Conference Proceedings, p. 1035 (1974).

7. D. A. Martin, F. E. Brantley, and D. M. Yergensen, "Decomposition of Gypsum in a Fluidized-Bed Reactor," Bureau of Mines Report of Investigation 6286 (1963).

8. M. Hartman and R. W. Couglin, "Reactions of Sulfur Dioxide with Limestone and the Influence of Pore Structure," Ind. Eng. Chem. 13(3), 248 (1974).

9. N. P. Phillips, Radian Corporation Technical Note 200-045-10-01 (September 1974).

10. N. P. Phillips, Radian Corporation Technical Note.

11. J. A. Cusumano and R. B. Levy, Catalytica Associates, Inc., EPRI TPS 75-603 (October 1975).

12. K. H. Stern and E. L. Weise, "High Temperature Properties and Decomposition of Inorganic Salts, Part I. Sulfates," NSRDS-NBS-7 (October 1966).

13. P. J. Fiscalora, O. M. Uy, D. M. Meunow, and J. L. Margrave, J. Am. Ceramic Soc. 51, 574 (1968).

14. G. J. Vogel *et al.*, "Reduction of Atmospheric Pollution by the Application of Fluidized-Bed Combustion and Regeneration of Sulfur-Containing Additives," Annual Report, July 1973 - June 1974, Argonne National Laboratory, ANL/ES-CEN-1007 (1974).

15. H. Schultz, E. A. Haltman, and W. B. Booher, "The Fate of Some Trace Elements During Coal Pretreatment and Combustion," Trace Elements in Fuel, Advances in Chemistry Series, No. 141, Chapter 11, p. 139, 1975.

16. A. Rehmat and S. C. Saxena, "Single Nonisothermal Noncatalytic Solid-Gas Reaction: Effect of Changing Particle Size," Ind. Eng. Chem. Process Design Develop., in press.

17. C. D. Prater, Chem. Eng. Sci. 8, 284 (1958).

18. A. Bondi, R. S. Miller, and W. G. Schlaffer, Ind. Eng. Chem. Process Design Develop. 1, 196 (1962).

19. J. Wei, Chem. Eng. Sci, 21, 1171 (1966).

20. D. Luss and N. R. Amundson, A.I.Ch.E. J. 15(2), 194 (1969).

21. G. S. G. Beveridge and P. J. Goldie, Chem. Eng. Sci. 23, 913 (1968).

22. J. Shen and J. M. Smith, Ind. Eng. Chem. Fundament. 4, 293 (1965).

23. C. Y. Wen and S. G. Wang, Ind. Eng. Chem. 62(8), 30 (1970).

24. R. H. Knapp and R. Aris, Arch. Ration. Mech. Anal. 44(37), 165 (1972).

25. K. J. Cannon and K. G. Denbigh, Chem. Eng. Sci, 6, 145-155 (1957).

26. K. B. Bischoff, Chem. Eng. Sci. 18, 711 (1963).

27. D. R. Stull and H. Prophet, JANAF Thermochemical Tables, 2nd Edition, NSRDS-NBS 37 (1971).

LIMESTONE AND DOLOMITE FOR THE FLUIDIZED-BED COMBUSTION OF COAL: PROCUREMENT AND DISPOSAL

Prepared by

Bernard S. Friedman
Consultant

for the

Argonne National Laboratory

October, 1975

TABLE OF CONTENTS

LIMESTONE AND DOLOMITE FOR THE FLUIDIZED-BED COMBUSTION OF COAL: PROCUREMENT AND DISPOSAL

This report assesses the potential demand, supply and cost as well as the disposal aspects associated with the use of limestone or dolomite as sulfur-accepting additives in the fluidized-bed combustion (FBC) of coal. It also assesses the market for the regeneration by-products: sulfur and sulfuric acid.

I. LIMESTONE/DOLOMITE SUPPLY, DEMAND AND COST

A. The Preferred Acceptor

Flue gas desulfurizer wet scrubbers require limestone. Dolomitic limestones are not acceptable for these scrubbers because of their high content of magnesium carbonate. This readily absorbs SO_2 at wet scrubber temperatures to form $MgSO_4$ and $MgSO_3$, salts which are quite soluble (particularly the sulfate) and readily leached when the discarded spent acceptor is exposed to rain or ground water, leading to unacceptable levels of water pollution. Regeneration of the sludge (which would "cure" the problem by converting $MgSO_4$ and $MgSO_3$ to insoluble $MgO/MgCO_3$) is not likely to be practiced.

Fluidized-bed combustion units, on the other hand, are permitted to use dolomite because magnesium oxide does not readily absorb (retain) SO_2 at the temperatures at which these units operate. In fact, dolomite is preferred for pressurized FBC units because of its better SO_2 absorption characteristics. This is attributed to the decomposition of the magnesium carbonate to magnesium oxide which greatly increases the porosity of the stone thus facilitating the reaction of the SO_2 with the calcium carbonate.

It is to be noted that because of its greater reactivity towards sulfur dioxide and consequent greater utilization (75-80%) of the calcium carbonate present, dolomite containing 50% $CaCO_3$ is the equivalent of limestone analyzing 96% $CaCO_3$. Thus, the choice between limestone and dolomite for the FBC units will depend on the relative ease and feasibility of regeneration as well as on cost and availability of each stone at the preferred plant site.

To regenerate or not to regenerate, however, is a question which will need to be resolved on the basis of technology, capital and economics:

Con

1) Regeneration is not yet a technically feasible process. Even though the outlook seems favorable, much R&D needs to be done.

2) Capital for regeneration equipment and daily operating expense will be considerable because of the enormous quantity of acceptor to be regenerated. For example, a 600-MWe FBC plant burning about 4800 tons/day of coal (4%S) will sulfate 1200 tons/day of dolomite. Assuming a useful life of 5 cycles[a], 960 tons will be regenerated and recycled along with 240 tons fresh stone. The 240 tons discarded[b] will offset decrepitation (about 1.5% per cycle[a]) and loss in activity.

3) Considerable capital for equipment -- and heavy outlays for daily operating expenses -- will be required for the recovery of sulfur from the SO_2 liberated during regeneration.[c]

4) It will be necessary to market or stockpile sulfur (about 135 tons/day in the above example).

Pro

1) Regeneration will greatly reduce the amount of fresh dolomite purchased (1200→240 tons/day for the above 600-MWe plant).

2) Regeneration will greatly reduce the amount of SSD[d] that will need to be marketed or otherwise disposed of (1200→120[e] or 150/200[f] tons per day).

---

[a] W. Zielke, et al, J. Air Pollution Control, 20: 3, 164 (1970) cite data suggesting this is feasible.

[b] Very probably after regeneration.

[c] Alternatively, capital and operating expense for producing sulfuric acid via oxidation of the SO_2.

[d] SSD = solid sulfated dolomite; SSL = solid sulfated limestone.

[e] If regenerated before disposal.

[f] Discarded in unregenerated condition from FBC unit operating at atmospheric pressure/10 atm., respectively.

B. Source and Price

Limestone and dolomite deposits suitable for commercial exploitation are somewhat scattered. Thus commercial quantities of dolomite (54%$CaCO_3$), but not limestone, are found in the Chicago area (Materials Service Corp., Thornton, Illinois quarry) and in the Toledo area (Ohio Lime Co. - Woodville, Ohio). As to price: Over the phone, Ohio Lime quoted $2.25/ton F.O.B. quarry for 8 mesh to 3/8" dolomite, or about $5/ton delivered to Toledo (18 miles distant).

High-grade limestone (96%$CaCO_3$) is available to the Chicago area from the Mississippi Lime Co., St. Genevieve, Miss. quarry. Commonwealth Edison uses this stone for the flue gas desulfurizer wet scrubber at the Romeoville, IL. 163-MWe plant. The stone costs[a] $6.50/ton-3/4" size, delivered by barge.

It appears, then, that the quarry price will run $2-$3/ton for either limestone or dolomite. Transportation will add $0.5/ton (if the quarry is close enough to move the stone by belt, truck shuttle, etc.), $1-$2 (25-mile haul by truck or train), $2.5-$3.5 (longer haul by unit train or barge). Thus site location will determine the delivered cost: $2.5 low to $6.5 high. Crushing to a size optimum for FBC units may add $0.25 to $1.0/ton.[b]

C. Demand

Estimates of the required tonnage of acceptor involve the following assumptions:

Coal per MWe	8 tons/day
Sulfur Content	4%
SO_2 Absorption	70%[c]
$CaCO_3$/S	2/1
$CaCO_3$ in Dolomite	50%
$CaCO_3$ in Limestone	96%
Dolomite/Coal (wt)	1/4
Limestone/Coal (wt)	1/4

[a] Estimate: by phone call, 8/75, to Commonwealth Edison, Chicago, Illinois.
[b] Estimate: by phone call, 10/75, to National Limestone Institute, Inc., Washington, D.C.
[c] To reduce SO_2 in flue gas to level equivalent to 1.2 lbs $SO_2/10^6$ BTU (about same as burning 0.7%S coal).

Because of their small size and sporadic operation, current requirements for the FBC experimental units listed in Table I are miniscule. However, their output of SSD or SSL will help supply experimental lots of material for end-use tests.

Table I

FBC-PD Units

Organization	MWe	Sulfur-Acceptor tons/day[a]
BCURA[b]	0.7	1.4
Exxon	0.7	1.4
Combustion Power	1.0	2.0
Pope, Evans and Robbins Co. (PE&R)	1.1	2.2
ANL	0.075	0.15
Approx. Total		7.15

[a] Assuming no regeneration.
[b] National R&D Corp. of Great Britain.

Some of these experimental units are not operating now, but PE&R is building a 30-MWe plant at Rivesville, W.Va., scheduled for completion in 1976. ANL is designing a 1- to 3-MWe Components Test and Integration Facility (CTIF). A number of companies have submitted proposals, in response to a RFP, to build FBC pilot plants in the range of 20 to 60 MWe.

Assuming once-thru use of acceptor, PE&R data indicate the new 30-MWe unit will require about 96 tons of Greer limestone (80%$CaCO_3$) to absorb the SO_2 liberated during the combustion of 240 tons of coal (4.3%S) per day. This would produce about 80-85 tons/day of solid sulfated (spent) lime (SSL). However, if regeneration permits recycling of the limestone, say an average of five times, the production of SSL would drop to about 16 tons/day. This would still provide ample quantities for end-use testing.

In attempting to project future requirements for dolomite or limestone as well as the potential supply of spent stone, several assumptions had to be made:

- The pilot plants would operate successfully
- Subsequent demonstration plants would operate successfully and show economic advantages over conventional coal-burning boilers
- No economically feasible process would be developed for the desulfurization of coal, eliminating the need for wet scrubbers, or for an acceptor in FBC units
- Nuclear and fossil fueled plants would remain competitive so that new plants of each type would continue to be built throughout the next two decades
- Breeder nuclear, MHD or fusion reactors would not become commercially feasible before 1995.

On the basis of these assumptions, and postulating that demonstration and commercial plants will involve 10x to 30x scale-ups of successful pilot plants -- one may project the expansion of fluidized technology, over the next two decades, to be approximately that shown in Table II and plotted in Figure 1.

Wet sludge (spent limestone from wet scrubbers) production, it should be noted, is and will be a great deal larger. Estimates of current and projected output are given in Table III. This table projects wet scrubber limestone needs only until about 1985 because it is believed that if the demonstration FBC plants operate successfully, especially so if the commercial-size FBC units succeed -- new coal-burning utility plants built after 1985 will most likely be FBC units.

The combined requirements (21.6 million tons/year of dolomite for the FBC units plus 58 million of limestone for wet scrubbers) amount to about 10.5% of the current national production. The U.S. reserves are enormous. Therefore a national shortage is very unlikely.* However, at a given site one but not the other stone may be locally available -- or neither.

*Noted added in proof: The paper, "The Use of Lime, Limestone and Other Carbonate Material in the New Coal Era," presented by Stephen T. Benza and Ann E. Lyon at the Second Symposium on Coal Utilization, October 21-23, 1975, Louisville, Ky. provides a good review of limestone and its use in coal mining and coal utilization. R. Malhotra and R. L. Major also present pertinent information in their paper, "Electric Utility Plant Flue Gas Desulfurization: A New Market for Lime and Limestone and Other Carbonate Materials" (Illinois State Geological Survey, June, 1974, pp 10-14).

Table II

Fluidized-Bed Combustion

Stage[a]	Plants #@Mwe	Type	Expected Completion	Coal[c,d] Each Plant	Coal[c,d] Sub-total	Coal[c,d] Running Total	SSL/SSD[d,e] with Regen.	SSL/SSD[d,e] w/o Regen.
Pilot Plant[b]	1@30	atm.	1976	0.24	0.24	0.24	0.01	0.06
	2@60	press.	1980	0.5	1.0	1.24	0.06	0.31
Demonstration	1@200	atm.	1981	1.6	1.6	2.84	0.14	0.71
	2@300	press.	1987	2.4	4.8	7.64	0.4	1.91
Early Stage[f]	5@1,000	atm.	1987	8.	40.	48.	2.4	12.
Commercial[f]	5@1,000	press.	1992	8.	40.	88.	4.4	22.
Enthusiastic Stage, Comm.[f]	25@1,000	both	1995	8.	200.	288.	14.4	72.
Total(1995)	36,000[g,h]					88 MM/yr	4.3 MM/yr	21.6 MM/yr

[a] Demonstration and commercial plants each dependent on success of plants in the prior stage.
[b] PE&R unit at Rivesville, Va.
[c] Averaging 4% sulfur.
[d] Thousands of tons/day. SSL = solid sulfated lime; SSD = solid sulfated dolomite.
[e] Running total.
[f] These are projections only.
[g] Rounded figure.
[h] The report of Subpanel V, "Coal and Shale Processing and Combustion," prepared for the President by the Chairman, U.S.A.E.C., 12/1/73, projected an installed capacity of 40,000 MWe by the year 2000, but suggested it might well be greater than that.

Table III

Plants Utilizing Wet Scrubbers

	MWe	Coal[h]	Sludge[g,h]
Installed	1,200[a] - 2,340[c]		4-7
Under Construction	5,500[a] - 4,440[f]		16-13
	6,780	55	20
Planned[b]	13,000[d]	104	39
Projected[b,e]	25,000[d]	200	75
Total as of 1980	45,000[k]	359	134
(MM/yr)		(107)	(40)
Additional to 1985	10,000[d,i]	80	30
Projected to 1985	10,000[d,j]	80	30
Total as of 1985	65,000	519	194
(MM/yr)		(156)	(58)

[a] M. R. Beychok, Chem. Eng./Deskbook Issue, Oct. 21, 1974, page 79
[b] H. S. Rosenberger, et al, Chem. Eng. Progress, May, 1975; see last paragraph on page 67
[c] Arthur P. Hurter, Jr., ANL Report ES-39, Nov., 1974, Table 11, p. 65
[d] Assuming 1/2 of the installations will utilize limestone and the other 1/2 will use a different absorption/desorption process; rounded to nearest thous.
[e] Additional capacity needing SO_2 removal in order to meet primary ambient air standards by 1980 (see last paragraph p. 75, ref. c)
[f] By difference
[g] Solids basis
[h] Thousands of tons/day; rounded figures.
[i] Contracted as of 6/30/75: reported in "A Status Report on Electric Utility Generation Equipment" issued 7/24/75 by Kidder, Peabody and Co.
[j] Estimated: assumes rate of new orders placed during 1976-79 will be reduced 50% by impact of new nuclear plants (95,000 MWe nuclear on order for period 1980-85)[i]
[k] Rounded to nearest thousand

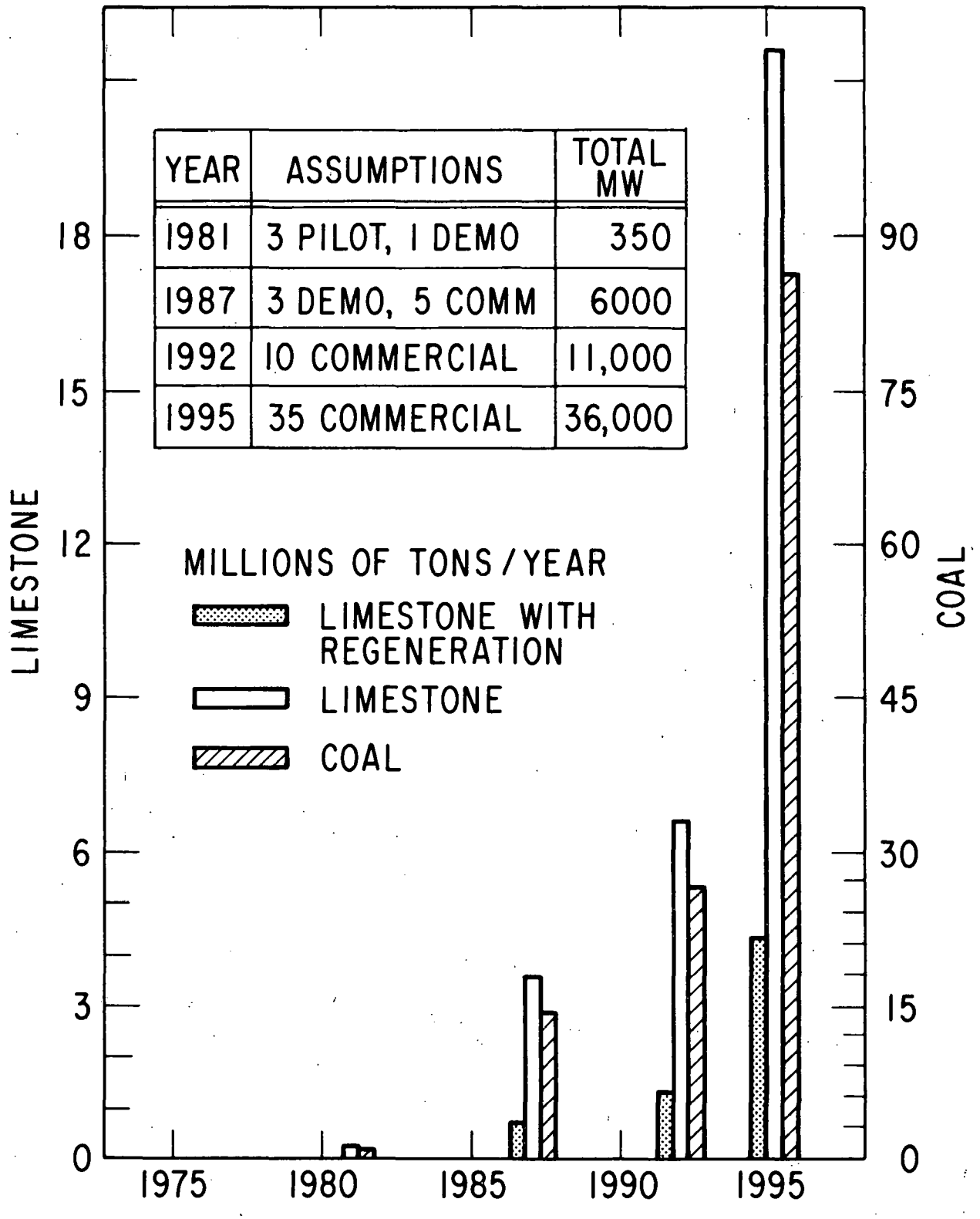

Figure I

*Note that the vertical scale for limestone (left margin) is larger than that for coal (right margin)

II. DISPOSAL OF SPENT STONE

A. Utilization as Soil Amendment for Peanuts (Source of Calcium)

Recent reports by PE&R indicate rather favorable results were obtained by the Virginia Agricultural Experiment Station with a ton sample of sulfated bed material of "high" sulfur content when the material was applied to a plot planted with peanuts. Below is a quotation from the PE&R Quarterly Report #3, January - March, 1975:

> "Dr. D.L. Hallock of the V.P.I. Tidewater Research Center has issued a complete report on the results of the peanut crop, treated with sulfated bed material from the FBM.* Based on this first season of testing, the results are very encouraging. Table 5 shows that at one farm the average crop values of the peanuts fertilized with the bed material (No. 19 and 20) were $51.00 and $72.00 per acre higher than the control standard. A control standard is a site not fertilized with a supplemental calcium source. These also compared favorably with the crop values from the sites fertilized with landplaster (No. 2 thru 7), the most commonly used calcium source. The average crop value of all the sites fertilized with 800 lbs/acre of landplaster (two different grades) was $519.00 per acre. The average crop value of all sites fertilized with 800 lbs/acre of FBM bed material was $516.50 per acre - only $2.50 per acre less than the landplaster fertilized sites.
>
> At the sites where the soil was of the Woodstown loamy fine sand variety the crop value per acre was higher when the FBM bed material was used. The crop value of Woodstown sites fertilized with 800 lb/acre FBM bed material was $533.00 per acre, whereas the crop value of Woodstown sites fertilized with 800 lb/acre landplaster

*This is the 1.1MWe fluidized-bed pilot plant at Alexandria, Va. (Footnote added)

was $530.00 per acre. This is a crop value increase of nearly $3.00 per acre when FBM bed material is substituted for landplaster as a calcium source on farms of the Woodstown type soil.

As reported in Quarterly Report No. 2, the price of landplaster in 1974 was about $26.00 per ton spread. At this price the use of FBM bed material as a landplaster substitute becomes very attractive.

In his comments, Dr. Hallock states that soil analyses indicated that readily available calcium levels in the fruiting zone were increased by these materials even soon after application. Also, effects of these materials on soil pH were minimal which probably is advantageous for materials utilized for supplemental calcium sources.

In preparation for another season of testing, sulfated bed material is being packaged for shipment to Tidewater Research Center. A more comprehensive study is planned this season with treatment being applied to different plots at different times during the growing season. Last year the bed material was applied only at one time."

These favorable results were obtained with spent bed material (SSL) from Test 621 using Greer (low cost) limestone. In this test no salt was fed to the bed. Yet PE&R operational experience has indicated* that besides limestone (550 lbs 80%$CaCO_3$) a catalyst (48 lbs of salt) must be present in order to secure a high level (e.g. 90%) absorption of the sulfur dioxide released in burning one ton of coal (4%S). On the other hand it is understood (phone conversation with Wayne McCurdy of ERDA-FE) that at least initially, salt will not be used in the new 30-MWe unit at Rivesville because the Monongahela Power Company on whose power plant site the unit is being installed is very worried that corrosion, a problem with some neat**coals, will be seriously aggravated when salt is added to the firebox.

*p.114, U.S. Department of the Interior, Office of Coal Research report 1974-1975
**i.e., no additives

At any rate, Dr. D. L. Hallock of the Tidewater Research Center, Suffolk, Va. is conducting additional and more extensive tests of PE&R spent lime. This material* will be applied as a calcium source to different plots of peanuts on two test sites representing different soil conditions -- at different times throughout the season -- to determine the optimum application time. Thus 800 lbs/acre will be used as preplant disk-in, 800 lbs more at emergence (June 1), 800 lbs additional at first flower (June 15), 800 lbs at normal flower (July 1). These treatments will be compared to regular landplaster.

Observations and data will be secured regarding:

- Yields, grades, acres value per treatment
- Pod breakdown (rot disease) incidence near maturity
- Soil analyses of fruiting zone and pH and contents of available Ca, Mg, K, and P. Also, if possible, other soil analyses during the growing season for evidence of calcium availability in the fruiting zone
- Daily precipitation at or near test sites
- Observations for phytotoxic effects, disease problems, etc.

PE&R also reports (April, 1975) that they are corresponding with a Mr. H. W. Elder of the Office of Agricultural and Chemical Development, Tennessee Valley Authority concerning TVA's ability and willingness to undertake a study of the use of spent bed material as an agricultural nutrient:

> The intent was to have Mr. Elder's organization evaluate the sulfated limestone as a liming agent and as a source of nutrient sulfur. It appears they are capable of performing extensive testing; however, at a prohibitive cost.
>
> A small sample was sent to Mr. Elder earlier in the year for analysis of toxic substances which might

*Presumably "salt-free" SSL (Footnote added)

> rule out its use in agriculture. His reply was: "Based on a cursory look at the material you sent, our agronomists felt that the lime bed material would not be toxic."
>
> The Office of Agricultural and Chemical Development has agreed to do preliminary green house testing, without charge, to determine the feasibility of the sulfated limestone's use as an agricultural nutrient. Any further testing will depend on the results of these tests.
>
> In response to their offer of preliminary testing a five-gallon sample of spent bed material has been sent to their facility at Muscle Shoals, Alabama. The bed material was from Test No. 620.

Growers have traditionally applied finely ground gypsum over the top of the peanut plants at the early bloom stage to supply the calcium needs of peanut kernels and pods. In a paper delivered at the ACS national meeting in Chicago (August 1975) Astor Perry of Carolina State University reported:

> Initial tests indicated that wet gypsum (a by-product of wet-process phosphoric acid plants) could meet the calcium requirements of peanuts and that it could best be applied broadcast using fertilizer spreading equipment. Replicated date and rate of application tests conducted at on-farm locations compared wet gypsum with finely ground and granular forms* as to their effect on yield and quality. No significant differences were found between sources or date of application when equivalent amounts of calcium sulfate in the fruiting zone were used. Grower and dealer acceptance of wet gypsum have been rapid as the method of application is desirable to both parties. Wet gypsum is now applied to approximately 50% of the peanut acreage in North Carolina and Virginia.

*Natural gypsum (Footnote added)

Mr. Perry indicated by phone that the wet gypsum has a trace only of H_3PO_4 and is only slightly more soluble than natural gypsum. The phosphoric acid plant -- which has a tremendous stockpile of the material -- charges $5/ton for it F.O.B. the plant. However, the farmer pays $25/ton to the distributor firm which spreads the wet gypsum on the land on a custom basis. The distributor uses a specially equipped truck-spreader which "broadcasts" the gypsum over a wide swath. The dosage is usually 0.7 ton/acre per year.

The peanut acreage in North Carolina and Virginia, Mr. Perry said, is 170,000 and 105,000 respectively. Total U.S. acreage has been limited since the 1930's by federal regulation to 1,610,000 (a 75% penalty is imposed on those who exceed their allotted acreage). However, yield of peanuts per acre has doubled over the last 50 years; consumption has not kept pace; thus the price structure is often weak.

Mr. Perry indicated that Oklahoma and Texas have access to natural deposits of gypsum, but North Carolina and Virginia do not. He believes that Georgia peanut growers utilize wet gypsum from a phosphoric acid plant in Florida.

Thus, this market for SSL -- if substituted by all peanut growers pound for pound (as Hallock did) for currently used "wet" gypsum by-product - or for natural gypsum - would equal about 1.12 million tons/year (1.6 million acres x 0.7 ton/acre). This amount could well be supplied by the SSL expected in 1987.[a] However, the annual production of "wet" gypsum (27 million tons/year in 1973) plus the availability of enormous stockpiles of "wet" gypsum make the peanut growers a highly improbable market for SSL, except, of course, where distribution costs favor SSL. SSD would need to be tested to determine what effect, if any, its magnesia content would have on the peanut crop.

Incidentally, some wet gypsum is used in North Carolina and Virginia for road construction and for recovering soil from salt water intrusion, e.g., coastal land inundated by ocean water as a result of hurricanes.

B. As Soil Amendment to Control pH

T.D. Hinesly, Professor of Soil Ecology at the University of Illinois, Urbana, indicates[b] that waste dolomitic and calcitic materials from FBC plants are sufficiently high in calcium carbonate equivalence[c] to suggest that these materials may

---

[a] See Table II: 12,000 tons/day (if no regeneration is practiced) times 300 stream days equals 3.6 million tons/year.

[b] Proposal to ERDA-FE dated July, 1975: "Agricultural Value of Sulfated Dolomitic and/or Calcitic Limestone Generated as Waste Materials in Fluidized-Bed Combustion of Coal"

[c] The spent stones from the ANL-PDU analyzed 68-85%.

be useful in correcting soil acidity conditions to optimum pH (6.2 to 6.5) levels for growing crops. Typically 600-800 lbs/acre of natural limestone is required annually just to maintain soil pH at optimum levels in areas (e.g. corn or soybean farms) where high levels of nitrogen fertilizers are applied. Hinesly estimates that in the midwest corn area where about 60 million acres (about 1/3 of the total cropland in the U.S.) is treated with relatively large amounts of nitrogen fertilizers, as much as 30 million tons of SSL might be utilized (1000 lbs/acre) per year.

Illinois, for example, uses 3.7 to 4.9 million tons per year of limestone -- not enough, Hinesly says, for proper soil pH maintenance. He estimates that at least 8 million tons of SSL might potentially be used each year in Illinois for soil pH maintenance on cropland.[a] His estimate is about the same as quoted in the official statement of need.[b]

He suggests there is a potential for 50 million tons/year in the Southeastern Upland region, and another 100-120 million in the humid Eastern half of the U.S.

Thus, a total of 180-200 million tons might be used annually on agricultural lands.[c] Even greater amounts would be used if dolomitic waste limestone is used to correct magnesia deficiencies of grazing land.

In such an agricultural economy the 4.3 to 21.6 million tons/year of SSD/SSL postulated for 1995 (Table II) could be easily absorbed. However, several problems or potential problems will have to be resolved or explored and tests made before this market could be exploited; e.g.,

1. Response of each crop and soil type to continuous use of SSD or SSL for pH control.

2. Assessment of any adverse effect on soil and water-runoff. Any ill-effect on plants, animals, birds, fish, etc.?

3. Logistics and cost of transportation, distributing and spreading on cropland - as compared to natural limestone and/or dolomite.

---

[a] Incidentally, Illinois leads in consumption of aglime (limestone plus dolomite 5.2 million tons in 1974); Missouri is next, 4.62 million; Iowa, 3.32; Tenn., 2.75; Ky., 2.2; Ohio and Pa. each 2 million.

[b] Based on figures submitted to the USDA by state agriculture officials and/or colleges.

[c] Larry Cline of the National Limestone Institute (1315 16th St., N.W., Washington, D.C. stated that U.S. consumption (34.4 million tons in 1974) should have been about 92 million for best farming practice.

4. Competition from wet scrubber spent lime/limestone sludge -- which will be available in large quantities (Table III); e.g., 40 million tons[a]/year in 1980; 58 million in 1985.

5. Competition from natural limestone available at $0.5 to $10/ton (average $2) at the crusher's plant.

Hinesley proposes to make tests of SSL on Northern Illinois corn land and on Southern Illinois grazing lands (brome, orchard or tall fescue).

The author would certainly recommend approval for the kind of study proposed by Dr. Hinesly. It is further recommended that soil tests be initiated, if suitable quantities of SSD/SSL are available, in the counties surrounding each FBC plant as it is being built. This would make possible development of a ready market for the SSD/SSL the plant is expected to produce when it is fully operational.

Incidentally, Hinesly and others have suggested that the sulfur content of the unregenerated SSD or SSL may well qualify them a more desirable aglime[b] than the natural stones. They point out that as SO_2 is removed from flue gas emitted by power plants, etc., the sulfur content of the soil throughout the country will no longer be replenished by absorption from the air.

C. Utility as Structural Material

Wallboard - One of the uses considered for SSL was in the manufacturing of gypsum board (wallboard utilized for the lining of walls, partitions and ceilings -- sometimes called stucco or plasterboard.)

In 1969, 94 gypsum board plants in North America produced 9×10^9 sq ft of gypsum board, most commonly 1/2" thick. It is estimated that this consumed 74 million long tons of gypsum ($CaSO_4 \cdot 2H_2O$) -- in the form of stucco ($CaSO_4 \cdot 1/2H_2O$).

B. W. Nies of U.S. Gypsum wrote[c] that:

> Although various additives or modifiers may be used in the core of gypsum board, they ordinarily amount to not more than 2% of the total by weight. The quality of the finished board and efficiency of its manufacture

---

[a] solids basis
[b] agricultural liming agent
[c] Kirk-Othmer, Encyclopedia of Chemical Technology, second edition, Volume 21, page 621

> are overwhelmingly dependent on the qualities of the stucco supplied to the board machine. Total impurities in the stucco including naturally occurring inert mineral substances should not exceed 12%. Soluble salts and hygroscopic clays are especially deleterious and their combined total should not exceed 0.2%.

Consequently, it is not likely that SSL, which usually contains only about 35-40% of $CaSO_4$, or SSD with its high content of magnesium oxide or carbonate, will find a ready market in the wallboard industry.

Other Structural Uses - The Coal Research Bureau of West Virginia University has investigated[a] the use of spent lime plus fly ash for the manufacture of cement or cinder block, facing-quality brick, mineral wool, cracking beds, ceramic casting and glaze coated materials. Of these, mineral wool production seems to have some promise.

D. Disposal as Waste

Landfill or open-pit disposal of the spent stone is not expected to cause serious pollution problems. Thus, Westinghouse[b] reporting their leaching tests on ANL spent stone, indicated that their results agree well with BCURA[c] tests -- and concluded:

> From the low leachate concentrations of magnesium and heavy metal elements, it is expected that the disposition of the spent sorbent from the fluid bed combustion process will most likely not cause pollution except for the high calcium and sulfate concentrations. Although one must point out that variation in operating conditions may alter the compositions of the spent sorbent, which in turn affects the leaching characteristics.

---

[a] Technical Report #60, 1970 Characterization and Utilization Studies on Limestone Modified Ash

[b] Westinghouse Monthly Report, Research Triangle Park, October 1974 pages 6-11

[c] National R&D Corp., Pressurized Fluidized Bed Combustion, November 1973, pages 50-53 OCR Contract 14-32-0001-1511

III. SULFUR OR SULFURIC ACID FROM REGENERATION

Plants equipped to regenerate and recycle the acceptor limestone will produce commercial quantities of sulfur dioxide. The regeneration process favored by ANL is a reductive decomposition which involves treating the sulfated stone with CO at >1900°F. This is done by adding coal to the hot sulfated lime (removed from the combustion chamber) and passing an appropriate amount of air through the mixture. The sulfur dioxide liberated by this treatment may be utilized directly for manufacture of sulfuric acid* (by oxidation) or it may be converted to marketable sulfur by reduction with coal, char or methane.

Because one step (conversion of SO_2 to sulfur) is eliminated, direct conversion of SO_2 to sulfuric acid is favored.* However the question arises: what to do with the unmarketable sulfuric acid in periods of economic downturn. No problem is anticipated in long-term stockpiling excess sulfur (in solid block) when the market falters, but this is not true for excess sulfuric acid, tank storage of which would probably be limited to about one or two weeks' production. However, in either instance, this exigency could be handled by shutting down the regenerator for the duration, transferring the sulfated stone to storage for subsequent sale as aglime, etc., or dumping it.

As shown in Table IV, the output of recovered sulfur (via removal from natural gas, petroleum, tar sand crude) surpasses production by the Frasch process.

Assuming the coal burned in the FBC plants listed in Table II will contain 4% sulfur and that the

- absorption effectiveness is 70%
- regeneration release is 90%
- conversion of SO_2 to sulfur is 90% efficient

the total sulfur production from these plants would equal 1.78 million long tons per annum in 1995, or roughly 17% of the current U.S. output of sulfur (Frasch plus Recovered).

Referring to Table III it is seen that 156 MM/yr of coal will be consumed in plants utilizing wet scrubbers. It is estimated that an equal number of plants will utilize absorber/desorber materials (other than limestone), which must be regenerated for recycle. This would be a source of an additional 3.15 million long tons/yr of sulfur or 30% of the current U.S. output.

*Especially if the plant is located in a favorable market area for the sulfuric acid.

Table IV

World Sulfur Production*

ELEMENTAL SULFUR	Millions of Long Tons
Frasch	14.22
U.S.	7.90
Poland	3.15
Mexico	2.22
Others	0.95
Recovered	15.33
Canada	6.80
U.S.	2.63
Western Europe	2.60
Others	3.30
Other	2.70
NON-ELEMENTARY SULFUR	
Pyrites	10.3
Other	7.0
TOTAL	49.55

*Texasgulf data, page 9, June 9, 1975 C&EN

Would demand grow fast enough to absorb this new production (30% by 1985; 47% by 1995)? Probably so, since the market growth[a] required -- about 2.7%/year 1976-85 and 1.3% 1986-95 -- is lower than the growth rate, 3.5%, experienced by the sulfuric acid industry during the past decade.

As shown in Table V, the projected amount of sulfur recoverable by 1985 from coal combustion and conversion as well as from shale oil could be absorbed without upsetting the market. However, one must keep in mind the current overproduction in Canada[b]: 6.8 million long tons recovered from natural gas and tar sands oil in 1974 by Western Canadian plants; 4.9 tons shipped; 1.9 stockpiled; inventory 13 million tons. If and when shipping problems are resolved, Canada could easily upset the world market supply/demand balance. On the other hand, Frasch plants provide a safety valve; unlike involuntary (recovered) sulfur producers they can be, and often are, shut down or started up as the market warrants.

Market quotations (October 27, 1975) reflect the current supply/demand picture:

$25/long ton f.o.b. Alberta, Canada for U.S. delivery

$57.50-58.50/long ton f.o.b. vessels, Gulf Ports for crude, bright, molten domestic

$61-67/long-ton, ex-Tampa, Florida for dark sulfur

While sulfuric acid manufacture consumes most of the sulfur produced (about 87-90%), there is considerable effort (e.g., $1 million budget for 1975 R&D by the Sulfur Development Institute of Canada) to develop new uses for sulfur. Some of the most promising were reported in 1972[c]:

---

[a] Compounded rate

[b] Chem. & Eng. News, June 9, 1975, p. 10

[c] Hydrocarbon Processing, July 1972, pages 79-85; also the 4/25/75 issue of the Globe and Mail

Table V

U.S. Sulfur Supply and Demand

	Millions of long tons/year	
Current U.S. Production		
Frasch	7.9[c]	
Recovered	2.63[c]	
		10.53
Projected (by 1985)		
From FCB units utilizing and regen. limestone	0.09	
From other absorption/desorption scrubbers	2.6	
Coal gasification and liquefaction	1.2[a]-3.6[b]	
Shale Oil	0.14[e]	
		4.03-6.43
Total Supply		14.56-16.96
Consumed in Mfg. H_2SO_4		
Current	9.5[d],	
Projected growth	4.27[f]	
Total Demand		13.77

[a] Pessimistic (realistic?) estimate that only about 1/3 of President Ford's goal of 1.5 million B/D will be attained
[b] Based on full achievement of President Ford's goal
[c] Table IV. No large increase is expected in recovered sulfur -- now almost totally from desulfurization of oil and natural gas
[d] Chem. & Eng. News, June 2, 1975, page 33
[e] Assuming production and refining of 500,000 B/D containing average of 0.8%S
[f] Assuming growth for 1974→1984 will equal that of 1964→1974

Sulfur As A Structural Material*

Rigid Sulfur Foams have been developed (Chevron Chemical Co.) for insulation e.g. sub-soil insulation for highway and pipeline construction. Other applications: insulating material for drilling sites in Northern Muskeg country to protect the top layers of the permafrost from melting, and to insulate the support structure of northern pipelines. It will also find application in construction of airstrips and buildings in the far north. The potential Canadian market for sulfur in the form of rigid-foam insulation is estimated at 300,000 tons/year.

Sulfur-Asphalt Mixes (low density thermal asphalt) display exceptional properties in resisting upheavals of road surfaces by frost penetration ("Cost fast approaching that of conventional asphalt paving material"). The mixture laid on top of low-grade aggregate acts as an insulator between the actual road surface and the roadbed. Field tests (on roads) have produced encouraging results. It is estimated that the potential Canadian market for sulfur-asphalt road building materials could consume more than 600,000 tons of sulfur per year.

Concrete: "Sulfur in a hot-pour mix with poor quality cement has produced a concrete mixture that is proving superior to concrete made from the best Portland cement" -- "two or three times better". Estimate of Canadian market is 100,000 tons sulfur/year.

Impregnant for Porous Materials - Impregnating concrete with sulfur under high pressures increased compression strength from 7,000 to 20,000/sq. in. Ceramics, wood, and other fibrous products, gain strength, stiffness, moisture- and acid-resistance when impregnated with sulfur.

Surface Bond Construction - "This interesting construction technique was developed at the Southwest Research Institute in the early 1960s. Cinder or concrete blocks are stacked without mortar to form the desired wall configuration. A thin sulfur coating is then brushed or sprayed on both exterior surfaces and within minutes hardens to form a strong, hard, moisture impervious surface. The resulting wall is significantly stronger than that obtained with conventional mortar joints, skilled labor is not required and rate of construction is greatly accelerated. A building erected in this manner in San Antonio, Texas, some 7 years ago is still in excellent condition, although the same cannot be said for some of the neighboring buildings of conventional cinder block construction."

*Alan H. Vroom, Hydrocarbon Processing, July, 1972, 79-85

Traffic Paints - "Hot-melt traffic paints based on sulfur have received considerable study by a number of companies and organizations in the United States, France and Canada. One U.S. company is marketing a sulfur composition for experimental evaluation as a traffic paint. The advantages claimed for this type of product are lower applied cost and maintenance cost plus elimination of the need for diverting traffic because of the quick cooling and setting of the paint. Earlier work in Canada indicated there were some cold weather problems to be solved, but another Canadian company is currently considering a development program aimed at the 10,000-15,000 ton Canadian annual market for traffic paints."

IV. CONCLUSION

The potential logistics problems arising from the use of limestone or dolomite as sulfur-accepting additives in the fluidized-bed combustion of coal appear to be manageable.

Supply - While the maximum demand projected for 1987 (about 3.6 million tons/year) would have negligible impact on the national supply (1974 production of limestone was 751/million tons/year), there may be some local imbalances. Thus the siting of a large plant, e.g., 600-MWe, would have to take into consideration not only the availability of coal (1.44 million tons/year) but the availability of a suitable source of dolomite (0.38 million tons). A plant equipped to regenerate the stone would require only 1/5 of this amount.

The advent of commercial plants (starting 1987) is likely to develop annual requirements of 6.6 million tons by 1992 and 21.6 million by 1995.

Price - The going price for limestone or dolomite is about $2 to $3 at the quarry. Transportation will add $0.5 (nearby quarry) or as much as $3.5 (quarry located two or three hundred miles distant, requiring unit train or barge). In some instances, a particular geographic situation would enable the utility to recover some of this cost. Thus, if there are no limestone quarries in the vicinity, farmers and/or fertilizer companies might be willing to purchase the discarded acceptor for use as aglime (agricultural liming agent).

Disposal - Leaching tests conducted by Westinghouse and BCURA indicate that landfill or open-pit disposal of the spent stone should not pose serious pollution problems. At least it will not be nearly as serious as that involved in dumping untreated wet scrubber sludge.

If the fresh stone is trucked or shipped in from a nearby quarry, it should be feasible to load the returning empty trucks or RR cars (unit train) with spent stone for dumping into the quarry.

Marketing of the spent stone for use as aglime appears promising; however, testing on various soils is certainly a prerequisite and should be a continuing activity prior to and during the operation of pilot and demonstration plants.

Geography will determine the marketability and the price. Where a limestone quarry is close by, the utility may have to give the spent stone away; where a natural source is not conveniently located, the farmer or distributor may be willing to purchase the stone at prices ranging $0.5 to $3/ton (f.o.b. plant) depending on the distance of the nearest natural aglime source.

Sulfur By-Product - The sulfur dioxide liberated in the regenerator can be converted to marketable sulfur or oxidized to produce sulfuric acid. The current U.S. market and price structure for sulfur is threatened by the heavy excess (two million tons in 1974) produced and stockpiled in Western Canada, and the lower prices quoted there ($28 F.O.B. Alberta vs $58/ton F.O.B. Gulf Ports). However, if the FBC plant is located close to a sulfuric acid plant, the sulfur dioxide or sulfur by-product would produce a reasonably good revenue* (probably $2 million to $3 million/year for a 600-MWe plant).

In the event no ready market is found, the sulfur can be stockpiled (as in Canada) in a stable fashion as massive blocks -- with minimum environmental risk -- while waiting for a market to develop. It is much more difficult and costly to stockpile sulfuric acid; therefore when the acid cannot be sold, one must shut down the regeneration unit and dispose of the sulfated stone as aglime or discard it by dumping.

*and probably net a satisfactory profit